2013-01-10

Role of Elemental Sulfur and Polysulfide in Corrosion Mediated by Sulfate Reducing Bacteria

Johnston, Shawna Lee

UNIVERSITY OF CALGARY

Role of Elemental Sulfur and Polysulfide in Corrosion Mediated by Sulfate Reducing Bacteria

by

Shawna L. Johnston

A THESIS

SUBMITTED TO THE FACULTY OF GRADUATE STUDIES

IN PARTIAL FULFILMENT OF THE REQUIREMENTS FOR THE

DEGREE OF DOCTOR OF PHILOSOPHY

DEPARTMENT OF BIOLOGICAL SCIENCES

CALGARY, ALBERTA

JANUARY 2013

Abstract

Sulfate reducing bacteria (SRB), such as *Desulfovibrio vulgaris* sp. Hildenborough, are strict anaerobes which reduce sulfate to sulfide, which is toxic and leads to reservoir souring and pipeline corrosion. SRB can be controlled through nitrate injection. Nitrate stimulates the nitrate reducing, sulfide oxidizing bacteria (NR-SOB) which reduce nitrate to nitrite. Nitrite is inhibitory to SRB, as it blocks a key sulfate reduction enzyme. Nitrite and oxygen (from periods of oxygen ingress) can also react chemically with sulfide to produce elemental sulfur (S) or polysulfide (PS), both of which are also inhibitory to SRB. In this way, nitrite and oxygen seem to dually inhibit SRB. However, both S and PS are very corrosive species, and their formation in pipelines is undesirable. Recent data suggests that sulfur formation during nitrate injection may occur, which may increase corrosion risk. SRB can overcome nitrite and oxygen stress, as well as S and PS stress. This raises the question: what role are SRB playing in pipeline corrosion?

Oxygen and nitrite were added to live and autoclaved *D. vulgaris* cells, and it was found that *D. vulgaris* could remove some polysulfide through an electron transport chain involving the hybrid cluster proteins Hcp1 and Hcp2. While making an *hcp1* mutant, a genomic island was found, which improves oxygen tolerance at the expense of growth rate.

Subsequent studies demonstrated that live *D. vulgaris* is able to prevent the formation of S and PS up to an oxygen: sulfide ratio of 1:1, although this did not translate to a decrease in weight loss corrosion. S and PS were formed with oxygen under biotic (live cells), abiotic (autoclaved cells) and chemical (high sulfide media) conditions. Corresponding pitting corrosion increased as biotic<abiotic<chemical. Properties of the

sulfur formed in each condition were examined, and it was found that the presence of *D. vulgaris* changed the properties of the sulfur, seemingly decreasing the severity of pitting. These findings indicate that biocide programs should be carefully considered before administration, and that once started, they should only be used under oxygen free conditions. Also, these results present the possibility of using biosurfactants as corrosion inhibitors.

Acknowledgements

A Ph.D. is certainly not an individual undertaking, and I have so many people to thank. I have had the most fortunate opportunity and experience to work under the supervision of Dr. Gerrit Voordouw, who has taught me how to carry out honest and open minded scientific research. Gerrit has been a continuous and valuable source of support, generosity and guidance since I began in the Voordouw lab as a summer student, and throughout all of my years in graduate school. As a summer student, I was fortunate to, and very much enjoyed learning from Dr. Alexander Grigoryan, Dr. Casey Hubert and Johanna Voordouw, who kindly and patiently taught me the many skills and techniques that I needed to start my project, and that I used throughout my entire Ph.D. Johanna has been of immeasurable help, both in and out of the lab. Not only has she done countless PCR's and made all kinds of mutants for me, but has also been a good friend to talk to and always had kind words to share.

Shiping Lin and Dr. Janine Wildschut were the first of many wonderful friends and mentors I met working in the Voordouw lab. Over the years, I saw many changes take place within the lab, which was a relatively small group when I started. Gerrit received the NSERC IRC in Petroleum Microbiology, and our group began to expand. Through this, I met Dr. Tom Jack, who has also been of endless help and support. He has provided much guidance about experiments, data analysis, and navigating the industrial side of things, and was always happy to help or talk about anything I needed. Tom also holds the largest collection of literature of anyone I know, and always had a reference for anything I might need. The start of the IRC also brought Dr. Rhonda Clarke to the group, whose

help with administrative and organizational details has been priceless. She is always cheerful and has also been a great companion outside of the lab as well.

I was so fortunate to meet and learn from many people along my journey: Dr. Adewale Lambo, Dr. Sean Caffrey, Dr. Hyung-Soo Park, Dr. Lisa Gieg, Dr. Akhil Agrawal, Marcy Yurkiw, Esther Ramos, Jane Fowler, Carolina Berdugo Clavijo and many others as well.

To all of my dear and most special friends, here and around the world, your encouragement and love are beyond words. The little things – coffee breaks, small words of support and simply just talking mean so much, and I love all of you dearly.

Most importantly, my family has provided unbending strength and support to me throughout this entire venture, as they were and continue to be for everything else as well. To my parents, words cannot thank you enough, and I love you with all my heart.

Dedication

For my grandmothers

Table of Contents

List of Tables

List of Figures and Illustrations

List of Symbols, Abbreviations and Nomenclature

Symbol	Definition
μL	microliter
Amp	ampicillin
API	American Petroleum Institute
Apr	APS reductase
APS	adenosine-5'-phosphosulfate
ATP	adenosine-triphosphate
bp	base pair
CAP	calf alkaline phosphatase
CO_2	carbon dioxide
COG	cluster of orthologous groups
CSB-A	Coleville synthetic brine medium, modified
dH_2O	distilled water
DNA	deoxyribonucleic acid
dNTP	deoxy-ribonucleotidetriphosphate
DR	direct repeat
Dsr	dissimilatory sulfite reductase
E	potential
E_{corr}	corrosion potential
EDTA	ethylenediaminetetraacetic acid

EPS	extrapolymeric substance
$Fe(OH)_3$	iron hydroxide
$Fe_2(CO_3)_3$	iron carbonate
FeS	iron sulfide
GC	gas chromatography
GC-MS	gas chromatography-mass spectroscopy
GC-PFPD	gas chromatography-phosphorus flame photometric detector
gDNA	genomic deoxyribonucleic acid
GEI	genomic island
H_2O_2	hydrogen peroxide
HCl	hydrochloric acid
Hcp	hybrid cluster protein
HGT	high gelling temperature
HPLC	high-pressure liquid chromatography
I_A	anodic current
I_C	cathodic current
I_{corr}	corrosion current
IOB	iron oxidizing bacteria
IPTG	isopropyl-β-D-thiogalactoside
IRB	iron reducing bacteria
IW	injection water
kb	kilobase

L	liter
LGT	low gelling temperature
$(CH_3)_xS_n$	methyl sulfide
MHGC	Medicine Hat Glauconitic C field
MIC	microbially influenced corrosion
mL	millilitre
MLP	mid log phase
mM	milimolar
N_2	nitrogen
NACE	National Association of Corrosion Engineers
nm	nanometer
NO	nitric oxide
Nrf	nitrite reductase
NR-SOB	nitrate reducing-sulfide oxidizing bacteria
NS-tSRB	North Sea-thermophilic sulfate reducing bacteria
O_2^-	superoxide
OD	optical density
PC	Postgate medium C
PCE	percholorethylene
PCR	polymerase chain reaction
PE	Postgate medium E
PW	produced water
PWRI	produced water reinjection

PS	polysulfide, central chain sulfurs, S_n^{2-}
qPCR	quantitative polymerase chain reaction
RNA	ribonucleic acid
Ros	oxygen : sulfide ratio
ROS	reactive oxygen species
S	elemental sulfur, S_8
$S_2O_3^{2-}$	thiosulfate
$S_4O_6^{2-}$	tetrathionate
Sat	ATP sulfurylase
SCOB	sulfur compound oxidizing bacteria
SDS	sodium dodecyl sulfide
SRB	sulfate reducing bacteria
TE	Tris-EDTA
TPP	triphenylphosphine
TPPO	triphenylphosphate
TPP-S	triphenylphosphine-sulfide; total of S and PS
tRNA	transfer ribonucleic acid
tRNA-Met	methionine- transfer ribonucleic acid
UV	ultraviolet
V	volume
WP	water plant
WP-LS	Widdel-Pfennig, lactate-sulfate medium
X-gal	5-bromo-4-chloro-indolyl-β-D-galactopyranoside

Chapter One: Introduction

1.1 The sulfur cycle

The biogeochemical sulfur cycle is a complex series of chemical and biological reactions which transform sulfur through its eight possible oxidation states, outlined in Table 1-1 (Madigan et al., 2003). Of these, three are of greatest significance: -2 (sulfide), 0 (elemental sulfur) and +6 (sulfate). Sulfur is found predominantly in the environment in sediments and minerals (e.g. gypsum and pyrite), and in the oceans as sulfate. The subsurface naturally contains sulfate, sulfur and sulfide which are present due to various chemical mechanisms such as: thermochemical sulfate reduction, thermal degradation of organic sulfur compounds and dissolution of pyritic materials (Anthony et al., 2009).

The sulfur cycle, as with other biogeochemical cycles, is largely driven through the actions of microorganisms, as outlined in Figure 1.1 (Tang et al., 2009).

In the reductive arm, sulfate can be reduced to sulfide by the sulfate reducing bacteria (SRB), such as *Desulfovibrio* and *Desulfobacter* species. Sulfur reduction to sulfide is another possible reduction reaction, being carried out by *Desulfuromonas* species and a few archaea.

Additionally, within the reductive arm, sulfate can be assimilated by microorganisms into various cellular components through assimilatory sulfate reduction (White, 2000).

Within the oxidative arm of the cycle is the oxidation of sulfide to sulfate, carried out by sulfur compound oxidizing bacteria (SCOB). This is carried out both aerobically, by various sulfur chemotrophs; and anaerobically by phototrophic purple and green sulfur bacteria (Madigan et al., 2003). Chemolithotrophs, such as the ε-proteobacterium *Sulfuromonas denitrificans* strain can also oxidize sulfide to either sulfur or sulfate while reducing nitrate (NO_3^-) to nitrite (NO_2^-), and

are known as nitrate reducing, sulfide oxidizing bacteria (NR-SOB) (Gevertz et al., 2000). The oxidation to sulfur or sulfate depends on the nitrate to sulfide ratio (N/S), with sulfate forming at high ratios (N/S > 2.2), and S/PS forming below this ratio (Gevertz et al., 2000, Hubert et al., 2003, Lin et al., 2008). Sulfide also reacts chemically with oxidizing agents, such as oxygen or nitrite, to form sulfur. This reaction occurs at a significant rate, hence most SCOB live at aerobic/anaerobic interfaces 'catching' sulfide as it diffuses up from anaerobic areas. As sulfide oxidation is mediated by a diverse range of microorganisms, sulfide oxidizing activity has been detected in many environments, regardless of pH (Mohapatra et al., 2008).

Table 1-1 Oxidation states of sulfur compounds. Adapted from (Kleinjan, 2005).

Oxidation State	***Sulfur Compound***
-2	Sulfide (H_2S, HS^-)
-1	Disulfide (S_2^{2-})
0	Sulfur (S_8)
+1	Dichlorodisulfane (S_2Cl_2)
+2	Sulfoxylate (SO_2^{2-})
+3	Dithionite ($S_2O_4^{2-}$)
+4	Sulfur dioxide (SO_2), sulfite (SO_3^{2-})
+5	Dithionate ($S_2O_6^{2-}$)
+6	Sulfate (SO_4^{2-})

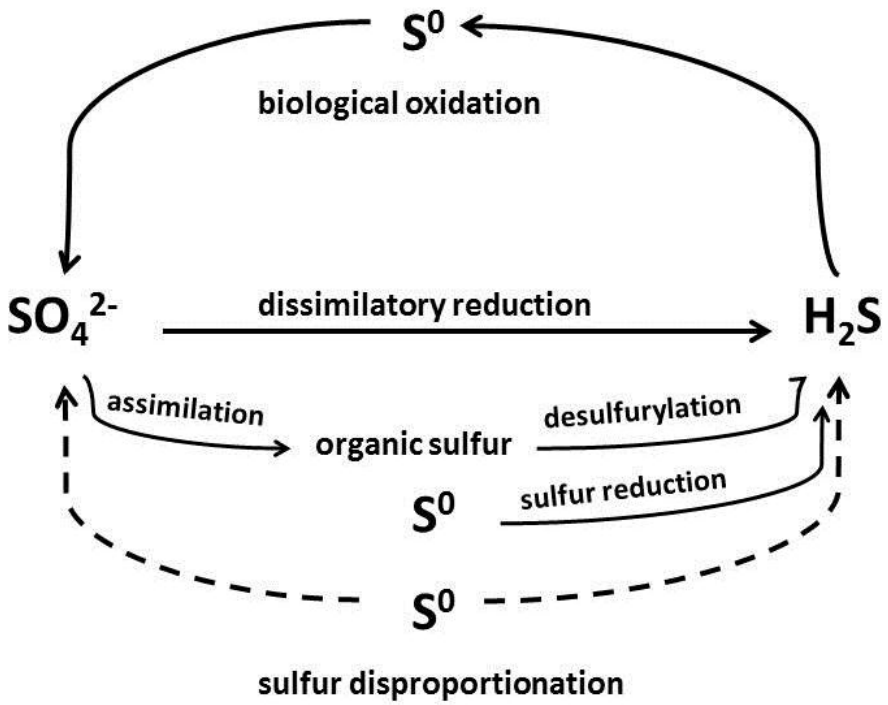

Figure 1.1 Microbial sulfur cycle according to (Tang et al., 2009).

1.2 Sulfate reducing bacteria

SRB use sulfate as the terminal electron acceptor, reducing it to sulfide while oxidizing organic compounds to generate a proton motive force and ATP (White, 2000). This process is known as dissimilatory sulfate reduction. Sulfate must first be activated by the addition of two phosphates from ATP, to make adenosine-5'-phosphosulfate (APS) which is carried out by ATP sulfurylase (Sat). Electrons from the oxidation of organic compounds are transferred to APS reductase (Apr) which reduces APS to sulfite. Sulfite is then reduced to sulfide by dissimilatory sulfite reductase (Dsr) (White, 2000). The model SRB, *Desulfovibrio vulgaris* Hildenborough, has a nine component Dsr system in three genomic regions (VIMSS). The first cluster comprises *dsrA* and *dsrB* which encode the α and β subunits of Dsr, respectively; and also *dsrD* of which the function is unclear (VIMSS 2012). The γ subunit of Dsr, encoded by *dsrC*, is located elsewhere in the genome. The third cluster has genes for *dsrP*, an integral membrane protein; *dsrO*, a periplasmic iron-sulfide binding protein; *dsrJ*, a periplasmic cytochrome c; *dsrK*, a cytoplasmic iron-sulfide binding protein; and *dsrM*, an inner membrane protein (VIMSS 2012).

1.3 SRB in the environment

SRB, such as *D. vulgaris* are ubiquitous in anaerobic environments, such as soils, marine sediments and oil reservoirs. Because sulfate reduction is an anaerobic process requiring an environmental redox potential of -300 to -400 mV relative to SHE, SRB are anaerobes requiring strictly anaerobic conditions for growth. These organisms are key components in global sulfur and carbon cycles, as they couple the reduction of sulfate with the oxidation of organic carbon to produce hydrogen sulfide, acetate and carbon dioxide (Haveman et al., 2004). SRB catalyze an estimated 50% of carbon mineralization in marine sediments worldwide (Jorgensen and Bak,

1991). However, organic carbon, capable of serving as an electron donor for sulfate reduction, is often most abundant near the aerobic to anaerobic transition zone, forcing SRB to live near this physiological edge. Other bacteria also seek this organic carbon or other compounds, such as sulfide; hence lots of community interactions take place at the oxic/anoxic transition areas. Of interest are the nitrate-reducing, sulfide-oxidizing bacteria (NR-SOB), which reduce nitrate to nitrite and ammonia while oxidizing sulfide to sulfur or sulfate (Greene et al., 2003). SRB and NR-SOB are interdependent, as the toxic sulfide produced by SRB is the electron donor required for NR-SOB metabolism. However, the nitrite produced by NR-SOB is inhibitory to SRB (Greene et al., 2003), as is the oxygen they would encounter living at this transition zone. As *D. vulgaris* frequently encounters both oxygen and nitrite in the environment, it follows logic that it would possess some means of coping with these metabolic obstacles. The following sections describe in more detail the modes of inhibition by oxygen and nitrite, and the mechanisms *D. vulgaris* possesses to overcome these.

1.4 Oxygen

The highest sulfate reduction rates in sediment gradients are often recorded near the zone of oxygen depletion (Jorgensen and Bak, 1991, Battersby et al., 1985). Because the gradient may shift vertically, microaerobic (typically 1% air by volume) or fully aerobic (100% air) conditions may occur transiently in regions in which SRB reside. Hence SRB must be able to temporarily survive full or partial air exposure, or move with the shifting gradient to new regions of the desired level of anaerobicity.

Numerous gene expression studies on the effects of oxidative stress on SRB have been carried out (Mukhopadhyay et al., 2007, Santana and Gonzalez, 2009, Pereira et al., 2008,

Wildschut et al., 2012, VIMSS). Previously, transcriptomic and proteomic studies of *D. vulgaris* were carried out at exposure to 0.1% pure oxygen, and full air exposure (Mukhopadhyay et al., 2007). SRB are well able to handle continuous exposure to 0.1% oxygen, but dramatic changes in gene expression were seen when exposed to air, the most notable being a downregulation in central metabolic pathways (sulfate reduction, ATP synthesis, electron transfer and lactate uptake). This has also been seen in our experiments with exposure to oxygen, as lactate oxidation rates slowed (described in Chapter 7).

The direct effects of oxygen stress on SRB are becoming clearer; and the resulting inhibition is likely a combination of factors such as the production of reactive oxygen species (ROS) such as peroxide (H_2O_2) and superoxide (O_2^-), which react with cellular macromolecules. Oxygen also disrupts thermodynamic equilibria due to the increase in redox potential, and leads to the direct inactivation of key metabolic enzymes, such as metalloproteins (Pereira et al., 2008, Brioukhanov et al., 2010).

In *D. vulgaris* and other representatives of this genus, oxygen survival is promoted by oxygen-reducing enzymes and enzymes removing ROS which arise from partial oxygen reduction (Dolla et al., 2007). The former include terminal oxidases typically found in aerobes (cytochrome *c* oxidase, Cox; cytochrome *bd* oxidase, Cbd), as well as the anaerobe-specific rubredoxin:oxygen oxidoreductase (Roo). The latter also include enzymes typical for aerobes (superoxide dismutase, catalase), as well as for anaerobes (superoxide reductase and the rubrerythrins). Because *D. vulgaris* does not grow with oxygen as the electron acceptor, the terminal oxidases and reductases likely serve a protective function, as shown for Roo by Wildschut and colleagues (Wildschut et al., 2006). The completed genome sequences have confirmed that *Desulfovibrio* spp. have large families of methyl-accepting chemotaxis proteins (Heidelberg et al., 2004,

Deckers and Voordouw, 1994), some of which contain redox-prosthetic groups for the sensing of environmental oxygen concentration or redox potential (Fu et al., 1994, Xiong et al., 2000). Hence, *Desulfovibrio* spp. can escape from or remove oxygen to promote their anaerobic growth in shifting gradients of aerobicity.

An SRB with the capacity to derive energy for growth from the reduction of sulfate as well as of oxygen may never have evolved, as a search for such metabolically versatile SRB in environments with strongly shifting diurnal oxygen gradients has proved negative (Sigalevich et al., 2000, Sass and Cypionka, 2007). Apparently, microbial cells can maintain growth, while shifting their metabolism from oxygen to nitrate reduction (e.g. *Escherichia coli*) or from nitrate to sulfate reduction (e.g. *D. desulfuricans* ATCC 27774), but not from oxygen to sulfate reduction, suggesting that the degree of genetic reprogramming required for this lifestyle change may be too extensive.

1.5 Nitrite

As discussed, NR-SOB reduce nitrate to nitrite, and this nitrite is often taken up again and can be further reduced to nitrogen (N_2) or ammonia (NH_3). The excreted nitrite also disperses into the environment where it can inhibit the *dsr* of SRB. Dsr has a high affinity for nitrite and slowly reduces it to ammonia (Kaster et al., 2007), in essence, suffocating SRB.

However, some SRB, including *D. vulgaris*, possess a periplasmic nitrite reductase (Nrf) which reduces nitrite to ammonia to relieve nitrite inhibition (Greene et al., 2003). Nrf has two subunits, NrfH and NrfA. NrfH contains four c-type haems and is the electron donating subunit; while NrfA has five c-type haems and is the actual site of nitrite reduction. Nrf genes are also

widely distributed in pathogenic bacteria (Greene et al., 2003) where they likely function against nitric oxide (NO) stress during host invasion (Poock et al., 2002).

1.6 Polysulfide

Oxygen and nitrite can also react chemically with sulfide to produce sulfur and/or polysulfide (S and PS). Polysulfides are defined as soluble, unbranched sulfur chains represented by S_n^{2-} in their most simple form (Kleinjan, 2005). Solution pH determines length 'n' of the chain, with n = 4 to 6 at neutral pH and shorter chains at higher alkalinities (Kleinjan, 2005). Both S and PS can be produced by chemical reaction between sulfide and compounds of a higher oxidation state (Table 1-2) such as: sulfur, ($S^0 = 1/8\ S_8$) (Kleinjan, 2005), hydrogen peroxide, H_2O_2 (Correa et al., 2002), tetrathionate, $S_4O_6^{2-}$ (Klimmek et al., 1991), nitrite, NO_2^- (Haveman et al., 2005) or oxygen, O_2 (Hamilton, 2003). These compounds can easily react to oxidize sulfide (-2 oxidation state), elemental sulfur (oxidation state 0) or polysulfides (oxidation state 0/-1). However, oxidizing past sulfur to sulfate (+6) with nitrite or oxygen, while thermodynamically allowed, is kinetically blocked at elemental sulfur, and a microbial catalyst is required to fully oxidize sulfide to sulfate (Table 1-2). This kinetic block is evident by the large piles of elemental sulfur seen around gas plants (an end product of sulfide removal), which sit exposed to the environment for years and do not chemically oxidize to sulfate. It should be noted however, that these sulfur piles harbour *Thiobacillus* species which catalyze the oxidation to sulfuric acid in the presence of water. However, reactions of sulfide and nitrite, catalyzed by bacteria such as NR-SOB, have a mechanism that allows the complete oxidation to sulfate.

It was found that S and PS are also inhibitory to SRB, as discussed in detail in Chapters 3 and 4. Polysulfide inhibition of SRB was first observed during studies with nitrite and thermophilic

SRB from the North Sea (NS-tSRB) in 2007 (Kaster et al., 2007). It was observed that when 0.25, 0.50, or 1.0 mM nitrite was added in the middle of the logarithmic growth phase (mid log phase, MLP) to NS-tSRB that the concentration of sulfide decreased, and that the cultures developed a yellow colour and a white precipitate also formed. As shown in Figure 1.2, the nitrite was completely removed, but the NS-tSRB remained inhibited. Acetate utilization was also completely inhibited, showing that the cells had become metabolically inactive. These data indicated that the sulfide oxidation products, namely sulfur and polysulfide, were causing the permanent inhibition of growth, even after the nitrite had been removed (Kaster et al., 2007). As a result, it appears that nitrite can inhibit SRB both by blocking *dsr* and by chemically reacting with sulfide to form S and PS. Oxygen may also lead to a similar two-pronged inhibition. Previous macroarray hybridizations with RNA extracted from wild type strain of *D. vulgaris* incubated with 5 mM nitrite for 30 minutes showed a strong downregulation of growth and sulfate reduction genes (ATP synthases and the *dsr* operon), while *nrf was* strongly upregulated (8.7-fold change). However, the most strongly upregulated gene was *hcp2* (255-fold). This gene was upregulated 16-fold in an *nrf* mutant exposed to 5 mM nitrite (Haveman et al., 2004). Chapter 3 discusses the role of the Hcp's in overcoming S and PS stress.

Table 1-2 Formation of sulfur and polysulfide through reactions with sulfide.

Sulfide with:	***Reaction***
Sulfur	$HS^- + n/8\ S_8 \rightarrow S_{n+1}^{2-} + H^+$
Tetrathionate	$(n+1)\ HS^- + n\ S_4O_6^{2-} \rightarrow 2n\ S_2O_3^{2-} + S_{n+1}^{2-} + (n+1)\ H^+$
Nitrite	$4\ HS^- + 2NO_2^- + 7\ H^+ \rightarrow NH_4^+ + 4\ S^0 + ½\ N_2O + 3\ ½\ H_2O$
Oxygen:	
Low concentration	$2\ H_2S + O_2 \rightarrow 2\ S^0 + 2\ H_2O$
High concentration	$H_2S + 2\ O_2 \rightarrow H_2SO_4$ (requires microbial catalyst)

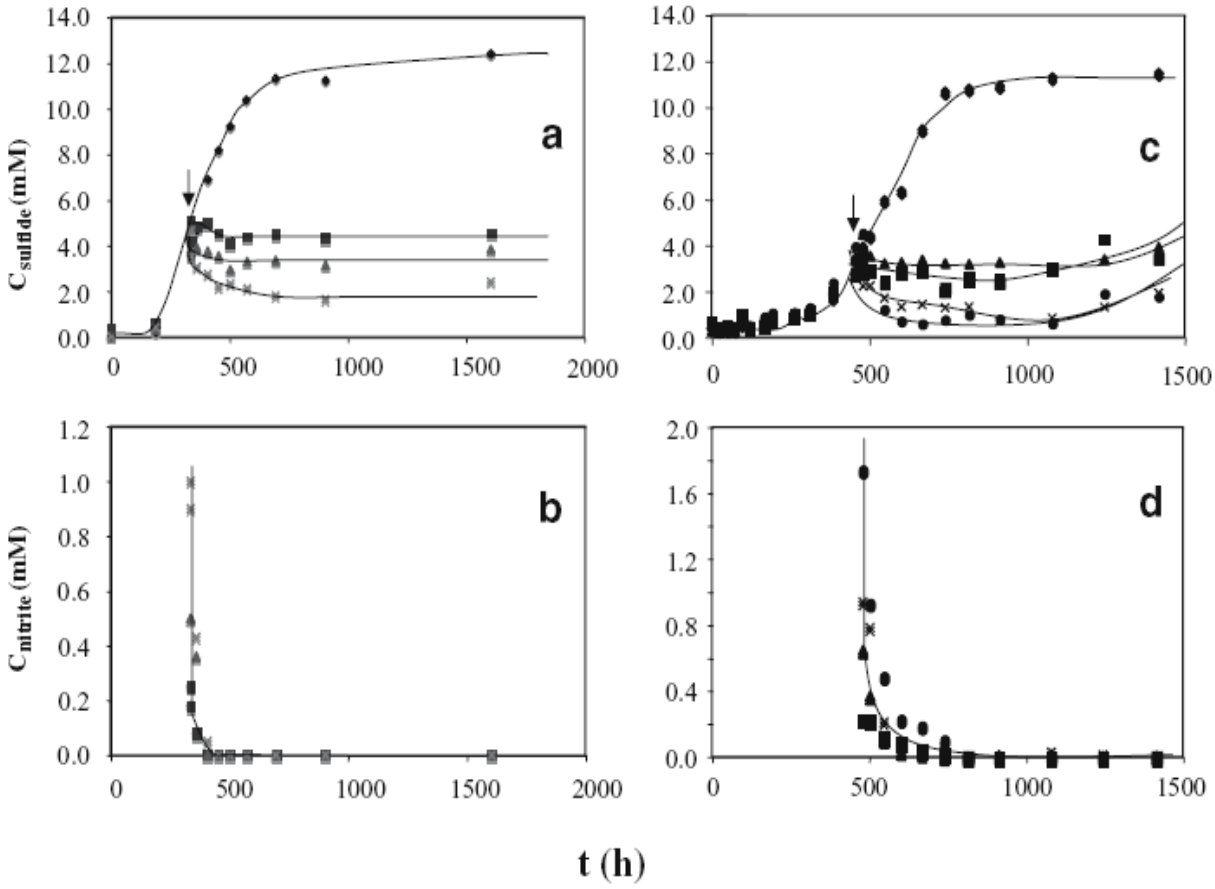

Figure 1.2 From (Kaster et al., 2007). Effect of nitrite on the growth of NS-tSRB1 and NS-tSRB2 monitored as the concentration of sulfide versus time. (a) NS-tSRB1 was grown in defined medium-1 containing acetate, proprionate and butyrate as electron donors, and either 0 mM (◆), 0.25 mM (■), 0.5 mM (▲), or 1.0 mM (✖) of nitrite was added at the indicated time (downward arrow). (b) Residual concentration of nitrite as a function of time. Symbols are for the same experimental conditions as in a. (c) NS-tSRB2 was grown in defined medium-2 with lactate as the sole electron donor, and either 0 mM (◆), 0.25 mM (■), 0.5 mM (▲), 1.0 mM (✖), or 2.0 mM (●) of nitrite was added at the indicated time (downward arrow). (d) Residual concentration of nitrite as a function of time. Symbols are for the same experimental conditions as in control.

1.7 Genomic Island in *D. vulgaris* strain Hildenborough

As discussed in section 1.5, nitrite is inhibitory to *D. vulgaris*, and this inhibition can be relieved by Nrf (Haveman et al., 2004). The gene expression pattern of *D. vulgaris* changes strongly upon nitrite addition with decreased expression of genes for enzymes involved in sulfate respiration and increased expression of genes for Nrf and hybrid cluster proteins, Hcp1 and Hcp2. While attempting to make a mutant lacking the *hcp1* gene, we discovered that this gene is readily deleted as part of a larger 47 kb region bracketed by 50 bp direct repeats (DRs). The deleted region contains 52 annotated genes (Table 1-3) with a gene for a site-specific recombinase (DVU2001) located near the 5' end. The 3'-DR is part of a tRNA-Met gene, which is retained following homologous recombination of the DRs. These features strongly suggest that the 47 kb region is a genomic island (GEI) that can be excised through homologous recombination of the 5'- and 3'-DRs, catalyzed by the DVU2001 recombinase (Dobrindt et al., 2004). Plating of the wild-type strain, used in our laboratory, on nutrient-rich, lactate- and sulfate-containing PE medium gave colonies containing and colonies lacking the GEI. PCR amplification of DNA extracted from GEI^+-cells with primer pairs p346/p347 or p348/p349, gave products of 801 and 1004 bp in agreement with theoretical expectations (Figure 1.3, Table 2-6). No product was obtained with primers p346 and p349, as their hybridization positions are separated by 47.5 kb (Table 2-6). However, use of the latter with DNA from GEI^--cells gave a fragment of 951 bp (Figure 1.4), whereas no product was obtained with the other primer pairs.

Table 1-3 Survey and location of genes in the GEI. The primer pairs used to confirm the GEI are listed. The genes confirmed to be within the GEI are noted (DVU2000 – DVU2051).

Dvu No.	Gene Name	Base Pair Coordinates		Primer(s)	Amplicon Size (bp)	GEI[a]	GEI[b]
1976	Chaperonin GroEL	2050958 ..2052601	-	p318/p319	500	yes	yes
1983	Cation-transporting ATPase, E1-E2 family	2072210 ..2074963	-	p320/p321	634	yes	yes
1996	Quaternary ammonium compound-resistance protein QacC, putative	2077184 ..2077513	+			yes	yes
1999	Sulfate transporter family protein	2079560 ..2081704	+	p322/p323	729	yes	yes
	5' screening primers	2082193 - 2082970	+	p346/347	777	yes	no
	50 bp 5' DR	2082600 ..2082649	+			yes	no
2000	Hypothetical protein	2082654 ..2082743	-			yes	no
2001	Site-specific recombinase, phage integrase family, authentic frameshift	2082778 ..2084039	+			yes	no
	Region between Dvu2001 and Dvu2003	2084039 ..2084977	-	p336/p337	1100	yes	no
2002	Hypothetical protein	2084394 ..2084816	+			yes	no
2003	Transposase, IS5 family, truncation	2084977 ..2086239	-			yes	no
2004	ISDvu4, transposase	2086357 ..2087406	+			yes	no
	Region between Dvu2004 and Dvu2007	2087406 ..2087978	-	p338/p339	500	yes	no
2005	Hypothetical protein	2087546 ..2087647	+			yes	no
2006	Hypothetical protein	2087712 ..2087867	-			yes	no
2007	Nuclease, putative	2087978 ..2088394	-			yes	no
2008	Hypothetical protein	2088618 ..2088752	-			yes	no
2009	Conserved domain protein	2088755 ..2089138	+			yes	no
2010	ISD1, transposase OrfB	2089119 ..2089943	-			yes	no
2011	ISD1, transposase OrfA	2089964 ..2090230	-			yes	no
2012	Hypothetical protein	2090399 ..2090584	-			yes	no
2013	Hybrid cluster protein-1 (Hcp1)	2090668 ..2092329	-	p286/p287	2856	yes	no
2014	Rubredoxin:oxygen oxidoreductase-1 (Roo1)	2092404 ..2093579	-			yes	no
2015	Hypothetical protein	2093666 ..2093794	+			yes	no
2016	GGDEF domain protein	2093764 ..2094645	-			yes	no
2017	ISDvu5, transposase	2094689 ..2095830	-			yes	no
2019	Conserved hypothetical protein	2096176 ..2098245	-			yes	no
2020	Conserved hypothetical protein	2098260 ..2100758	-			yes	no
2021	Hypothetical protein	2100755 ..2101222	-			yes	no
2022	Conserved hypothetical protein	2101222 ..2104698	-	p326/p327	1008	yes	no
2023	Hypothetical protein	2104703 ..2105242	-			yes	no
2024	Conserved hypothetical protein	2105239 ..2106303	-			yes	no
2025	Conserved hypothetical protein	2106300 ..2108851	-			yes	no
2026	Conserved hypothetical protein	2109863 ..2110453	-			yes	no
2027	Hypothetical protein	2110636 ..2110950	+			yes	no
2028	Conserved domain protein	2111168 ..2111395	-			yes	no
2029	ISDvu2, transposase OrfA	2111440 ..2111838	+			yes	no
2030	ISDvu2, transposase OrfB	2111835 ..2112677	+			yes	no
2031	Hypothetical protein	2112978 ..2113208	-			yes	no
2032	ERF family protein	2113963 ..2114676	+	p328/p329	625	yes	no

2033	Hypothetical protein	2114748 .. 2116019	+			yes	no
2034	Hypothetical protein	2116022 .. 2116387	+			yes	no
2035	Plasmid stabilization system family protein	2116384 .. 2116671	-			yes	no
2036	Helix-turn-helix protein, CopG family	2116661 .. 2116900	-			yes	no
2037	cobS protein, putative	2116979 .. 2117953	+	p330/p331	794	yes	no
2038	Hypothetical protein	2118007 .. 2118303	+			yes	no
2039	Hypothetical protein	2118372 .. 2118647	+			yes	no
2040	Hypothetical protein	2118657 .. 2118944	+			yes	no
2041	Conserved hypothetical protein	2118990 .. 2119965	+			yes	no
2042	Fic family protein	2119999 .. 2120793	+			yes	no
2043	Conserved hypothetical protein	2120862 .. 2122463	+			yes	no
2044	Hypothetical protein	2122572 .. 2122697	+			yes	no
2045	Hypothetical protein	2122690 .. 2122872	+			yes	no
2046	Hypothetical protein	2123012 .. 2123182	+			yes	no
2047	Hypothetical protein	2125275 .. 2125439	+			yes	no
2048	Hypothetical protein	2125651 .. 2125821	-			yes	no
2049	Transposase OrfA, IS3 family, degenerate	2126385 .. 2126851	+			yes	no
2050	Transposase OrfB, IS3 family, degenerate	2126667 .. 2127417	+			yes	no
2051	Hypothetical protein	2127643 .. 2128941	-			yes	no
	3' screening primers	2128697 .. 2129677	+	p348/p349	980	yes	no
	50 bp 3' DR	2129157 .. 2129207	+			yes	yes
	tRNA-Met	2129162 .. 2129238	-			yes	yes
2052	Glycosyl transferase, group 2 family protein	2129341 .. 2130063	+	p332/p333	700	yes	yes
2053,2054	Hypothetical proteins	2130293 .. 2131065	+, -			yes	yes
2055	Methionyl-tRNA synthetase	2131143 .. 2133134	-			yes	yes
2056,2057	Hypothetical proteins	2133136 .. 2133258	+,-			yes	yes
2058	HD/G domain protein	2134985 .. 2135596	+			yes	yes
2059	Glycosyl transferase, group 2 family protein	2135611 .. 2136603	+			yes	yes
2066	Site-specific recombinase, phage integrase family	2146192 .. 2147616	-			yes	yes
2069	DNA processing protein DprA, putative	2149978 .. 2151969	-	p334/p335	1103	yes	yes

Determination of the nucleotide sequence of the 951 bp fragment (Figure 1.4) confirmed deletion of the GEI as indicated in Figure 1.3. Southern blot analysis indicated hybridization patterns for the two strains in agreement with expectations based on the genomic maps (Figure 1.3), as well as that the wild-type strain used in our laboratory was largely GEI^+. From comparison of the intensities of hybridizing SalI fragments the wild type strain appeared to be approximately 97% GEI^+ (Figure 1.5).

The genotypic stability of a freshly colony purified GEI^+-strain was also investigated. Initial anaerobic cultures in WP-LS lacked the 951 bp PCR product obtained with primers p346/p349 indicating absence of GEI^--cells. However, this PCR product became detectable after multiple transfers, indicating excision of the GEI under these conditions. In contrast when a small fraction (1%) of GEI^+-cells was added to a culture of GEI^--cells and the co-culture was transferred multiple times in defined lactate- and sulfate-containing medium (WP-LS, Table 2-1), the fraction of GEI^+-cells was not found to increase as judged by analysis of Southern blots as in Figure 1.5.

The specific function of the GEI in *D. vulgaris* during oxygen and nitrite stress is discussed in Chapter 3. The discovery of the GEI again highlights the numerous protective mechanisms possessed by *D. vulgaris* against common metabolic inhibitors in its environment.

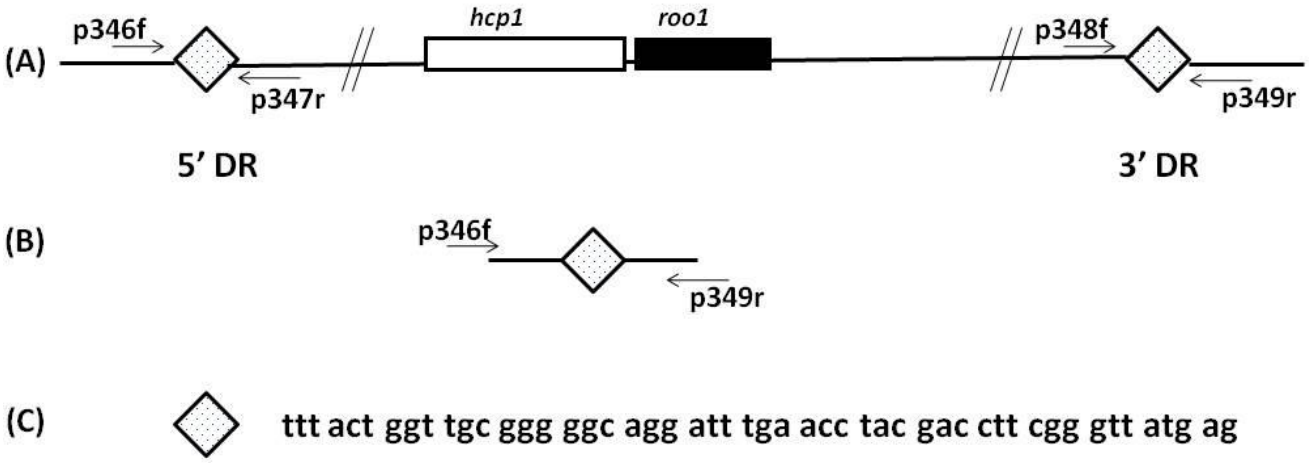

Figure 1.3 Survey of the GEI-containing region.

A. Map for the GEI⁻ strain indicating the direct repeats (DRs) and genes for DVU2013 *hcp1* and DVU2014 *roo1*. The two DRs are separated by 47 kb. Positions of PCR primers are indicated. A survey of all genes in this region is provided in Table 3.2. The 3′-DR is part of a tRNA-Met gene.
B. Map for the GEI⁻ strain. The complete nucleotide sequence of the 951 bp PCR product obtained with primers p346f and p349r is shown in Figure 1.4.
C. Sequence of the 50 bp DR bracketing the GEI.

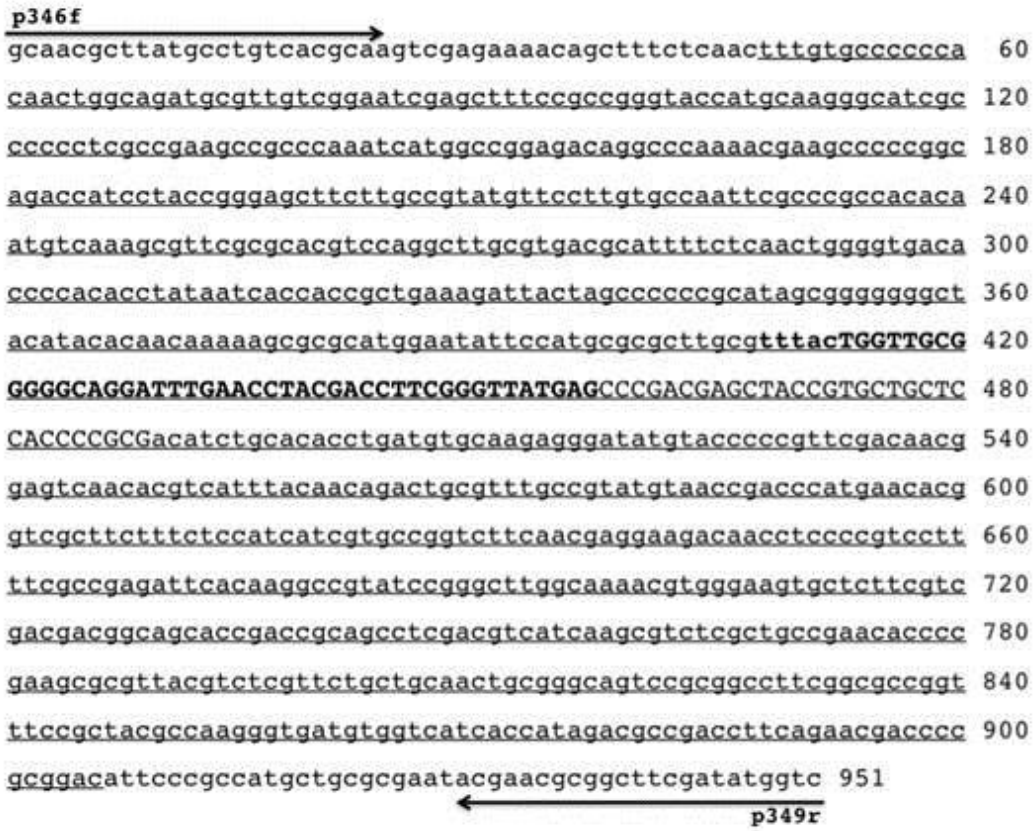

Figure 1.4 Nucleotide sequence of the 951 bp product obtained by PCR of chromosomal DNA from the GEI⁻-strain using primers p346f/p349r. The positions of primers p346f and p349r are indicated. The 50 bp direct repeat sequence is indicated in bold (nucleotides 408-457) and the 77 bp tRNA-Met gene is indicated in uppercase (bp 413-489). The portion of the sequence confirmed by sequencing is underlined.

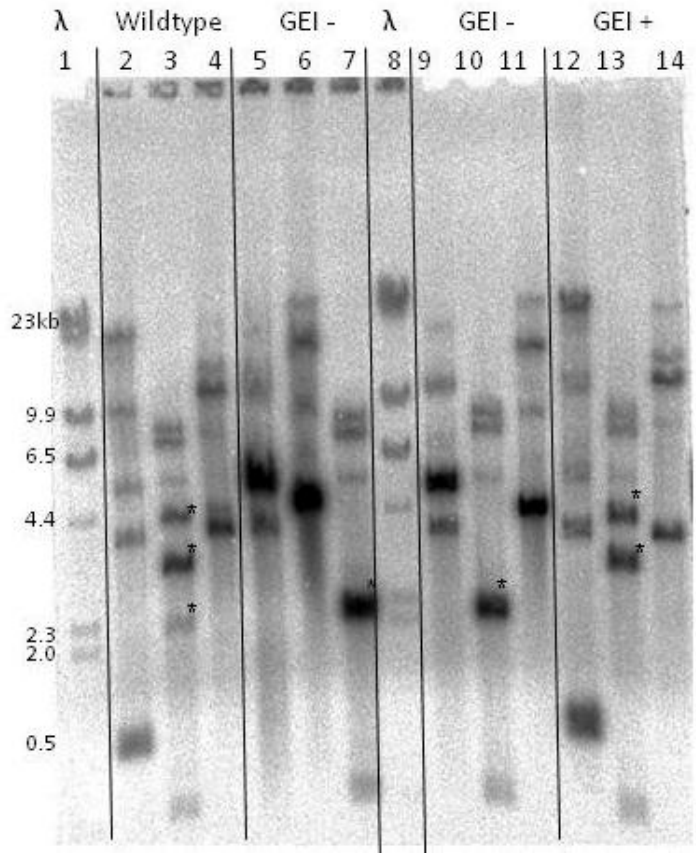

Figure 1.5 Southern blot of chromosomal DNA isolated from the wild type, the GEI$^-$- and the GEI$^+$-strains. Lanes 1 and 8 are bacteriophage λ DNA digested with HindIII. Chromosomal DNAs of *D. vulgaris* strains were digested with EcoRI (lanes 2, 5, 9 and 12), SalI (lanes 3, 6, 11 and 13), and PstI (lanes 4, 7, 10 and 14). All indicated lengths are in kilobases (kb). The blot was hybridized with the radioactively labeled 951 bp PCR product amplified from the GEI$^-$-strain with primers p346f and p349r. Qualitative inspection indicates that the wild-type pattern more closely resembles that of the GEI$^+$- than that of the GEI$^-$-strain. The intensities of bands of 4066 and 2986 bp in the SalI digest of the GEI$^+$- strain and of 2087 bp in the SalI digest of the GEI$^-$-strain were used for quantitation. These are marked (*).

1.8 Industrial applications

What is the importance of being able to inhibit SRB metabolism? While SRB are critical players in global carbon and sulfur cycles, the sulfide produced as a by-product of SRB metabolism creates serious problems for numerous industries, especially the petroleum industry. Here, sulfide leads to reservoir souring (a facility is considered sour when the total sulfur content in the gas or oil is greater than 0.5%; (Jones, 1996)) pipeline corrosion, reduced product recovery and worker safety issues. Current methods of coping with SRB activity involve the application of costly and toxic biocides, such as glutaraldehyde, into pipelines and above-ground facilities, and sometimes into the reservoir. However, with the understanding of the inhibitory actions of nitrite, new research has shown that nitrate injection is a safe and effective way to remove sulfide, as it stimulates the resident NR-SOB, which excrete the dually-inhibiting nitrite.
In this context, oxygen ingress into pipelines from routine operational activities might even be viewed as beneficial for SRB and souring control. However, S and PS are corrosive towards steel, as discussed in Chapters 5 and 6. This presents a double edged sword – does nitrate injection to control souring pose an increased corrosion risk? Corrosion is a serious problem, as described in detail in the following section.

1.9 Corrosion

Corrosion is a natural deterioration phenomenon due to reactions of a product with its environment. This process has enormous financial and safety implications, especially for the energy industry. The cost of corrosion can be divided into two main categories: direct costs and indirect costs. Direct costs refer to the expenses associated with repairing corroded pipe (i.e. digging up a pipe and replacing a section); indirect costs refer to additional expenses incurred

due to pipeline failure, such as loss of revenue from disrupted supply, legal costs, environmental clean-up, loss of reliability and increased costs of corrosion management. The annual direct cost of corrosion in the United States is equivalent to 3.1% of the annual Gross Domestic Product (GDP), which equated to $276 billion in 2002; a staggering amount which nearly doubles when the indirect costs are included (Koch et al., 2002). Worldwide, the annual cost of corrosion in 2011 was US $2.2 trillion, or 3% of the world's GDP (WCO, 2012).

In Alberta, there are approximately 415,000 km of oil and gas transmission lines that are under the jurisdiction of the Energy Resources Conservation Board (ERCB). From a corrosion perspective, even if each meter of pipe is designed, installed, operated and mitigated 99.99% properly, problems can still be expected on 41.5 km of pipe distributed throughout the system. On average, 800 pipeline 'releases' (ruptures and leaks) are reported to the ERCB in Alberta each year (Board, 2007).

As corrosion is a natural, energetically favorable process, it can be quite challenging to mitigate and likely cannot be altogether eliminated, although with careful steps it can be controlled. The energy cycle of steel demonstrates the difficulty in controlling corrosion, as the iron oxide is processed into the less stable but more desirable iron steel, which has a propensity to return to its original state.

1.9.1 Corrosion theory

In general, four elements are needed to generate a corrosion cell: an anode, a cathode, an electrical conductor and an electrolyte. At the anode, iron dissolution (oxidation) occurs as in equation 1-1:

$Fe \rightarrow Fe^{2+} + 2e^-$ **(Equation 1-1)**

Each oxidation (anodic) reaction requires a complementary reduction (cathodic) reaction, which collectively are referred to as 'redox' reactions. These reactions vary with pH and the presence of oxygen. The associated cathodic reactions in acidic solution are shown in equations 2 and 3; and for neutral or basic solution in equations 4 and 5 (Jones, 1996).

Acidic solution:

$O_2 + 4H^+ + 4e^- \rightarrow 2H_2O$ (aerobic) **(Equation 1-2)**

$2H^+ + 2e^- \rightarrow H_2$ (anaerobic) **(Equation 1-3)**

Neutral or basic solution:

$O_2 + 2H_2O + 4e^- \rightarrow 4OH^-$ (aerobic) **(Equation 1-4)**

$2H_2O + 2e^- \rightarrow H_2 + 2OH^-$ (anaerobic) **(Equation 1-5)**

The metal surface acts as a conductor, transporting electrons between the anodic and cathodic sites, and dissolved salts and minerals present in the water contacting the metal surface can act as an electrolytic fluid (Jones, 1996).

As the anodic and cathodic reactions involve the movement of electrons, anodic and cathodic currents are generated (I_A and I_C, respectively, see Figure 1.6), which are of opposite sign and are dependent on the potential (E) of a given metal. The potential of a metal can be measured relative to various electrodes, and the values discussed here will be presented as volts relative to a Standard Hydrogen Electrode (SHE). An Evan's diagram (mixed potential plot) can be generated by plotting both the anodic and cathodic half reactions for each chemical species involved, for example zinc and hydrogen (Figure 1.7). The point of intersection of the appropriate reactions (e.g. hydrogen reduction and zinc oxidation in (Figure 1.7)), represents the corrosion current, I_{corr} (x-value) and the corrosion potential, E_{corr} (y-value) (Jones, 1996).

Corrosion rates can be determined from the I_{corr} value. It should be noted that the corrosion current for a given material varies with the environment.

In general, any process which increases I_{corr} will increase corrosion; conversely, any process which decreases I_{corr} will limit corrosion.

1.9.2 Microbially influenced corrosion

There are numerous mechanisms which can lead to the establishment of a corrosion cell (Jones, 1996) outlined in Table 1-4. Of particular interest is microbially influenced corrosion (MIC). MIC is defined as corrosion affected by the presence and activities of microorganisms (Jones, 1996). Biological activity leads to changes in the type and concentrations of ions, pH and oxygen levels, altering the chemical and electrochemical environment on a given surface (Herrera and Videla, 2009a). This results in the subsequent establishment of electrochemical circuits and therefore corrosion cells. MIC tends to cause pitting corrosion, which is the most unpredictable and damaging type of corrosion (Evans, 1981). MIC can occur under both aerobic and anaerobic conditions. A brief discussion of the main bacteria known to cause corrosion follows.

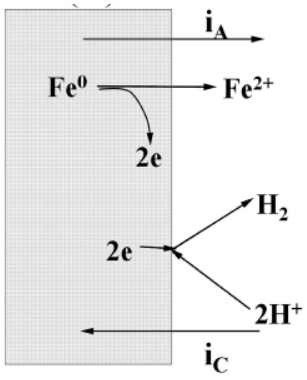

Figure 1.6 Anaerobic corrosion of iron. Generation of anodic (I_A) and cathodic (I_C) currents at an iron surface (Caffrey et al., 2008).

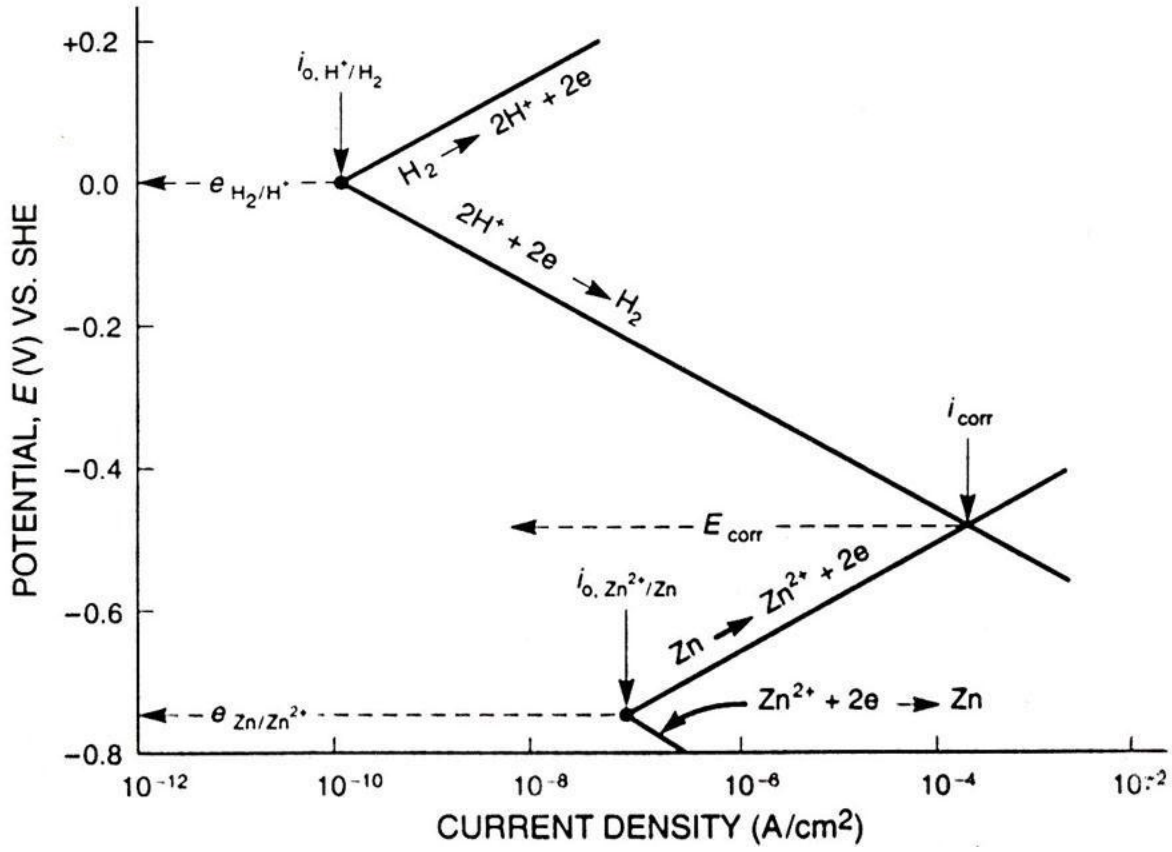

Figure 1.7 Evans diagram showing the polarization of anodic and cathodic half-cell reactions for zinc in an acidic environment, to give a mixed corrosion potential, E_{corr}, and a corrosion current, $I_{corr.}$ The corrosion rate can be calculated from I_{corr} (Jones, 1996).

Table 1-4 Types of corrosion. Adapted from (Jones, 1996).

Type	***Mechanisms Include:***	***Examples***
Uniform	Anaerobic attack and neutral pH, aerobic attack on uniformly exposed surfaces	Under disbonded coating, sour service
Intergranular	Grain boundaries depleted or loaded with alloying elements	Sensitized stainless steel
Galvanic	Active and noble metals in contact	Attack at welds
Pitting	MIC, concentration cells, localized loss of passivating film	under deposit corrosion, under disbonded coating
Crevice	Concentration cells, water retention	Gaps or interfaces at fasteners, gaskets
Dealloying	Graphitic corrosion	Cast iron pipes
Hydrogen damage	Hydrogen induced cracking	under sulfurcrete weights, sour service
EAC	Stress corrosion cracking, corrosion fatigue	under disbonded coating
Erosion corrosion	abrasion of metal surface in contact with electrolyte	oil sands transport pipes

1.9.2.1 Aerobic MIC

Aerobic bacteria and certain fungi contribute to iron corrosion through a variety of mechanisms, such as: (a) excretion of exopolymeric substances (EPS); (b) oxidation of sulfide; (c) oxidation of iron; and (d) production of acidic metabolites (Jones, 1996).

The production of EPS aids in the adherence of bacteria to surfaces, and thus establishment of biofilms which alter local chemistry and can create differential aeration/concentration cells. Here, regions of low oxygen or chemical concentration become anodic, with the associated cathodic reaction occurring at either the regions of high oxygen or chemical concentration (Figure 1.8). EPS production also creates anaerobic environments which allow for the proliferation of anaerobic bacteria (Jones, 1996).

Sulfide-oxidizing bacteria, such as *Thiobacillus thiooxidans*, oxidize sulfide and/or sulfur to sulfate, which will be present as corrosive sulfuric acid. The sulfide may also be incompletely oxidized to sulfur, which is known to be an aggressive corrosion agent (Dowling, 1992). Sulfide can also be oxidized through chemical reaction with any oxygen present in the system; or from chemical oxidants added to control souring (Johnston et al., 2009).

Iron oxidizing bacteria (IOB) such as *Thiobacillus ferrooxidans*, along with some species of *Gallionella, Sphaerotilus* and *Pseudomonas* oxidize ferrous ions (Fe^{2+}) to less soluble ferric ions (Fe^{3+}) (Jones, 1996). This activity has two main implications: (1) the utilization of Fe^{2+} will pull the anodic reaction forward, increasing the corrosion rate; and (2) Fe^{3+} will readily

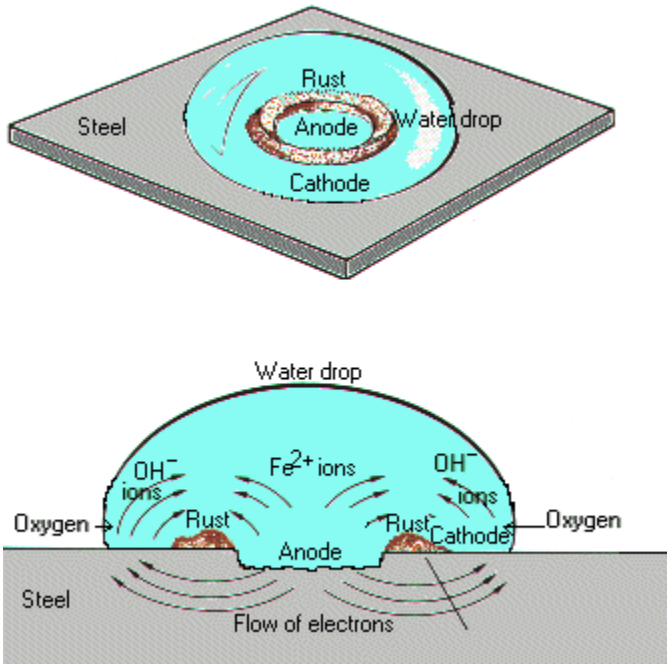

Figure 1.8 Differential aeration cell. The regions with higher oxygen concentration act as a cathode, drawing electrons from the anodic region and initiating pit formation. The Fe^{2+} ions produced from the anodic reaction combine with the OH^- ions formed from the cathodic reaction to form $Fe(OH)_2$, or rust. This theory can be applied to other types of concentration cells as well (England, 2012).

.

precipitate as ferric oxides which grow into large, solid tubercles and can block pipe flow. These deposits can also lead to the formation of differential aeration cells; with the region underneath the deposit being anodic (Jones, 1996). The cathodic reaction in an aerobic environment (from Equation 1-4) will lead to increased hydroxide production. This will favor more iron hydroxide ($Fe(OH)_3$) and iron carbonate ($Fe_2(CO_3)_3$) precipitation, leading to increased tubercle growth. Tubercles also lead to the creation of anaerobic environments (Jones, 1996).

1.9.2.2 Anaerobic MIC

Anaerobic MIC is mainly attributed to the activities of sulfate reducing bacteria (SRB) and iron reducing bacteria (IRB) (Jones, 1996).

SRB comprise a diverse group of organisms, and were implicated as causative agents of MIC as early as the 1930's (Von Wolzogen Kuhr and Vlugt., 1934). SRB are capable of using a wide variety of carbon sources, such as lactate, fumarate, ethanol, straight chain alkanes and various aromatic compounds (White, 2000). Some can also grow autotrophically using H_2 as the electron donor through the use of hydrogenases (White, 2000, Caffrey et al., 2008).

There are different theories as to the exact mechanism of how SRB increase corrosion. The two classical theories include (a) cathodic depolarization and (b) secondary effects of sulfide production (Jack, 1990).

Cathodic depolarization refers to the acceleration of the cathodic reaction (Equation 1-3) due to SRB consumption of cathodic hydrogen as an electron source for sulfate reduction. Here, SRB act as a hydrogen sink, which increases the electron demand from the anode, thereby increasing corrosion. Some SRB are capable of utilizing hydrogen via hydrogenase enzymes, which carry out the reversible oxidation of molecular hydrogen (White, 2000). While hydrogenase activity has been shown to increase cathodic currents on steel electrodes, leading to increased corrosion

rates; this remains controversial (Jones, 1996). Microbes that produce hydrogen, such as *Clostridium acetobutylicum*, can also influence corrosion reaction rates by unbalancing the local redox chemistry (Jack and Ward, 1983, Jones, 1996). Cathodic hydrogen may be formed if a corrosion cell is present, or if a system is under impressed current cathodic protection. Sulfide produced by SRB is the most reduced form of sulfur, and is highly soluble and reactive. It can be easily oxidized to S or PS, both of which are corrosive agents (Dowling, 1992, Schutt and Rhodes, 1996). Microbially produced sulfide reacts readily with anodic ferrous ions to produce insoluble iron sulfide:

$SO_4^{2-} + 9H^+ + 8e^- \rightarrow HS^- + 4H_2O$ **(Equation 1-6)**

$Fe \rightarrow Fe^{2+} + 2e^-$ **(Equation 1-7)**

$4Fe + SO_4^{2-} + 8H^+ \rightarrow FeS + 3Fe^{2+} + 4H_2O$ **(Equation 1-8)**

Iron sulfide is a conductor and is cathodic with respect to steel; and can therefore establish aggressive corrosion cells (Jones, 1996). In some situations, iron sulfide layers can passivate the steel surface from further corrosion, however, the level of protection is highly dependent upon the formation of a complete, continuous and adhesive barrier (Smith and Miller, 1975). Often, defects in the iron sulfide layer result in accelerated corrosion rates of the exposed areas of metal, since the small exposed area will be anodic to the larger FeS cathode, resulting in rapid pitting corrosion because of the high electron demand of the large cathodic area (Dexter and LaFontaine, 1998). Sulfide can also interfere with the formation of other passivating layers (Smith and Miller, 1975). Sulfide is also a poison which prevents cathodic hydrogen from leaving the metal surface, and promotes entry of cathodic hydrogen into the steel matrix, where it will concentrate at voids and imperfections. This leads to formation of pressurized "blisters" in the steel, and consequently to hydrogen induced cracking (Jones, 1996).

IRB are facultative anaerobes, which reduce ferric ions back to ferrous ions, and can also play a role in anaerobic steel corrosion. The common assumption is that production of the soluble ferrous iron compounds facilitates the removal of ferric oxide passivating films, exposing the vulnerable steel underneath. IRB have also been implicated in biofilm production, and help create anaerobic niches for SRB to flourish (Herrera and Videla, 2009b).

1.9.3 Summary of MIC – complex dynamics

The microbial involvement in corrosion processes is highly complex and situational, and the activities of microorganisms typically increase I_{corr}, as was discussed.

It should be noted that the division between aerobic and anaerobic microbial processes when it comes to corrosion is not black and white. For example, both aerobic and anaerobic bacteria are capable of producing EPS and establishing biofilms, as it is a beneficial mode of acquiring nutrients, especially in a pipeline setting where nutrient-containing fluids are continuously flowing by (Madigan et al., 2003.). Both aerobes and anaerobes can also produce acidic metabolites, such as acetate and carbon dioxide (Jack, 1990).

Therefore, one must examine the corrosion products formed to determine whether a given environment would be capable of supporting a predominantly aerobic or anaerobic metabolism. For example, the presence of iron hydroxide ($Fe(OH)_3$) would indicate oxidizing conditions; whereas the presence of iron sulfide (FeS) indicates a reduced, anaerobic environment.

It is most likely that complex community interactions are taking place, with the community composition depending on the local chemistry and available substrates. A recent study (Duncan et al., 2009a) examined a microbial community from an Alaskan North Slope oil field. Analysis of 16S rRNA revealed a complex microbial community, consisting of thermophilic hydrogen-using methanogens, syntrophic bacteria, peptide- and amino acid fermenting bacteria, iron

reducers, sulfur/thiosulfate-reducing bacteria, and sulfate-reducing archaea. These microbes can contribute to metal corrosion by generation of organic acids, CO_2, sulfur species, and via hydrogen oxidation and iron reduction. This finding highlights the complexity of microbial corrosion systems (Duncan et al., 2009b).

Overall, there is likely no single corrosion mechanism taking place in a given environment. Rather, multiple mechanisms involving diverse chemical and microbial interactions are likely occurring simultaneously. Thus, one of the main challenges of corrosion science is pulling apart the different mechanisms at play, which are often complex and intertwined.

1.9.4 Corrosion prevention

Corrosion mitigation typically involves the use of pipeline coatings, biocides/metabolic inhibitors (Hubert et al., 2005), chemical inhibitors and/or cathodic protection (Jones, 1996). There are two types of cathodic protection; sacrificial anode and impressed current. To understand sacrificial anode cathodic protection, we must first understand galvanic connections and series. Contact between two electrically dissimilar materials is referred to as a galvanic connection. Looking at a galvanic series for various metals in seawater (Figure 1.9), it can be seen that zinc, for example, is a very "active" metal; meaning that it has a very low reduction potential, and will give up electrons easily. This means that zinc will act as the anode when galvanically coupled to a metal of higher reduction potential (Jones, 1996). It should be noted that galvanic series are specific to the environment they were generated for, and the values will change in different environments (e.g. seawater versus freshwater).

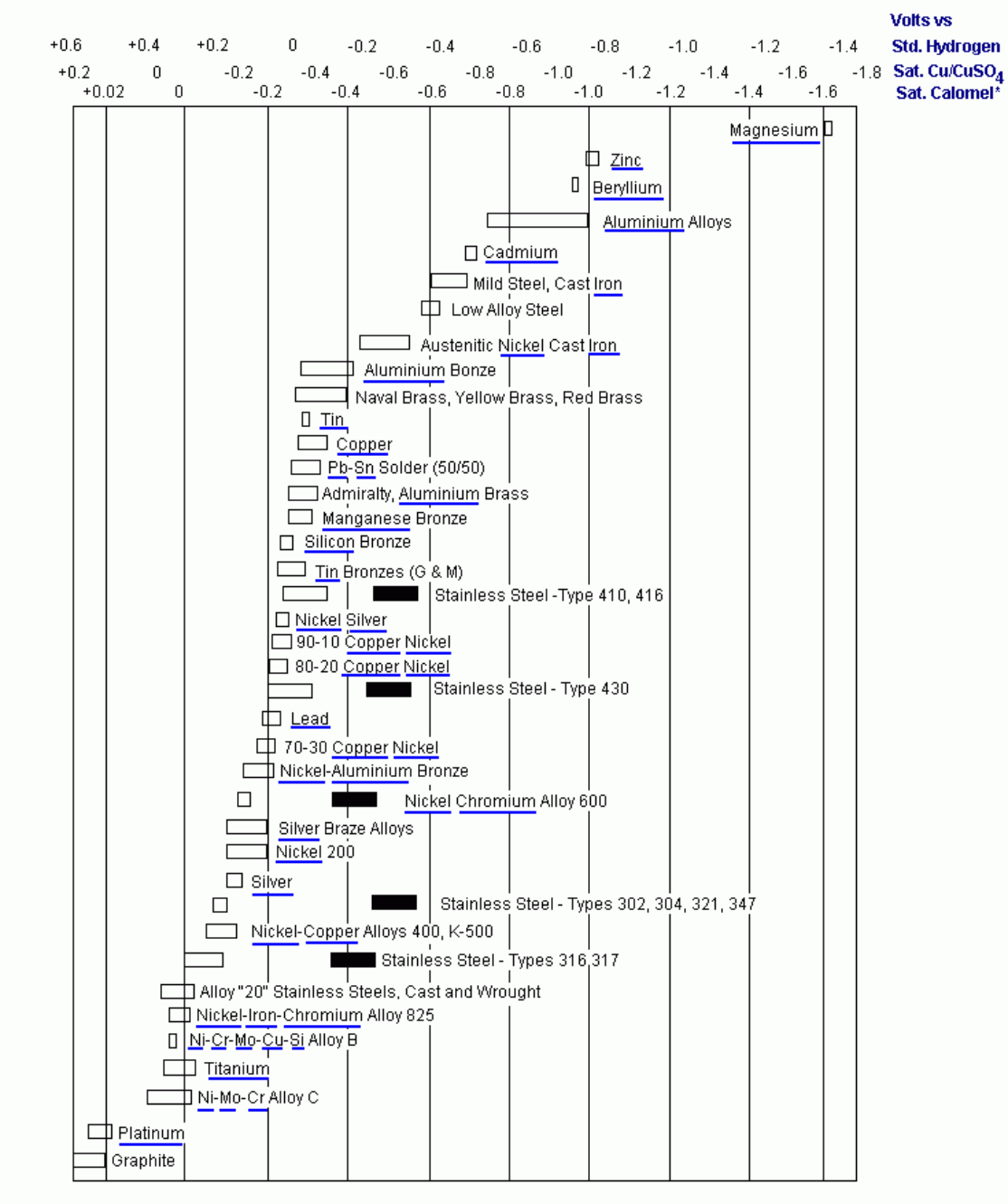

Figure 1.9 Galvanic series of common metals in seawater. The most anodic (active) metals are at the top, with the most cathodic (noble) metals at the bottom .

Sacrificial anodic protection involves linking a metal which is more active than steel, such as zinc or magnesium, to the pipeline. This will cause the anode to preferentially corrode and leave the pipe intact (Jones, 1996). For example, a zinc disc attached to a ship's iron rudder will slowly corrode while the rudder remains intact (Jones, 1996). Steel pipes may also be coated with zinc and thus will similarly protect a pipe from atmospheric corrosion (Jones, 1996).

In impressed current cathodic protection, a negative potential is applied to the pipe through an above ground rectifier and the system is grounded with an inert groundbed, such as graphite. By keeping the potential on the pipe negative; the cathodic current is increased (Figure 1.6) and the anodic reaction is therefore limited. This process causes the region at the groundbed (anode) to become acidic as groundwater is oxidized as in Equation 1-9:

$2H_2O \rightarrow 2H^+ 2\,e^- + H_2O_2$ **(Equation 1-9)**

$H_2O + ½\,O_2 \rightarrow 2e^- + 2OH^-$ **(Equation 1-10)**

The pH around the pipe (cathode) becomes basic due to reducing reactions on pipe surfaces exposed to groundwater (Equation 1-10) and promotes the precipitation of a protective, or passivating, calcium carbonate scale, which will also help to decrease I_{corr}.

1.10 Summary and objectives

As discussed in section 1.7 nitrate injection has been successful for souring control, but may increase the risk of corrosion through formation of S and PS, which is discussed in Chapter 6. S and PS can also form during periods of oxygen ingress into pipelines, and these compounds present a corrosion problem. However, as discussed, SRB are able to remove nitrite, oxygen and some S and PS (Chapters 3 and 4) from their environment. What, then, does this mean in terms

of corrosion? SRB are causative agents in corrosion, but may be able to prevent the formation of potentially more corrosive sulfur species.

As there is little understanding of S and PS formation in pipelines, and of how SRB are affecting its formation, removal, and potential corrosivity; the present work aimed to study what exactly SRB are doing in terms of corrosion caused by S and PS. Specific objectives were to:

1. Examine the phenotype and function of the GEI and its role in oxygen and nitrite stress in *D. vulgaris.*
2. Study the gene expression profiles of wild type *D. vulgaris* when exposed to sulfur-polysulfide to determine the basis of S/PS inhibition at a genetic level.
3. Study the polysulfide metabolism of mutant strains of *D. vulgaris* lacking either or all of *nrf, hcp1* or *hcp2* with induction of polysulfide formation through the addition of tetrathionate, oxygen or nitrite.
4. Determine the iron corrosion rates under conditions where *D. vulgaris* is unable to remove the excess polysulfide that is formed by chemical reaction.
5. Study the influence of SRB on the physical properties of S and PS
6. Determine the functional role of SRB during conditions of oxygen ingress
7. Determine if sulfur formation during nitrate injection occurs in an oilfield and pipeline system.

1.11 Hypothesis

Polysulfide is an aggressive corrosion agent. Mutant strains of *D. vulgaris* lacking Nrf or the Hcp's will not be able to remove S and PS and will therefore cause higher corrosion rates. Higher corrosion rates will also be observed under conditions where *D. vulgaris* is unable to

remove excess S and PS. *D. vulgaris* will confer some degree of corrosion protection through its ability to remove oxygen, nitrite, S and PS.

Chapter Two: Methods and Materials

2.1 Bacterial strains and media

Wild type *Desulfovibrio vulgaris* strain Hildenborough NCIMB 8303 was cultured in defined Widdel-Pfennig medium (WP-LS, Table 2-1). Cultures were grown in 100 mL serum bottles sealed with butyl rubber stoppers containing 50 mL of WP–LS, and a headspace of 90% vol/vol N_2 and 10% vol/vol CO_2 (N_2-CO_2). *D. vulgaris* cultures were incubated at 30^{o}C with shaking. *Desulfuromonas acetoxidans* DSM 684 was obtained from the Deutsche Sammlung von Mikroorganismen und Zelkulturen and cultured in defined MMS medium (Table 2-2). *Thiomicrospira* sp. CVO, was obtained from environmental samples from the Coleville oil field in Saskatchewan, Canada (Hubert et al., 2003) and cultured in CSB-A medium (Table 2-3). Samples were taken anaerobically from stoppered serum bottles using syringes flushed with N_2-CO_2 gas described above.

2.2 Molecular methods

2.2.1 Dilution of DNA primers

Primers were reconstituted and diluted in TE (10mM Tris; 0.1 mM EDTA at pH 7.2) to make a 20 pmol/μL solution.

The volume of TE used was calculated with the equation

Vol. TE = (ODU x pmol/mL/ODU) / 200 (**Equation 2-1**)

Following this, 20 μL of the reconstituted primer was added to 180 μL fresh TE to make a final volume of 200 μL at a concentration of 2 pmol/μL.

2.2.2 Polymerase chain reaction (PCR)

The following was mixed in a microcentrifuge tube: 5 µL PCR buffer, 1 µL dNTP's, 1 µL of each primer (forward and reverse), 0.2 µL Taq polymerase, 2 µL template DNA, 39.8 µL dH_2O to make 50 µL total volume. The mixture was then placed in the PCR machine for 25 cycles of a determined program.

2.2.3 Whole cell PCR

First, 40 µL of cells from an overnight culture was obtained and centrifuged for five minutes at 13,000 rpm. The supernatant was discarded and the pellet resuspended in 20 µL TE. Of this, 10 µL was denatured for five minutes at 94°C and then 8.2 µL of the PCR mix described above and 32 µL of water were added to each tube; and the PCR program resumed.

2.2.4 Gel electrophoresis

The gels were run on 0.7 % HGT agarose gel, and λ DNA digested with HindIII was used as a ladder. On a piece of parafilm, 2 µL of sample with 2 µL of gel dye was mixed and placed into the gel well. Once the gel was loaded, the electrodes were attached and the gel was run at 60 V until the marker spots were approximately ¾ down the gel. To visualize, the gel was stained with 5 µL of ethidium bromide (10 mg/mL) and placed on a gentle shaker for 10 minutes. The gel was then washed four times with dH_2O and imaged.

Table 2-1 WP-LS medium.

Component	***(per L)***
NaCl	1.0g
KH_2PO_4	0.2g
$MgCl_2$	0.4g
KCl	0.5g
$CaCl_2$	0.15g
NH_4Cl	0.25g
Na_2SO_4	4.0g
Na Lactate	7.51g
1% resazurin	3 drops
WP-Trace Element solution	1ml
Selenite-Tungstate solution	1ml
$NaHCO_3$ 1M	30ml
Na_2S 1M	1ml

Table 2-2 MMS medium.

Component	***(per L)***
NaCl	7.0g
KH_2PO_4	1.0g
$MgCl_2$	1.2g
KCl	0.2g
$CaCl_2$	0.1g
NH_4Cl	0.25g
Na Acetate	0.68g
$NaHCO_3$ 1M	48ml
Sulfur	0.3g
Trace elements 2 solution	1ml
Vitamin solution	1ml
Vitamin B_{12} solution	1ml

Table 2-3 CSB-A medium.

Component	***(per L)***
NaCl	7.0g
KH_2PO_4	0.2g
$MgCl_2$	0.4g
KCl	0.5g
$CaCl_2$	0.15g
NH_4Cl	0.25g
Na_2SO_4	0.7g
$NaNO_3$ 2M	5ml
1% resaurin	3 drops
WP-Trace element solution	1ml
Selenite-Tungstate solution	1ml
$NaHCO_3$ 1M	30ml
Na2S 1M	5ml

Table 2-4 Postgate medium C (PC, saline or non-saline).

Component	***(per L)***
KH_2PO_4	0.5g
NH_4Cl	1.0g
Na_2SO_4	4.5g
$CaC_{l2} \cdot 6\ H_2O$	0.062g
$MgSO_4$	0.03g
Na-lactate, 70%	8.6g
Yeast extract	1.0g
$FeSO_4 \cdot 7H_2O$	0.004g
Na-citrate $\cdot\ 2H_2O$	0.3g
NaCl (omit for non-saline)	30g

Table 2-5 Postgate medium E (PE).

Component	***(per L)***
KH_2PO_4	0.5g
NH_4Cl	1.0g
Na_2SO_3	1.0g
$CaC_{l2} \cdot 6\ H_2O$	1.0g
$MgCl_2 \cdot 7H_2O$	2.0g
Na-lactate, 70%	3.5g
Yeast extract	1.0g
$FeCl_2 \cdot 4H_2O$	0.4g
Agar	15g

2.2.5 Purification of PCR products

A QIAquick PCR purification kit (Qiagen) was used to clean the PCR products. Briefly, 250 µL PB buffer was added to 50 µL of PCR product and centrifuged for 30 seconds at 13,000 rpm in a collection tube and the flow through poured off. Next, 750 µL of PE buffer was added and the centrifugation step repeated. Next, the column was placed in a 1.5 mL centrifuge tube and 30 µL EB buffer added and the mixture was let to stand for 1 minute and then centrifuged again for one minute at 13,000 rpm.

2.2.6 RNA extraction

RNA was extracted using the Invitrogen TRIzol Plus RNA purification kit. Briefly, mid log phase *D. vulgaris* cells were harvested by centrifugation and 1 mL of TRIzol lysing reagent was added per 1 x 10^7 cells and the mixture incubated at room temperature for five minutes. After this, 200 µL of chloroform was added per 1 mL TRIzol reagent, and the tubes were handmixed for 15 minutes and then centrifuged for 15 minutes at 8500 rpm at 4°C. The upper phase was collected and an equal volume of 70% was ethanol added, and this mixture was transferred to a spin cartridge and the tube was centrifuged for 15 seconds at 8500 rpm. Next, 700 µL of Wash Buffer I was added and centrifuged as before; followed by the addition of 500 µL Wash Buffer II and another centrifugation step, after which the flow through was discarded. The samples were then washed with RNAse free water, and incubated at room temperature for one minute, and the tubes centrifuged for two minutes at 8500 rpm. RNA quality and quantity were assessed using the ratio of absorbances at 260 and 280 nm (A_{260}/A_{280}), denaturing agarose gel electrophoresis with ethidium bromide staining, and with a Qubit fluorometer (Invitrogen, Burlington, Ontario, Canada).

2.2.7 DNA extraction

Cultures were cooled on ice and then centrifuged for 30 minutes at 3000 rpm at 4°C. After, cells were resuspended in 500 µL NaCl-EDTA (0.1 M NaCl, 0.15 M EDTA, pH 8) and transferred to a microfuge tube and centrifuged for 2 minutes at 14,000 rpm and 4°C. This pellet was then re-suspended in 280 µL of NaCl-EDTA and placed on ice. Next, 20 µL of lysozyme (5 mg/mL) was added and incubated for at least 10 minutes in a 37°C water-bath. Then, 24 µL of 25% (w/v) SDS was added and the tubes incubated for at least 10 minutes in a 68°C water-bath and periodically inverted to mix. After incubation, 72 µL of 5 M $NaClO_4$ and 420 µL chloroform:isoamylalcohol (24:1 v/v) was added and mixed well. The tubes were then placed on a slowly rotating wheel to continually invert the phases for at least 1 hour, or overnight. Next, the tubes were centrifuged for four minutes at 10,000 rpm at 4°C and the supernatant placed in a clean tube and 2 volumes of 95% chilled ethanol was added, and the tubes inverted to precipitate the DNA. The tubes were then centrifuged for 15 minutes at 4°C and the supernatant carefully removed, with care not to disrupt the pellet. Next, 200 µL of TE (10 mM Tris base, 0.1 mM EDTA pH 8) was added to allow the DNA to dissolve; and 20 µL of DNAse free RNAse (1 mg/mL) was added and left to stand at room temperature for at least 30 minutes. Next, 80 µL of phenol was added and the tubes inverted several times over a 10 minute period and they were again centrifuged for three minutes at 14,000 rpm at room temperature. After centrifugation, 180 µL of the upper phase was placed in a clean tube and 2.5 volumes of DNA precipitation mix (90 mL of 95% ethanol and 10 mL of 2.5 M Na-acetate pH 5.5) was added, and the tubes left to stand either for 30 minutes at -70°C or overnight at -20°C. Next, the tubes were centrifuged for 15 minutes at 14,000 rpm at 4°C and the pellets carefully washed with 350 µL of 70% (v/v) ethanol. After, the ethanol was completely removed by blotting on a Kimwipe and the DNA

allowed to air dry with the tubes upright. Finally, the DNA was redissolved in 50 to 200 µL TE, depending on the size of the pellet, and the final concentration determined by spotting on an ethidium bromide plate.

2.2.8 Southern blot

Chromosomal DNA from *D. vulgaris* was first digested with appropriate restriction enzymes, and the total volume of digested product run on a 0.7% HGT agarose gel and imaged as described above. Following this, the gel was placed in 100 mL of denaturing salt solution (0.5 M NaOH and 1.5 M NaCl, pH 8) and gently shaken for 30 minutes, and then washed twice with dH_2O. After washing, the gel was again shaken for 30 minutes with 100 mL Tris solution (1 M Tris-HCl and 1.5 M NaCl). Next, a glass plate was covered with 3 MM membrane and 100 mL of 10-fold diluted SSC solution (3 M NaCl and 300 mM tri-sodium citrate, pH 7) was poured onto the paper and the bubbles removed. The gel was placed face up onto the 3 MM membrane and bubbles removed and a piece of Hy-Bond membrane placed on top of the gel, and covered with three layers of 3 MM paper and a stack of paper towels and a stack of glass plates. The purpose of this step was to transfer DNA from the gel to the membrane by flow via the paper towels.

UV binding: The Hy-Bond membrane was then washed in a small volume of 1xSSC solution, and then transferred to a clean sheet of 3 MM membrane and dried for 10 minutes at 37°C. The DNA was then covalently bound to the Hy-Bond filter by exposure to UV light for 5 minutes.

For probing: 5 µL of clean PCR product was mixed with 10 µL dH_2O and 5 µL λ DNA (7.5 µL of 100 ng λ DNA in 250 µL dH_2O). This mixture was boiled for three minutes and then placed on ice for three minutes, and 6 µL of primer extension mix (containing dGTP, dATP, dTTP and random hexanucleotides) and 2 µL Klenow polymerase (2U/µL) was added and the mixture

vortexed well and centrifuged. Next, 2 μL of [α^{32}P] dCTP was added and the mixture was let to stand for four hours. Meanwhile, the Hy-Bond filter was incubated at 68°C with shaking in 45 mL prehybridization fluid (30 mL 6x SSC, 5 mL 10% (w/v) SDS, 10 mL of 50x Denhardt's solution (5 g Ficoll 400, 5 g polyvinlypyrollidone and 5 g BSA in 100 mL dH_2O)). After four hours, the [α^{32}P] labelled mixture was again boiled for three minutes and iced for three minutes, and then added to the incubating Hy-Bond filter, and left shaking at 68°C overnight. Next, the filter was washed twice with 50 mL of 1xSSC and then incubated for one hour at 68°C with 100 mL of 1xSSC with 0.2% SDS. After one hour, the Hy-Bond filter was dried with 3 MM paper and wrapped with Saran Wrap, and contacted with a clean Bas-III imaging plate (Fuji) and let to stand for four hours. The exposed plates were imaged and analyzed using a Fuji BAS1000 Bioimaging Analyzer.

2.2.9 Microarrays

Probe selection and microarray manufacturing were carried out as described by (Caffrey et al., 2007, Caffrey et al., 2008). RNA and genomic DNA (gDNA) were purified from cultures as described above in sections 2.2.6 and 2.2.7.

Amino-modified cDNA was produced from 10 μg of total RNA using the Invitrogen SuperScript indirect cDNA labelling system and random hexamers. Amino-modified gDNA was produced using 1 μg of gDNA with the Invitrogen BioPrime Plus Array CGH genomic labelling system. The amino-modified cDNA was then coupled with Alexa fluor 647 and the amino-modified gDNA with Alexa fluor 555. The dried cDNA and gDNA probes were mixed and diluted to 40 μl by using a hybridization solution containing 50% (vol/vol) formamide, 5× SSC, 0.1% (wt/vol) SDS, and 0.1 mg of herring sperm DNA/mL. This solution then was incubated at 98°C for 5 min and then kept at 60°C. Sixteen μL of 3× SSC solution was added to the wells at the

ends of the microarray slides to maintain proper chamber humidity, and then the hybridization solution was applied to a Corning UltraGAPS microarray slide, which had been prewashed according to the manufacturer's specification (Corning, NY). These microarrays contained 70-mer oligonucleotide probes for 3,368 of the 3,394 protein-coding sequences of the *D. vulgaris* chromosome and were constructed as previously described (Chhabra et al., 2006). The slides were incubated for 17 h in Corning hybridization chambers, washed according to the manufacturer's specifications, and dried in a centrifuge. The hybridized slides were scanned on a PerkinElmer Scanarray 5000 scanner. Spot and background intensities were quantified using the Spotfinder software of The Institute for Genomic Research (TIGR) (Schweizer, 1992). The gDNA channel was used as the control for the immobilized probe concentration, spot uniformity, and labeling efficiency, as described by (Talaat et al., 2002) and Chhabra et al., 2006. Spots were flagged and rejected if they were saturated, of irregular size, missing from one channel, or had a poor signal-to-noise ratio (less than two times the median local background level). A complete microarray analysis used RNA extracted from two independent biological samples that were hybridized to a minimum of four arrays that had duplicate spots. Data below the threshold of a low-pass filter were rejected. The remaining microarray hybridization intensities were normalized using total intensity normalization and then averaged for the duplicate spots and the four arrays. Hybridization intensity ratios, *Ri*, were calculated from the normalized, averaged cDNA and gDNA hybridization intensities (designated <cDNA*i*> and <gDNAi>, respectively), as

$$Ri = \langle cDNAi \rangle / \langle gDNAi \rangle \qquad \textbf{(Equation 2-2)}$$

Differentially expressed genes were discovered with significance analysis of microarrays using the Stanford tools package (Tusher et al., 2001), which averaged the normalized intensities for

each gene, *i*, and calculated *Ri*. An expression ratio, $R_{C,i}$, for gene *i* for two different conditions, A and B, was calculated as $R_C,i = Ri_{,A}/Ri_{,B}$. Genes were determined to be differentially expressed if they had at least a twofold-changed R_C,i and a q value of less than 5%. The q value measures the percentage of false versus significant calls for the twofold expression change. Functional categories for global analysis were defined by COGs (clusters of orthologous genes) (Tatusov et al., 1997). The bootstrap-supported hierarchical clustering tree was created using TIGR's multiple experiment viewer from genes identified as significant by a one-way ANOVA with adjusted Bonferroni's correction at the 1% confidence level (Saeed et al., 2003). The clusters were created using Euclidean distances and average linkages.

2.2.10 Quantitative PCR (qPCR)

RNA was extracted as described above from *D. vulgaris* cells, and the product obtained with primers for 16S rRNA was used as a control. Reverse transcription of RNA was carried out to make the cDNA template for the qPCR, generated using the SYBR GreenER Two Step qRT-PCR kit from 1 µg of RNA. Briefly, the following were mixed and kept on ice: 10 µL of 2X RT Reaction Mix (2.5µM oligo $(dT)_{20}$, 2.5 ng/µL random hexamers, 10 mM $MgCl_2$ and dNTPs), 2 µL RT enzyme mix, RNA template and DEPC treated water up to 20 µL. The contents were incubated for 10 minutes at 25°C, then for 30 minutes at 50°C, followed by five minutes at 85°C. Following the incubations, 1 µL of *E. coli* RNAse H was added and the tubes incubated for 20 minutes at 37°C.

The qPCR reaction was as follows: 12.5 µL of SYBR Green, 10.5 µL DEPC treated water, 0.5 µL of each primer and 1 µL of template. The qPCR was carried out on a BioRad iCycler thermal cycler according to the manufacturer's directions. The data were normalized to the 16S rRNA control and used as a reference. Primers 350f and 351r were used for the *hcp1* gene; primers 352f

and 353r were used for the *hcp2* gene. These primers amplified 123 base pair and 142 base pair regions of the *hcp1* and *hcp2* genes, respectively.

2.3 Mutagenesis

2.3.1 Restriction digestion

The following were mixed together and incubated in a 37°C water bath for 2 hours: 4 µL PCR product, 1 µL of each restriction enzyme, 12 µL dH_2O, 3 µL OPA (one-phor-all) buffer
The reaction was stopped by adding 0.1 M EDTA (1 µL per 10 µL digest) and incubated for 20 minutes at 65°C.

2.3.2 CAP treatment of the digestion product

Calf alkaline phosphatase (CAP) was used to remove the 5' phosphate from vectors cut with restriction enzymes to prevent self-ligation of the vector. CAP in particular was used as it is easily removed by either protease digestion or heating in the presence of EDTA. The following were mixed together and incubated in a 37°C water bath for 2 hours: 45 µL of digestion product, 140 µL water, 10 µL OPA (CAP buffer), 4 µL CAP. Next, a phenol extraction was carried out using 75 µL phenol in 200 µL of CAP treated product and this mixture was vortexed for five minutes, and then centrifuged for two minutes at 13,000 rpm. Then 200 µL of the top layer was removed and 2.5 times the volume of DNA precipitate mix added, and let to stand at -70°C for 20 minutes. The samples were again centrifuged for 10 minutes at 13,000 rpm at 4°C and washed with cold 70 % ethanol. The product air dried upside down for 15 minutes and dissolved in 20 µL TE and the sample verified with gel electrophoresis.

2.3.3 Competent cells

E. coli TG2 cells were grown overnight and then 0.2 mL was subcultured into 5 mL TY media for 2 hours. The cultures were then poured into 15 mL Falcon tubes and set on ice and centrifuged for five minutes at 3000 rpm at 4 °C using the IEC. The supernatant was discarded and the pellet resuspended in 3 mL cold $CaCl_2$ and let stand on ice for 15 minutes, and again centrifuged for three minutes at 3000 rpm at 4 °C. The supernatant was again discarded and the pellet resuspended in 1 mL cold $CaCl_2$ and stored in the fridge or snap frozen using liquid nitrogen.

2.3.4 Ligation

First, 100 µL of ampicillin (Amp) was spread onto TY plates and allowed to dry, and the vector and insert were ligated with a Rapid Ligation Kit (Roche). Briefly, the following were mixed and allowed to stand for five minutes at room temperature: 2 µL vector, 3 µL insert, 2 µL solution #2 (ligation kit), 3 µL H_2O, 10 µL solution #1 (ligation kit), 1 µL T_4 ligase (solution #3 in the ligation kit). Then 200 µL of competent *E. coli* cells were added. This solution was placed on ice for 45 minutes, then in a 42 °C bath for 90 seconds. The ligation product was then plated on TY/Amp plates with 20 µL IPTG and 40 µL X-gal to allow for blue/white colony selection. The plates were incubated at 37 °C overnight. The white colonies from the plates were picked and transferred to 1 mL of TY media with 4 µL Amp and grown overnight at 37 °C. The same procedure was used to ligate in the *cat* genes, only the ligation product was plated on TY-Cm plates with no ampicillin, IPTG or X-gal. Colonies picked after ligation of *cat* were grown in 1 mL TY with 4 µL Cm.

2.3.5 Purification of plasmids from cultures

Extraction and purification of plasmids from cultures were performed using a QiaPrep Spin Miniprep Kit (Qiagen). Briefly, the pelleted bacterial cells were resuspended in 250 μL P1 buffer and transferred to a micro centrifuge tube. 250 μL P2 buffer was then added and the contents mixed by inverting the tube several times. Then, 350 μL of N3 buffer was added, the tube inverted and then centrifuged for 10 minutes at 13,000 rpm. The resulting supernatant was pipetted into a spin column and centrifuged for 30 seconds and the flow through discarded. The spin column was washed by first adding 500 μL PB buffer followed by 30 seconds of centrifugation at 13,000 rpm; and then 750 μL of EB buffer and another round of centrifugation. The flow through after each round of centrifugation was discarded, and the column was then centrifuged for an additional minute. The DNA was eluted by adding 50 μL EB buffer to the column, allowing it to stand for one minute, and then centrifugation for one minute.

2.4 Genomic island

2.4.1 Construction of mutants strains

The genomic island described in section 1.7 has the *hcp1* and *roo1* genes, while the copies of *hcp2* and *roo2* are elsewhere in the chromosome. Strains, plasmids and primers used are listed in Table 2-6. For construction of the *hcp*2 mutant, the 500 bp region upstream of *hcp2* was PCR amplified using primers p256f and p259r. The PCR product was digested with BamHI and HindIII and ligated into pNOT19 digested with these same enzymes to produce pNOT256/259. The 500 bp downstream region was amplified with p257f and p258r and digested with BamHI and KpnI and then ligated into similarly digested pNOT256/259 to give pNOTΔ*hcp2*. The *cat* gene was inserted into the BamHI site to give pNOTΔ*hcp2*Cm. Insertion of the 4.5 kb *mob*-

containing NotI fragment from pMob2 completed construction of pNOTΔ*hcp2*CmMOB. This plasmid was transformed into *E. coli* S17-1 and then transferred into *D. vulgaris* by conjugation. Single cross-over integrants were selected on PE plates with kanamycin and chloramphenicol. Selection for the *hcp2* gene replacement mutant in medium containing chloramphenicol and sucrose was done as previously described (Fu and Voordouw, 1997). The mutant obtained lacked the GEI and is therefore referred to as *D. vulgaris* Hcp2$^-$ GEI(Hcp1)$^-$ or *D. vulgaris* Hcp2$^-$ GEI(Roo1,Hcp1)$^-$. The *nrf* mutant generated earlier (Haveman et al., 2004) was found to be GEI$^+$. A GEI$^-$ strain, *D. vulgaris* Nrf$^-$ GEI$^-$, was generated by plating a culture on PE plates and testing the genotype of isolated colonies. An *nrf* strain lacking both *hcp* genes, *D. vulgaris* Nrf$^-$ Hcp2$^-$ GEI(Hcp1)$^-$, was generated by repeating replacement of the *nrf* gene (Haveman et al., 2004) in the *D. vulgaris* Hcp2$^-$ GEI(Hcp1)$^-$ strain using a kanamycin-resistance cassette and G418 as the selective marker (Caffrey et al., 2008).

2.4.2 PRC analysis and Southern blotting.

Primers p208 to p211 were used to confirm the presence or absence of *nrfA* with PCR and p208 and p210 were used as probes. Primers p350 and p351 were used to verify pNOTΔ*nrfA*KmMOB, (Figure 2.1A). Primers p286 to p289 were used for the construction of the *hcp1* mutant; p298-f and p299-r were used as probes for the *hcp1* region (Figure 2.1B). Primers p256 to p259 were used in the construction of the *hcp2* mutant, and p256 and p259 as probes to verify the mutant genotype by Southern blotting (Figure 2.1C). PCR with primer sets p318 through p339 were used to determine the approximate size of the *hcp1* deletion region, within 4.5 kb at the 5' end, and 11 kb at the 3' end. Primers p346 to p349 were used to verify the homologous recombination sites and to screen for plus and minus strains. The deletion of the 50 kb genomic island was also confirmed and plus/minus strains compared using Southern blot analysis with

PCR fragments obtained with p346-f and p349-r as probes. Chromosomal DNA from plus and minus strains was digested with EcoRI, PstI and SalI. Probes were labeled with [α-^{32}P] dCTP by the random hexamer procedure and probe hybridization was visualized and analyzed as described above.

2.4.3 Frequency of deletion of the genomic island

Wild type *D. vulgaris* cultures were grown in PC medium in an anaerobic hood (Forma Scientific, Inc.). After two days, 10^{-5} dilutions were plated on PE; and 25 colonies were picked at random and grown up in 1 mL PC. Once the picked colonies had grown, whole cell PCR was performed using p346/p349 as a positive control, and p348/p349 as a negative control (Figure 2.1B). Strains with (D20) and without (D1, D3) the island were isolated and stored in PB stocks. The isolated strains were named initially in reference to the numerical order of the 25 colonies picked. These will be referred to as GEI$^+$ and GEI$^-$ strains. Southern blots were used to further analyze the wild type, GEI$^+$ and GEI$^-$ strains, as explained above.

2.4.4 Genotypic stability

A mixture of 5% of D1 (GEI$^-$) and 1% wild type (predominantly GEI$^+$) *D. vulgaris* was inoculated into 50 mL of anaerobic WP-LS medium. The OD_{600} was monitored and at mid log phase (OD_{600} = 0.250), a 5% subculture was made. This was repeated for six transfers. After 100 hours genomic DNA was extracted and digested with SalI; and Southern blots created using the PCR product obtained with p346 and p349 as the probe.

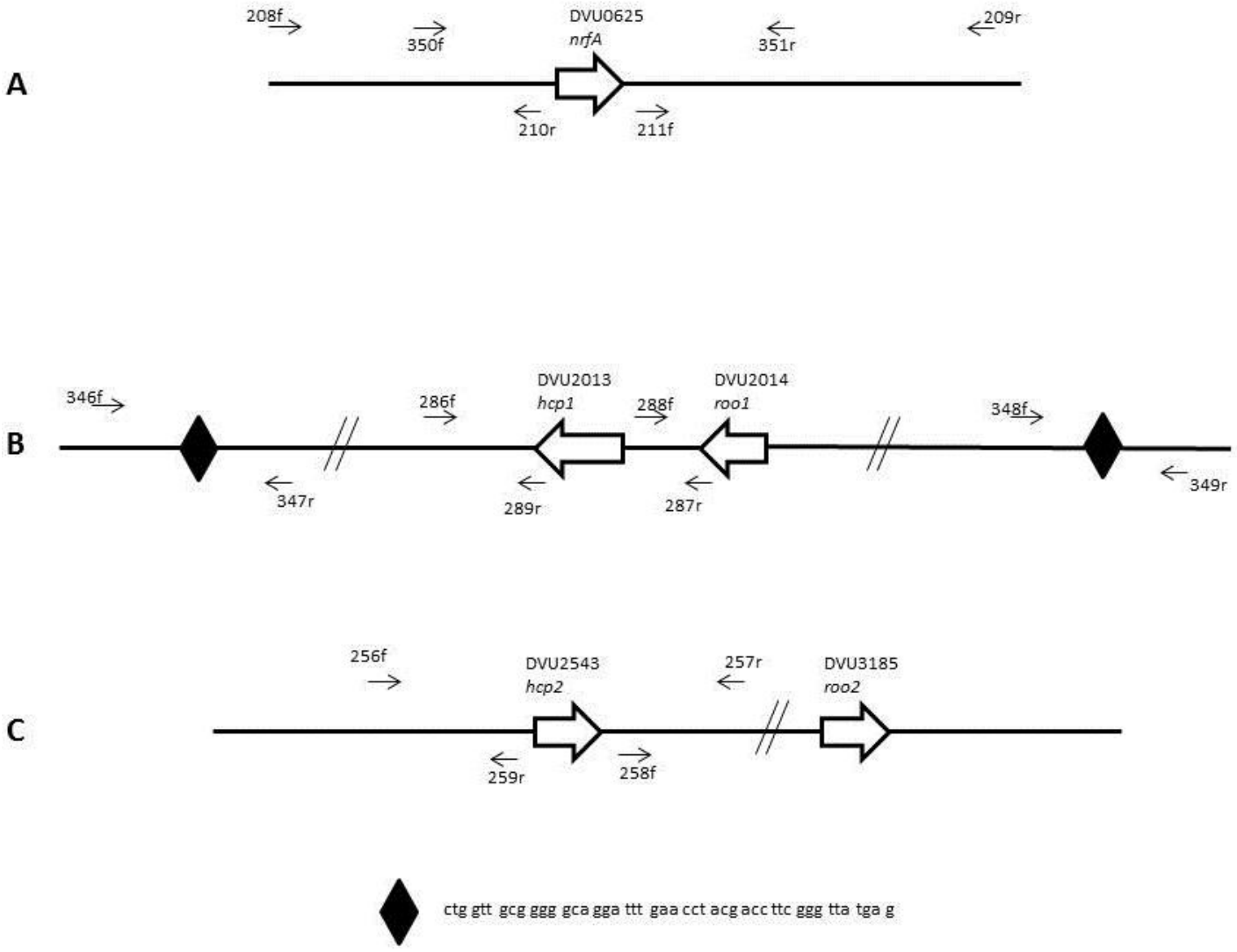

Figure 2.1 Primers used in the construction of the (A) *nrfA* mutant, (B) *hcp1* mutant and identifying the genomic island, and (C) *hcp2* mutant.

2.4.5 Sequencing

A known GEI minus strain was PCR amplified with gel purified primers p346/p349 and the bands verified with gel electrophoresis. The remaining PCR product was run on a 0.7% LGT agarose gel at 4ºC overnight. The resulting bands were visualized with UV light and excised; then melted down at 68ºC. Once melted, 1/3 of the total volume of TE saturated phenol was added and the sample vortexed and centrifuged for one minute. The top layer was removed and placed in a clean microfuge tube, and the phenol extraction was repeated three subsequent times until the top layer was clean. The product was dried with n-butanol, then 2.5 times the volume of 95% ethanol was added and the sample was placed at -70°C for 20 minutes, and then centrifuged for 15 minutes at 4°C. The resulting supernatant was drained and 500 µL of 70% ethanol was added and the sample centrifuged for an additional 5 minutes. The ethanol was poured off and the sample dried. Once dry, 20 µL of dH_2O was added. Approximately 4µL of product was run on a gel to verify that it was still present. The samples were taken to the University of Calgary DNA Sequencing Lab. The results were analyzed using GAP4 (Staden).

2.4.6 Native gel electrophoresis and hydrogenase activity staining

The GEI^+- and GEI^-- strains were grown on rich medium without added selenium and cell extracts prepared according to Valente et al., 2006. Native PAGE of crude extracts was performed on a 7.5% (wt/vol) polyacrylamide gel containing 0.1% Triton X-100 at 4 ^oC. The running buffer also contained 0.1% Triton X-100. The gel was placed in a solution of 50 mM Tris–HCl, pH 8, 0.5 mM methyl viologen and deaerated with argon, followed by incubation under a H_2 atmosphere. A 10 mM 2,3,5-triphenyltetrazolium chloride solution was used to visualize and fix the bands. This work was performed by the group of Dr. Ines A. C. Pereira at ITQB, Universidade Nova de Lisboa, Oeiras, Portugal.

2.4.7 Survival under microaerophilic conditions

Appropriate dilutions of the GEI$^+$- and GEI$^-$- strains were plated in duplicate (the air-exposed set and the anaerobic control set) on PE plates in the anaerobic hood. The sets were placed in separate 2 L steel jars. One of these was injected with 1% (vol/vol) air as detailed elsewhere (Wildschut et al., 2006). Following incubation for 5 days in the anaerobic hood at room temperature, the jars were opened and the plates placed in a 32°C incubator under anaerobic conditions for another 5 days. Colonies were then counted. The percentage of GEI$^-$-, relative to that of GEI$^+$-survivors (=100%) was calculated as done previously (Wildschut et al., 2006).

2.4.8 Analysis of motility and aerotaxis

For analysis of motility, 20 μL of a mid-log phase culture was placed at the center of a plate, containing PC and 0.3% (wt/vol) of agar. The spreading of the cells on the anaerobic soft agar plates was followed as a function of time by photographing the plate and determining the fraction of the total surface occupied by the cells. For analysis of aerotaxis, capillaries (20 μL) filled with 5 μL of PC and a headspace of air were sealed at the top and then transferred to the anaerobic hood in a sealed container. They were then inserted into a midlog-phase culture ($1x10^8$ cells/mL) of either the GEI$^+$- or the GEI$^-$-strain. At the indicated times the capillaries were briefly washed, the tops were broken off and their contents transferred to 1 mL of PC. The number of colony-forming units (CFU) was then determined by dilution plating. The aerobic capillaries containing PC were also inserted into an anaerobic mixture of GEI$^+$- and GEI$^-$-cells. The genotype of colonies obtained following plating was then analyzed by PCR.

Table 2-6 Bacterial strains, plasmids, vectors and primers used**.**

Strain, plasmid(s), primer or vector	***Genotype, phenotype, comment or sequence***
Strains	
D. vulgaris subsp. *vulgaris* strain Hildenborough	NCIMB 8303; isolated from clay soil near Hildenborough, United Kingdom
D. vulgaris HCP1/2	△*hcp1-hcp2*; Suc^r Cm^r
D. vulgaris NRF-HCP1/2	△ *nrfA-hcp1-hcp2*; Suc^r $Km^{r;}$
E. coli TG2	*supE, hsd*△*5, thi,* △ *(lac – proAB)F' [traD36, proAB*$^+$*, lacI*^{q}*, lacZ*△ *M15*] (Wahbi et al., 1996)
E. coli S17-1	*thi pro hsdR hsdM*$^+$ *recA* RP4-2 (Tc::Mu Km::Tn7) (D., 1990)
Plasmids and Vectors	
pUC19Cm	pUC19 containing the Cm gene
pNOT19	Cloning vector pUC19; NdeI site replaced with NotI site
pMOB2	Contains *oriT* of plasmid RP4 and *B. subtilus sacB* genes on a 4.5 kb NotI fragment; Km^r Cm^r pNOT△hcp2
pNOT△hcp2Cm, pNOT△hcp2CmMo pNOT△nrf-hcp2, pNOT△nrf-hcp2Km, pNOT△nrf-hcp2KmMob	
Primers	
p208-f	ccctctagaTGGCTGCTATGCTGCTCGC (690926 - 690948)
p209-r	cccgagctcCTGCCCTTCGACGGTG (693709 - 693726)
p210-f	cccggatccTTATTCATCGGCGACCTCTCT (691506 - 691525)
p211-r	cccggatccGCTCTTTCGCAAAGGTATG (693142 - 693162)
p256-f	tcgaaagcttCACACGTTGCGCAGCGTCGTA (2653299 - 2653319)
p257-r	tcgaggtaccCACCAGAACGTCAGCCCCCTT (2656129 - 2656149)
p258-f	tcgaggatccAGGCGACCCGACGAATGCAAG (2655581 -2655601)
p259-r	tcgaggatccTCCCTGGGCTGGATGTTGT (2653838 - 2653857)
p286-f	tcgaaagcttTGGATCATTGACGCCTAC (2092875 - 2092894)
p289-r	tcgaggatccATAATTACTGTTGCCGATCGC (2092324 - 2092344)
p288-f	tcgaggatccAAAGATTCGTTGAGGCTTCCA (2090610 - 2090630)
p287-r	tcgaggtaccCTCTTCTTCAAGTTCCTTGAG (2090062 - 2090082)
p346-f	GCAACGCTTATGCCTGTCACGCAA (2082197 - 2082217)
p347-r	CAATCCGGCACCTTCTTCTTTTGA (2082970 - 2082990)
p348-f	GCCTCCTCAAATAATGCTTTGTCG (2128698 - 2128721)

p349-r	GACCATATCGAAGCCGCGTTCGTA (2129678 - 2129701)
p350-f	GGCTCGGGCATGCGGATATGG (690884 - 690904)
p351-r	TCGGCCTTGACCGCGTCGAAC (693733 - 693726)
qPCR primers	
p350f	AACACCTATCTGGACCGTCTCTAC
p351r	TTTCTTGGCCTGTGCGATCA
p352f	CATGGATCGAACTGGCCATGGAAT
p353r	ACGAGGATGCACTTGCCCTT

2.5 Analytical methods

2.5.1 Aqueous sulfide

Aqueous sulfide concentration was determined using one of two colorimetric methods; copper sulfate or methylene blue. For the copper sulfate method, 50 µL of sample was combined with 950 µL of an acidic copper sulfate solution (5 mM $CuSO_4 \cdot 5H_2O$; 50 mM HCl) and immediately read at an optical density of 480 nm (Cordruwisch, 1985). For the methylene blue assay, 2 mL of zinc acetate solution (24 g $Zn(CH_3COO)_2$; 1 mL 20% (w/w) CH_3COOH, adjusted to 1 L dH_2O) was mixed with 30 µL of sample in a 25 mL tube. Next, 8.5 mL dH_2O and 2.5 mL of diamine reagent (600 mL dH_2O; 200 mL 12 N H_2SO_4; 2 g 4-amino-N,N-dimethylaniline, adjusted to 1 L with dH_2O), and 30 µL of iron-alum solution (10 g $NH_4Fe(SO_4)_2$ x 12 H_2O; 2 mL 12 N H_2SO_4, adjusted to 100 mL with dH_2O) were added and the tubes mixed. The tubes were left to stand for 7 to 10 minutes at room temperature, and then adjusted to 20 mL with dH_2O, and read at an optical density of 670 nm. When cultures became turbid due to sulfur and/or FeS precipitation, samples were placed in a microcentrifuge and filled with anaerobic gas, and then spun down for 30 seconds at 13,200 rpm. The supernatant was then used for the sulfide assay.

2.5.2 Nitrite

Nitrite concentrations were determined spectrophotometrically by mixing 50 µL of sample with 12 mL dH_2O and 250 µL of sulfanilamide/N-(1-napthyl)-ethylenediamine reagent and reading the optical density at 543 nm after 15 minutes of incubation at room temperature. Standards were made from a prepared 1M stock solution.

2.5.3 Nitrate

Nitrate was determined using high pressure liquid chromatography (HPLC) with a Waters 600E HPLC with a Gilson UV/VIS-151 UV detector set at 200 nm. All analysis and quantitation of

HPLC data was done using the Empower Pro Software (Waters). Standards were made from a prepared 1M stock solution.

2.5.4 Sulfate

Sulfate concentrations were determined either turbidometrically (Nemati et al., 2001) or by HPLC. For turbidometric analysis, 50 µL of sample was mixed with 950 µL conditioning reagent (50 mL glycerol, 75 mL concentrated HCl, 75 g NaCl, 100 mL 95% ethanol and 255 mL dH_2O) and excess ground $BaCl_2$. The mixture was vortexed and allowed to stand for 30 minutes and then read at an optical density of 420 nm. For HPLC analysis, a Waters IC-Pak A HC column (150 x 4.6 mm) with 24% acetonitrile, 2% butanol and 2% borate-gluconate concentrate as the eluent flowing at 2 ml min^{-1}, using a Waters 432 conductivity detector. Standards were made from a prepared 1 M stock solution.

2.5.5 Lactate and acetate

Using a Waters 515 HPLC, lactate and acetate concentrations were determined with an Alltech Prevail organic acid column (250 × 4.6 mm) with 25 mM KH_2PO_4 (pH 2.5) eluent flowing at 1 ml min^{-1} and a Waters 2487 UV detector set at 220 nm. Standards were made from a prepared 1M stock solution.

2.5.6 Elemental sulfur and polysulfide

2.5.6.1 Optical density

Initially, rates of polysulfide formation and reduction in the mutant strains were determined by monitoring the OD_{360} or OD_{410} (yellow colour) of the cultures as described by Klimmek, et al., (Klimmek et al., 1991). This method is purely qualitative, as no S or PS standards are available at a biologically relevant pH. Also, the yellow colour only represents the dissolved, polysulfide

(PS) component of S-PS; it does not represent the precipitated sulfur present. Hence, it should be made clear that this method does not measure sulfur.

2.5.6.2 Derivitization with methyl trifluromethanesulfonate

A more accurate method for quantifying polysulfides was then introduced. This method involved the chemical derivatization of polysulfides to methyl sulfides through a reaction with trifluromethanesulfonate (methyl triflate), and subsequent analysis using HPLC (Kamyshny et al., 2004):

$$S_n^{2-} + 2CF_3SO_3CH_3 \rightarrow (CH_3)_2S_n + 2CF_3SO_3^- \qquad \textbf{(Equation 2-3)}$$

The method described by (Kamyshny et al., 2004) for polysulfide quantification is able to resolve different polysulfide chain lengths, from S_2 to S_9. Dimethyldisulfide and dimethyltrisulfide were purchased commercially from Sigma and appropriate standards were made. Chain lengths Me_2S_4 to Me_2S_9 are not stable enough to be produced commercially, or synthesized off site and shipped. As such, these compounds were synthesized in house as described by (Rizkov et al., 2004). Preliminary polysulfide quantification data was obtained using this technique. Briefly, 100 µL of sample was mixed with 100 µL of methyl triflate and 900 µL of HPLC grade methanol. Immediately after mixing, 20 µL was manually injected into a C_{18} reverse phase column with a UV-Vis detector at 230 nm for 45 minutes at a flow rate of 0.5 mL min^{-1} with a 90% methanol eluent (Kamyshny et al., 2004). This technique proved to be very tedious for analysis as the polysulfides were separated by chain length, making it difficult to deduce the total concentration from the results.

2.5.6.3 Extraction with perchloroethylene or derivitization with triphenylphosphine

Subsequently, easier and more accurate methods of quantitating S and PS separately were developed. Elemental sulfur (S) was extracted by mixing 300 µL aqueous sample with 300 µL

perchloroethylene (PCE) and 50 µL of 10% (vol/vol) nitric acid. The mixture was placed on a rotating wheel for 15 minutes and then spun down for one minute at 13,200 rpm. 200 µL of the bottom PCE layer was then removed for analysis using a Waters 515 HPLC with a C_{18} reverse phase column (250 x 4.6 mm) and 95% methanol eluent flowing at 1 ml min^{-1} and a UV detector at 254 nm. To prepare standard solutions, S flour was first recrystallized in PCE to remove the insoluble fraction. The recrystallized S was then used to prepare standard solutions of 5 to 400 mg/mL in PCE, which were analyzed by HPLC.

The zero-valent sulfur (S^0) in S and in PS, i.e. excluding terminal sulfides, was determined by derivatization with triphenylphosphine (TPP) to produce triphenylphosphine sulfide (TPP-S). To derivatize, 100 µL of aqueous sample was mixed with 10 µL 6 N HCl and dried at 80^{o}C overnight. The dried sample was reconstituted with 100 µL deionized H_2O and 1 mL of a stock solution, containing 5 g TPP and 1 g triphenylphosphate (TPPO) per L of dimethylformamide. TPPO was added as an internal standard. Derivatized samples were stored and analyzed by either gas chromatography (GC) with a flame photometric detector and phosphorus filter (GC-PFPD) with a DB5 megabore column (0.53 mm x 30 m) or by GC-mass spectrometry (GC-MS). For GC-MS analysis, a 1-µL volume of the TPP-S extract was injected by an autoinjector (7683B series, Agilent Technologies, Santa Clara, CA) into a gas chromatograph (7890N series, Agilent) that was connected to a mass-selective detector (5975C inert XL MSD series, Agilent). The gas chromatograph was equipped with an HP-1 fused silica capillary column (length 50 m, inner diameter 0.32 mm, film thickness 0.52 µm; J&W Scientific) with helium as the carrier gas.

The areas of the TPP-S peaks obtained by either GC-PFPD or GC-MS were determined relative to that of TPPO to obtain the TPP-S concentration, which represents S^0 in both S and

polysulfide. The value for TPP-S is thus expected to be higher than that from S values obtained by PCE extraction and HPLC.

2.6 Oxygen addition

In order to add oxygen in the desired ratio of oxygen to sulfide (Ros), the volume of oxygen to be added to the headspace of a given serum bottle was calculated based on the sulfide concentration in the aqueous phase. For abiotic experiments these were determined following autoclaving and cooling. Using 41.2 mM as the concentration of gaseous oxygen at 23°C and 1 atm, the volume (V) of 100% (vol/vol) oxygen to add was calculated as:

$$V = (\text{mM } O_2 \text{ wanted in solution} \times 50 \text{ mL headspace})/41.2 \text{ mM} \qquad \textbf{(Equation 2-4)}$$

Pure oxygen (O_2) was then added to each bottle. The R_{OS} was the ratio of the added gas phase O_2 and the determined aqueous phase sulfide concentrations. The concentration of gas phase H_2S (approximately 12%) was ignored in this calculation.

2.7 Corrosion experiments and analysis

2.7.1 Coupons and preparation

Steel coupons (ASTM a366; 10 x 20 x 1 mm) were cleaned according to NACE protocol RP0775-2005. The coupons were polished with 400 grit sandpaper, placed into a dibutyl-thiourea HCl solution for two minutes, neutralized in a saturated bicarbonate solution for two minutes, rinsed with deionized water, then with acetone, and dried in a stream of air. Gloves and forceps were used to avoid leaving fingerprints on the coupons. The coupons were weighed thrice to 0.1 mg and the average weight was recorded as the starting weight. Coupons were placed in plastic holders (eppendorf tubes sliced into rings with a sterile razor blade) to prevent

them from contacting the glass walls or each other were placed in sterile 100 mL serum bottles. Sterile anaerobic WP-LS medium (50 ml) was added and the bottles were flushed with N_2-CO_2 and sealed with a butyl rubber stopper and crimped. Bottles were then amended and incubated for 30 days with shaking at 30^{o}C after which they were opened. During the 30 day incubation, the concentrations of aqueous sulfide, sulfate, lactate, S and TPP-S were monitored regularly. After 30 days, the bottles were opened and the corrosion coupons were cleaned and weighed, and the corrosion rates determined as per NACE protocol RP0775-2005.

2.7.2 Electrochemical corrosion monitoring methods

Linear polarization resistance (LPR) was used to assess corrosion rates as described by (Park et al., 2011a). Measurements were carried out using a Gamry Reference 600 potentiostat (Gamry, USA) and a test vessel equipped with three electrodes. An iron coupon (A366 carbon steel - 0.015% C) with an effective surface area of 6.7 cm^2 was used as the working electrode (WE). The WE potentials were measured relative to an Ag/AgCl reference electrode (RE-5B, BAS, USA). A platinum wire (5 cm; ø 0.05 cm) served as the counter electrode. Initial and final potentials for each scan were -0.02 V and 0.02 V relative to the open circuit potential. The scan rate was 0.125 mV/s. A nitrogen gas headspace was provided in the test vessel to maintain anaerobic conditions during the test. The corrosion rate was determined automatically from the measured polarization resistance (Rp) and corrosion current (I_{corr}). Double port serum bottles were used and the anaerobic LPR system was prepared in house. Electrical wires were soldered to the electrodes, and the junctions coated with epoxy and plastic shrink wrap. The wires were carefully inserted into blue rubber stoppers with three holes punched through. Two weight loss corrosion coupons were placed in the serum bottles, and then filled with 100 mL of WP-LS medium and the caps carefully fitted. LPR measurements were taken daily.

2.7.3 3D microscopy

Surface analysis was carried out using an Olympus STM6 3-axis measuring microscope at 200-fold magnification. At least 10 randomly selected pits were measured per coupon with the value for the deepest pit being reported as the maximum pit depth.

2.8 Analysis of sulfur morphology

Of two bottles of *D. vulgaris,* grown to mid log phase, one was autoclaved. Pure oxygen was added to each bottle to produce visibly equal amounts of sulfur precipitate (R_{OS} = 1.0 and R_{OS} = 1.5 for biotic and abiotic bottles, respectively). Oxygen (R_{OS} = 2.0) was also added to a bottle with high sulfide WP-LS medium. After incubating for 24 hours at 30^{o}C with shaking, a 1 mL sample was taken from each bottle and centrifuged at 13,200 rpm for 2 minutes. The supernatant was decanted and a portion of the suspended pellet was fixed to a slide. Non-concentrated samples were also fixed to slides. Elemental sulfur flour, dissolved in PCE and mixed with water to precipitate the sulfur was used as a control. Samples were examined and photographed with an Olympus BX51 microscope with a Retiga 2000R imager at 1000-fold magnification.

For partition tests 5 mL each of water and hexadecane were placed into three test tubes. A 1 mL sample of the biotic and abiotic incubations used for light microscopy was added to each tube. To the third tube, 1 mL of sulfur flour in water was added. For determining surface interactions and wettability, approximately 0.1 g of sulfur flour was added by syringe to uninoculated WP-LS medium and to a stationary phase culture of wild type *D. vulgaris.* The bottles were left to stand for several hours and observed periodically to see if sulfur remained on the surface, or if it sank to the bottom.

Chapter Three: Genomic Island of *Desulfovibrio vulgaris* sp. Hildenborough

3.1 Introduction

The discovery of the genomic island (GEI) was discussed in section 1.7. In this chapter, the specific phenotype and function of the GEI and its role in oxygen and nitrite stress are discussed.

3.2 Methods

All methods used in this chapter were described in Chapter 2. All primers, strains and vectors used are described in Table 2-6.

3.3 Results

3.3.1 Growth phenotypes of strains with and without the genomic island

The growth of GEI^+- and GEI^--strains in nutrient-rich PC (Table 2-4) is compared in Figure 3.1. Hydrogen from the gas atmosphere of the anaerobic hood was also available as an electron donor for sulfate reduction. Specific growth rate constants (μ) derived from the data in Figure 3.1 were $(0.141 \pm 0.007)\ h^{-1}$ and $(0.183 \pm 0.012)\ h^{-1}$ for the GEI^+- and the GEI^--strain, respectively. The wild type (data not shown) had $\mu = (0.142 \pm 0.007)\ h^{-1}$. Hence, the specific growth rate constants of the wild type and the GEI^+-strain were similar, in agreement with the fact that the wild type was mostly GEI^+ (Figure 1.5), whereas that of the GEI^--strain was 30% higher. No significant differences were observed in the stationary phase cell densities (OD_{600}), which were (0.62 ± 0.03), (0.65 ± 0.03) and (0.67 ± 0.05) for the wild type, the GEI^+-strain and the GEI^--strain, respectively.

Larger differences were seen in defined WP-LS medium (no yeast extract, lactate as the sole electron donor for sulfate reduction) with specific growth rate constants of (0.020 ± 0.002) h^{-1} and (0.058 ± 0.005) h^{-1} for the GEI^+-strain and the GEI^--strain, respectively (Figure 3.1). Hence, the specific growth rate constant of the GEI^--strain exceeded that of the GEI^+-strain by 3-fold in WP-LS medium. The stationary phase cell densities (OD_{600}) were (0.34 ± 0.05) and (0.42 ± 0.04) for the GEI^+-strain and the GEI^--strain, respectively.

3.3.2 Changes in global gene expression mediated by the genomic island

In order to determine the genetic basis for this different growth physiology, the gene expression profiles of the two strains grown in WP-LS were compared by microarray hybridization, with expression changes of more than 2-fold being considered significant. Relative to the GEI^+-strain, the GEI^--strain had increased expression of 36 genes and decreased expression of 62 genes. As shown in Table 3-1, genes up-regulated in the GEI^--strain included those for Fe-only hydrogenase (DVU1769-70), as well as several genes of the operon for the putative H_2:Hdr complex (DVU2399-2404). This complex has been proposed to act together with Fe-only hydrogenase and DVU2405 alcohol dehydrogenase in a bioenergetic cycle promoting anaerobic growth in defined lactate-sulfate medium (Haveman et al., 2003). Expression of DVU2405 alcohol dehydrogenase is among the highest of the entire genome and expression changes for this gene could not be determined by microarray hybridization due to signal saturation. The over-expression of Fe-only hydrogenase was confirmed by activity-stained native gels, which showed higher activities for Fe-only hydrogenase in the GEI^--strain, as compared to the GEI^+-strain (Figure 3.2).

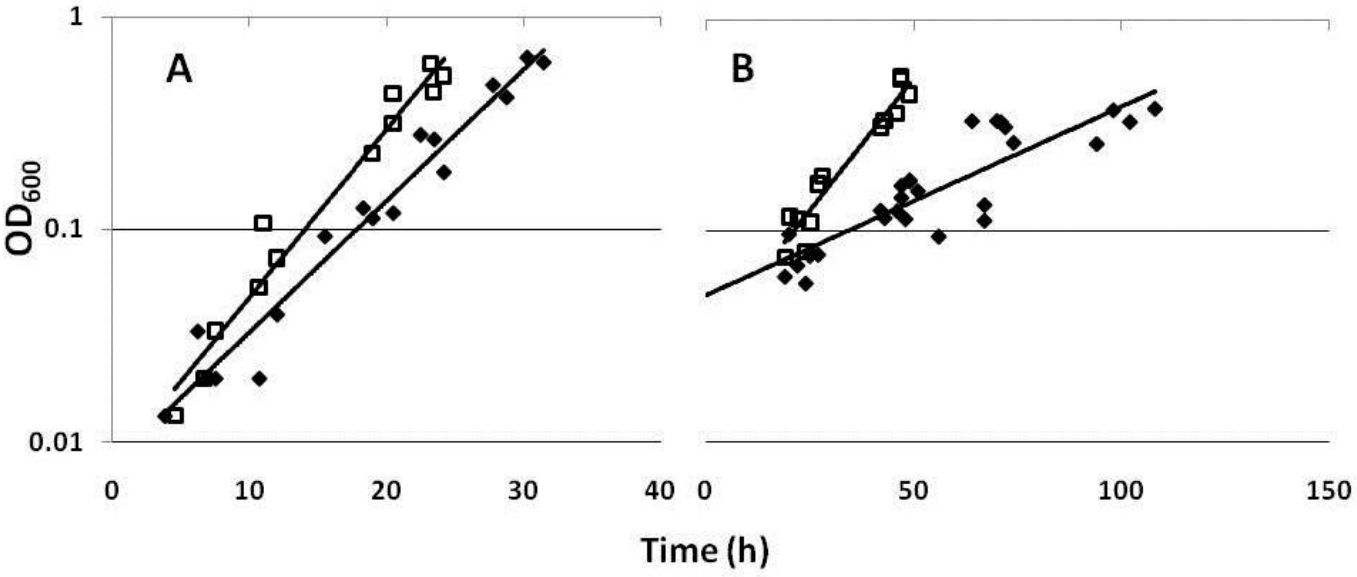

Figure 3.1 Growth rates of *D. vulgaris* GEI^{+}- and GEI^{-}-strains. Strains were grown in (A) rich medium C and (B) defined WP-LS. The cell density (OD_{600}, log scale), is plotted for the exponential growth phase of the GEI^{+}- (♦) and the GEI^{-}-strain (□). The data in (A) and (B) are for 3 and 5 independently conducted experiments, respectively.

Table 3-1 Top up- or downregulated genes in the GEI$^-$ strain relative to the GEI$^+$ strain of *D. vulgaris* Hildenborough grown in WP-LS medium.

Gene ID	Gene Name	^{2}Log^a		Gene ID	Gene Name	^{2}Log^a
DVU2401	"hydrogenase, iron-sulfur cluster-binding subunit, puta	3.59		DVU2667	"phosphate ABC transporter, periplasmic phosphat	-4.80
DVU2398	conserved hypothetical protein	3.22		DVU2752	rhodanese-like domain protein	-3.26
DVU2399	"hydrogenase, putative"	3.19		DVU2543	hybrid cluster protein-2 (Hcp2)	-3.25
DVU0948	conserved hypothetical protein	2.74		DVU1397	bacterioferritin	-2.88
DVU1769	"periplasmic [Fe] hydrogenase, large subunit"	2.62		DVU2325	mercuric transport protein periplasmic component	-2.80
DVU1147	"alginate o-acetyltransferase AlgI, putative"	2.56		DVU1704	conserved hypothetical protein	-2.78
DVU2449	S-adenosylmethionine synthetase	2.45		DVU0459	hypothetical protein	-2.73
DVU0949	conserved domain protein	2.33		DVU0305	ferredoxin II	-2.73
DVU2562	"acyl carrier protein, putative"	2.23		DVU2751	hypothetical protein	-2.70
DVU2290	"hydrogenase, CooU subunit, putative"	2.23		DVU2441	"heat shock protein, Hsp20 family"	-2.68
DVU2894	sigma-54 dependent transcriptional regulator	2.22		DVU0571	alanine dehydrogenase	-2.62
DVU2448	pantoate--beta-alanine ligase	1.90		DVU2442	"heat shock protein, Hsp20 family"	-2.57
DVU0764	DNA-binding protein HU	1.88		DVU1670	conserved hypothetical protein	-2.55
DVU2231	GTP-binding protein TypA	1.87		DVU0881	"translation elongation factor G, putative"	-2.50
DVU2567	conserved hypothetical protein	1.86		DVU2839	conserved hypothetical protein	-2.43
DVU0836	tRNA (guanine-N1)-methyltransferase	1.85		DVU2428	"lipoprotein, putative"	-2.43
DVU1317	ribosomal protein S8	1.81		DVU2988	phage shock protein A	-2.42
DVU3219	hypothetical protein	1.79		DVU1534	"membrane protein, putative"	-2.30
DVU3033	iron-sulfur cluster-binding protein	1.79		DVU1396	conserved hypothetical protein	-2.26
DVU0466	"anthranilate synthase, glutamine amidotransferase co	1.78		DVU1434	hypothetical protein	-2.26
DVU1299	ribosomal protein S7	1.77		DVU0773	hypothetical protein	-2.19
DVU0210	"tail sheath protein, putative"	1.77		DVU2753	C_GCAxxG_C_C family protein	-2.19
DVU1382	HesB family selenoprotein	1.73		DVU2574	"ferrous ion transport protein, putative"	-2.05
DVU1208	fatty acid/phospholipid synthesis protein PlsX	1.72		DVU0620	"endoribonuclease, L-PSP family"	-2.03
DVU1029	histidinol-phosphate aminotransferase	1.71		DVU1820	"preprotein translocase, YajC subunit"	-2.01
DVU2063	conserved hypothetical protein	1.70		DVU3217	hypothetical protein	-2.00
DVU2122	type II/IV secretion system protein	1.68		DVU2515	HD domain protein	-2.00
DVU2563	"beta-ketoacyl synthase, putative"	1.66		DVU2544	iron-sulfur cluster-binding protein	-1.99
DVU1770	"periplasmic [Fe] hydrogenase, small subunit"	1.65		DVU0024	conserved hypothetical protein	-1.98
DVU2413	radical SAM domain protein	1.63		DVU0883	"glutaredoxin, putative"	-1.95
DVU1329	"DNA-directed RNA polymerase, alpha subunit"	1.61		DVU0878	"dnaK suppressor protein, putative"	-1.93
DVU3310	"ATP-dependent RNA helicase, DEAD/DEAH family"	1.59		DVU1669	ribosomal large subunit pseudouridine synthase B	-1.92
DVU0467	anthranilate phosphoribosyltransferase	1.59		DVU0486	hypothetical protein	-1.91
DVU3094	rubrerythrin	1.57		DVU1283	UTP-glucose-1-phosphate uridylyltransferase	-1.90
DVU1308	ribosomal protein L22	1.52		DVU0302	"chemotaxis protein CheX, putative"	-1.88
DVU0262	hypothetical protein	1.49		DVU1109	ATPase domain protein	-1.87

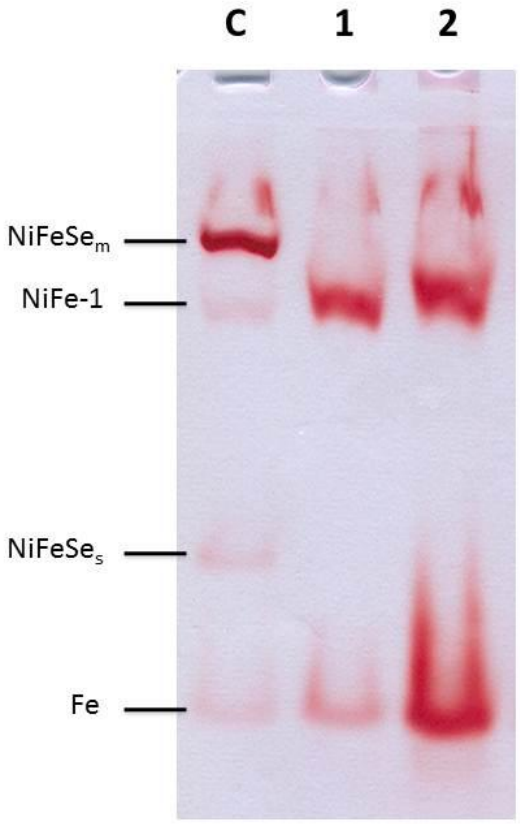

Figure 3.2 Native gel of *D. vulgaris* strains stained for hydrogenase activity. Lane C (control) contained *D. vulgaris* hydrogenases from top to bottom: membrane-bound NiFeSe-hydrogenase, NiFe-hydrogenase-1, solubilized NiFeSe-hydrogenase, and Fe-only hydrogenase. Lanes 1 and 2 are periplasmic extracts (89 μg of protein) from GEI$^+$- and GEI$^-$-strains, respectively. The cells were grown in the absence of added selenium to prevent overexpression of the NiFeSe-hydrogenase (Valente *et al*., 2006).

3.3.3 Phenotypic characterization under stress conditions

3.3.3.1 Oxygen

Since the presence of the GEI appears to compromise anaerobic growth on lactate- and sulfate-containing media, why is it maintained in wild-type *D. vulgaris* cells? The presence of genes for a rubredoxin:oxygen oxidoreductase homolog (DVU2014 Roo1) and for a hybrid cluster protein homolog (DVU2013 Hcp1) suggests that the GEI promotes survival under conditions of oxygen or nitrite stress. *D. vulgaris* has homologs for these genes, DVU2543 *hcp2* and DVU3185 *roo*2, elsewhere in the genome. Interestingly, the *hcp*2 gene is also significantly up-regulated in the GEI^+-strain (Table 3-1) and, consequently the *hcp*-genes are either absent (*hcp1*) or down-regulated (*hcp2*) in the GEI^--strain. Up-regulation of the Hsp20-family heat shock protein in the GEI^+ strain (Table 3-1: DVU2441-2442) also suggests that the GEI promotes survival under conditions of environmental stress.

The function of Roo2 was recently investigated by mutagenesis (Wildschut et al., 2006). Single cells of a *roo*2-mutant strain, plated on an agar surface and incubated in 1% (vol/vol) of air for 5 days showed 4% (i.e. 25-fold decreased) survival as compared to the wild type. As mutant construction involves the picking of single colonies and because 3% of GEI^--cells are present in the wild-type strain used, constructed mutants can also be GEI^-. PCR analysis of the entire mutant library of the Voordouw lab indicated that 9 of 31 constructed mutants are GEI^--strains. The constructed *roo*2-mutant strain is one of these and, therefore, this strain is a *roo1*-, *roo*2-double mutant. Relative to the GEI^+-strain (containing both the *roo1* and the *roo2* gene), the GEI^--strain (containing only the *roo2* gene), had a decreased microaerophilic survival of 27±10% (average of 3 experiments). This suggests that both Roo1 and Roo2 contribute to microaerophilic survival by about 4- and 6-fold, respectively.

3.3.3.1.1 Motility

Microaerophilic oxygen stresses vary spatially in habitats where *D. vulgaris* resides and the question thus arises whether GEI^+- and GEI^--cells occupy different niches in the resulting gradients. Motility of the two strains, as judged by spreading in soft agar (0.3% wt/vol) plates of anaerobic medium C, was similar (Figure 3.3a). In experiments with individual strains, the GEI^+-strain appeared to enter aerobic capillaries with up to 4-fold increased frequency as compared to the GEI^-- strain (Figure 3.3b). Less significant differences were observed in experiments with mixtures of the two strains. In these experiments medium C-containing, aerobic capillaries were inserted into an anaerobic mixture of GEI^+- and GEI^--cells. The genotype of colonies obtained following plating was then analyzed by PCR. Capillaries dipped into a mixture of 20% GEI^+-cells (N=126) had 10% of GEI^+-cells (N=31) at 5 min, and 33% of GEI^+-cells (N=36) at 15 min. Hence, no clear enrichment of GEI^+-cells in the aerobic capillary was observed in this experiment. Overall we conclude that the presence or absence of the GEI does not appear to strongly alter chemotaxis towards air.

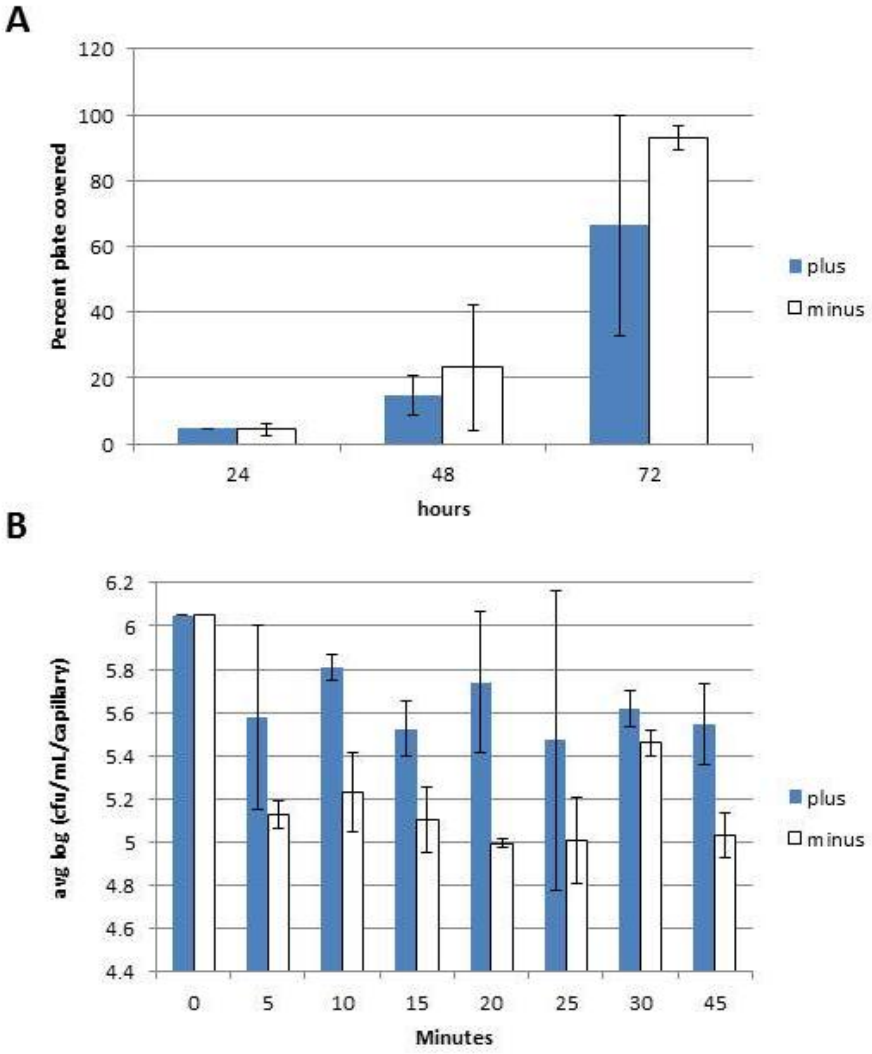

Figure 3.3 Motility of GEI^{+}- and GEI^{-}-strains. (A) Swimming in anaerobic soft agar plates. The fraction of the total surface occupied by the swimming cells was recorded as a function of time as the average of duplicate experiments. (B) Entry of strains in aerobic capillaries. Capillaries, containing medium C and a headspace of air were sealed at the top, transferred to the anaerobic hood and inserted into a midlog-phase culture of either the GEI^{+}- or the GEI^{-}-strain. The number of colony-forming units (CFUs) present in the capillaries was determined by dilution plating at the indicated times. The data at time zero reflect the CFU/ml of the midlog-phase culture. The data are averages of triplicate experiments; error bars represent the standard deviation.

3.3.3.2 Nitrite and polysulfide

The function of Hcps, which are present in a diverse range of bacteria, remains enigmatic. In pathogens Hcps contribute to survival in stressful environments including in macrophages (Flatley et al., 2005). A common feature of *hcp*-genes in pathogenic and environmental bacteria appears to be that they are up-regulated under conditions of nitrite stress. Transcription of the *hcp1* and *hcp*2 genes of *D. vulgaris* is also up-regulated in the presence of nitrite, the latter of the order of 100-fold (Haveman et al., 2004, Haveman et al., 2005, He et al., 2006). Nitrite is a strong, specific inhibitor of dissimilatory sulfite reductase, the enzyme that reduces sulfite to sulfide in all SRB (Haveman et al., 2004). Nitrite stress is rapidly alleviated in *D. vulgaris* by nitrite reductase (DVU0624-625 Nrf), which uses electrons derived from the oxidation of lactate for the reduction of nitrite to ammonia. It was reasoned that the function of Hcps was best evaluated in an *nrf*-mutant background, as nitrite persists for prolonged periods under these conditions (Haveman et al., 2004), whereas millimolar concentrations are removed within 24 h by Nrf^+-strains (Figure 3.4).

Chemical reaction of nitrite with sulfide, produced by *D. vulgaris*, gives rise to polysulfide, colouring the medium yellow, with nitrite being reduced to ammonia, i.e.:

$2HS^- \rightarrow HS\text{-}S^- + H^+ + 2e$ **(Equation 3-1)**

$HS\text{-}S^- + HS^- \rightarrow HS\text{-}S\text{-}S^- + H^+ + 2e$ **(Equation 3-2)**

$HS\text{-}S\text{-}S^- + HS^- \rightarrow HS\text{-}S\text{-}S\text{-}S^- + H^+ + 2e$ (etc.) **(Equation 3-3)**

is coupled to:

$NO_2^- + 8H^+ + 6e \rightarrow NH_4^+ + 2H_2O$ **(Equation 3-4)**

For an overall reaction:

$4HS^- + NO_2^- + 5H^+ \rightarrow HS\text{-}S\text{-}S\text{-}S^- + NH_4^+ + 2H_2O$ **(Equation 3-5)**

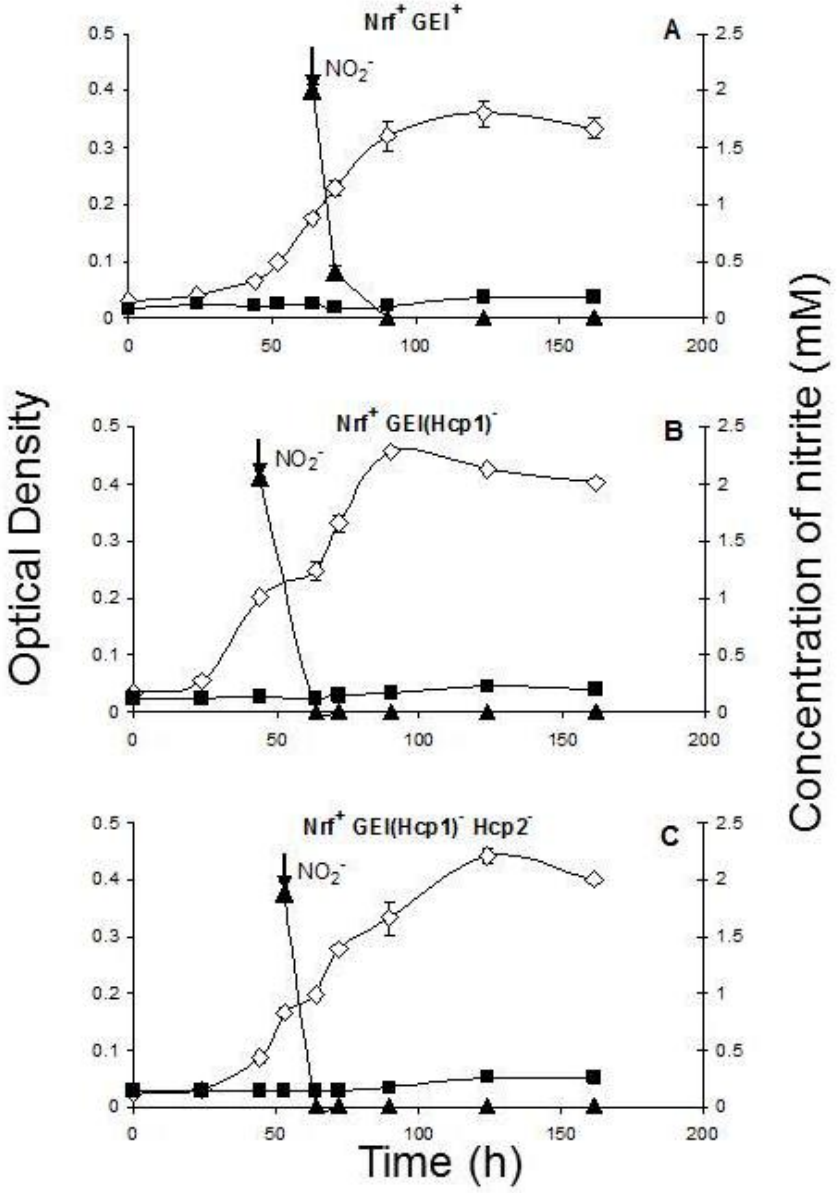

Figure 3.4 Nitrite removal by Nrf^+-strains of *D. vulgaris*. Nitrite (2 mM) was added (↓) in mid-log phase (sulfide concentration of 8-10 mM, lactate concentration of 20-25 mM) to cells growing in WP-LS. Time courses are shown for the concentration of NO_2^- (▲, scale on the right), for the cell density (◊, OD_{600}, scale on the left) and for the polysulfide concentration (■, OD_{410}, scale on the left). No significant polysulfide formation is observed in the Nrf^+-strains. The data shown are averages of duplicate experiments. Error bars represent standard deviation.

Although not indicated in the overall reaction (Equation 3-5), polysulfides with different chain lengths n are formed. When n>8 precipitation (↓) of elemental sulfur (S_8) ensues:

$HS\text{-}(S)_7\text{-}S^- \rightarrow S_8\downarrow + HS^-$ **(Equation 3-6)**

The nitrite-dependent formation of polysulfide can be monitored by determining the OD_{410} as a function of time. No sulfur precipitate was observed under these conditions (i.e. n<8), allowing the cell density to be monitored as OD_{600} (Figure 3.5). Cell growth stopped immediately following the addition of nitrite (Fig. 3.5). Increasing amounts of polysulfide were formed by the Nrf^--mutant (OD_{410}=0.10), the Nrf^-, $GEI(Hcp1)^-$ mutant (OD_{410}=0.20), and the Nrf^-, $GEI(Hcp1)^-$, $Hcp2^-$ mutant (OD_{410}=0.45). The latter formed polysulfide with the same kinetics and to the same extent as the abiotic control (Figure 3.5). In contrast, no polysulfide was formed in cultures of Nrf^+-strains due to the rapid removal of nitrite (Figure 3.54, OD_{410}<0.05). Polysulfide formed by reaction of nitrite and sulfide is inhibitory to SRB (Kaster et al., 2007). Hence, the *D. vulgaris* Hcps may contribute to an electron transport chain in which polysulfide is converted back to sulfide (i.e. redox half reactions 3-1 to 3-3 with the arrows pointed in the reverse direction) with the electrons possibly being provided by lactate oxidation. The resulting lower polysulfide concentrations may diminish polysulfide inhibition. In order to test this further, polysulfide and sulfur were generated by adding 2 mM tetrathionate ($S_4O_6^{2-}$) to a mid-log phase culture of *D. vulgaris*, containing an excess of 8-10 mM sulfide (Klimmek et al., 1991):

$n\ S_4O_6^{2-} + (n+1)\ HS^- \rightarrow 2n\ S_2O_3^{2-} + HS_{n+1}^- + nH^+$ **(Equation 3-7)**

In addition to sulfur/polysulfide (HS_{n+1}^-) this reaction leads to formation of thiosulfate ($S_2O_3^{2-}$) which is a known electron acceptor for SRB and is not inhibitory to either strain (results not

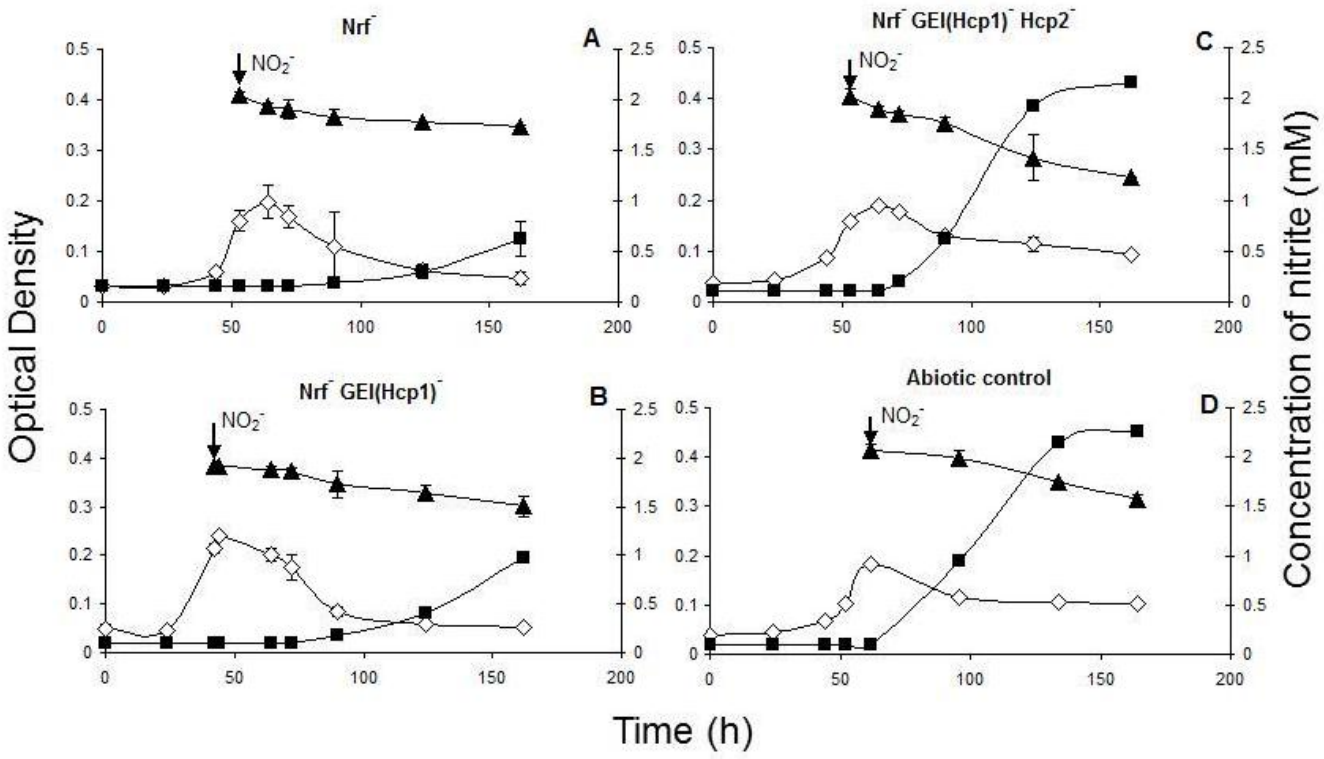

Figure 3.5 Effect of addition of 2 mM nitrite on Nrf$^-$-strains of *D. vulgaris*. Nitrite was added (↓) in mid-log phase (sulfide concentration of 8-10 mM, lactate concentration of 20-25 mM) to cells growing in WP-LS. Time courses are shown for the concentration of NO_2- (▲, scale on the right), for the cell density (◊, OD_{600} , scale on the left) and for the polysulfide concentration (■, OD_{410}, scale on the left). Genotypes of the strains used were (A) Nrf$^-$, GEI(Hcp1)$^+$, Hcp2$^+$; (B) Nrf$^-$, GEI(Hcp1)$^-$, Hcp2$^+$; (C) Nrf$^-$, GEI(Hcp1)$^-$, Hcp2$^-$. (D) represents an abiotic control in which 2 mM nitrite was added to a wild-type culture autoclaved in mid-log phase. The data shown are averages of duplicate experiments. Error bars represent standard deviation.

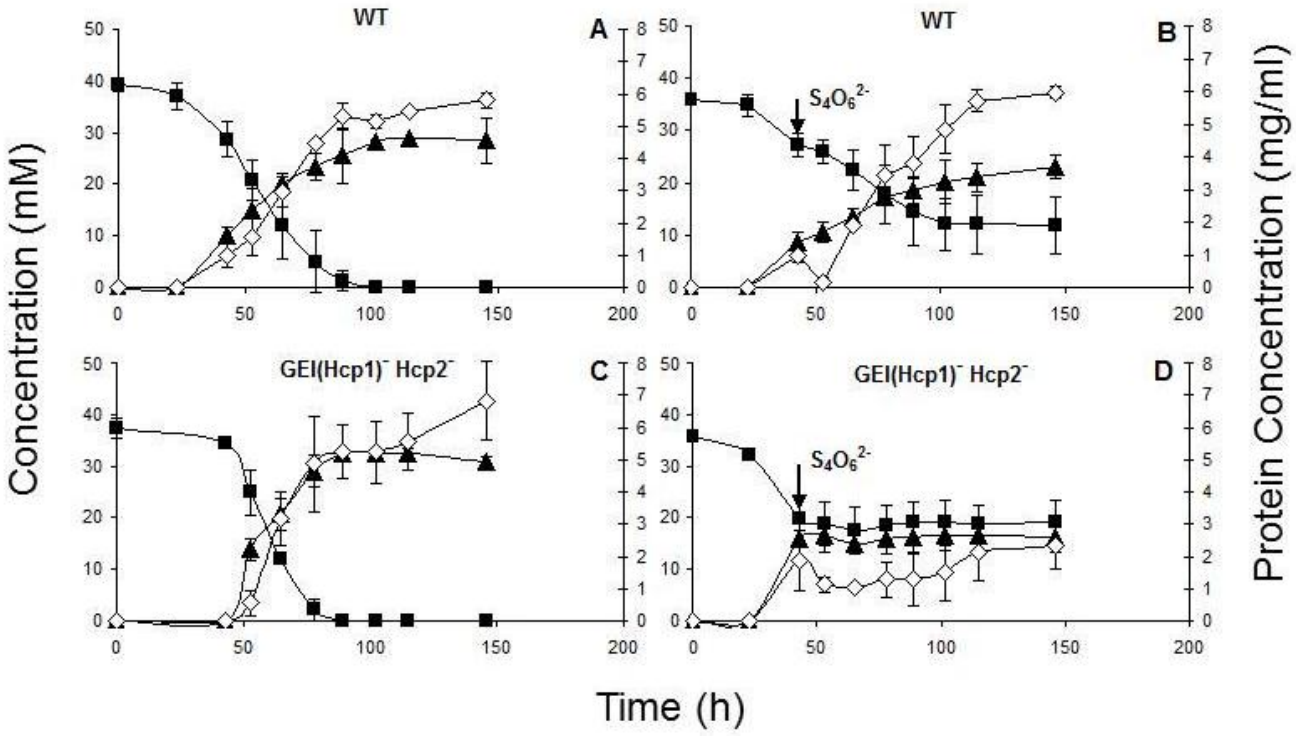

Figure 3.6 Effect of tetrathionate addition on *D. vulgaris* cultures. Cultures for (A, B) the wild type and (C, D) the GEI(Hcp1)$^-$, Hcp2$^-$ mutant strain in WP-LS were compared without (A, C) and with (B, D) 2 mM of added tetrathionate (↓). Time courses are shown for the concentrations of protein (◊, right hand scale), of lactate (■, left hand scale) and of acetate (▲). The results show strong inhibition of the mutant strain by the sulfur/polysulfide formed upon reaction of tetrathionate with the 8-10 mM of sulfide present in the medium. The data shown are averages of duplicate experiments. Error bars represent standard deviation.

shown). Because substantial sulfur precipitation was observed immediately following tetrathionate addition, protein concentrations were measured as a proxy for cell density. In addition, the concentrations of lactate and acetate were measured to monitor metabolic activity. Only marginal inhibition of both growth and metabolic activity were observed when tetrathionate was added to mid-log phase cultures of the wild-type strain (Figure 3.6), whereas the GEI(Hcp1)$^-$, Hcp2$^-$-strain was strongly inhibited (Figure 3.6). Because thiosulfate is not inhibitory, the observed inhibition is thus caused by S and PS. This inhibition can be largely (but not completely) prevented by the presence of Hcps or another gene product from the GEI. Corrosion rates of the individual mutant strains are discussed in more detail in Chapter 6.

3.4 Discussion

Genomic islands are mobile genetic elements that contribute to genome evolution through horizontal gene transfer (Dobrindt et al., 2004). Although discovered initially in pathogenic bacteria as elements that contribute to increased virulence, inspection of genome sequences has indicated that GEIs are also widespread in non-pathogenic, environmental bacteria. GEIs can be functional phages, which often but not always, insert in the genome at tRNA genes. In the case of *D. vulgaris* Hildenborough several GEIs representing functional phages have been discovered by comparing its genome with that of the closely related *D. vulgaris* strain DP4 (Walker et al., 2006). Because the sequence of the DP4 genome is now available (NCBI locus tag NC_008751), a more detailed comparison can be made. It appears that the two genomes are contiguous, i.e. have the same gene order and high sequence identity, over the entire length of the core genome (the fraction of the genome that does not include the GEIs). Genomic islands appear to be integrated always at tRNA genes and constitute the main source of intergenome variability.

Hence, the DP4 genome has GEI insertions at tRNA loci that are lacking in the Hildenborough genome and vice versa. The GEI discovered in the course of this study is not present in the corresponding region of the DP4 genome (DVUL1175-tRNAMet-DVUL1174, with DVUL1175 and DVUL1174 being homologous with DVU2052 and DVU1999 respectively). However, a homologous GEI is present in the DP4 genome inserted at the $tRNA^{Met}$ gene located between DVUL2617 and DVUL2563. This GEI consists of 53 genes (DVUL2616 to DVUL2564) of which many are conserved with the Hildenborough GEI, including those for the site-specific recombinase. However, the DP4 island does not include genes for Hcp1 and Roo1, but instead has genes functioning in carbohydrate capsule biosynthesis and export. Hence the origin of the current Hildenborough GEI is not clear. However, its lower GC content of 54.2%, as compared with 63% for the core genome, also indicates that it was acquired by horizontal transfer.

The Hildenborough GEI, inserted at the $tRNA^{Met}$ gene adjacent to DVU1999 (Table 1-3), was not included in the list of bacteriophage regions (R1-R6), presented by Walker and colleagues (Walker et al., 2006). Indeed, this GEI lacks typical phage genes. Yet, it can actively excise itself as we have shown here. The excision gives rise to a mixed population of GEI^+ and GEI^- cells that each have desirable properties. The GEI^+ cells are better equipped to survive microaerobic air exposure through the *roo1* gene product, whereas improved survival of nitrite stress may be mediated through the *hcp1* gene. In contrast, the GEI^- cells have superior anaerobic growth, especially under conditions in which lactate is the sole electron donor for sulfate reduction as in WP-LS medium. Previous proteomics and genomics studies of a *hyd* mutant of *D.vulgaris* Hildenborough, lacking genes for Fe-only hydrogenase (DVU1769-70), indicated that expression of the gene for DVU2405 alcohol dehydrogenase and of neighbouring genes for a putative H_2:Hdr complex (DVU2399-2404) were severely down-regulated (Haveman et al., 2003). These

results indicated that Fe-only hydrogenase, DVU2405 alcohol dehydrogenase and the H_2:Hdr complex participate in a bioenergetic cycle or pathway that promotes growth on lactate-sulfate medium (as in WP-LS). The increased expression of the components of this cycle or pathway in the GEI$^-$-strain likely explains its improved growth in WP-LS medium.

Hence in a laboratory culture in which the cells are kept under strictly anaerobic conditions with plenty of lactate and sulfate, the GEI$^+$-cells will be outcompeted. However, in a natural population, living in a soil or sediment gradient, the organism may have to tolerate small concentrations of oxygen or nitrite to access optimal concentrations of these energy substrates. These conditions would clearly favor the GEI$^+$-strain. Hence, the GEI$^+$- and GEI$^-$-populations, resulting from excision of the GEI, may inhabit distinct regions of soil and sediment gradients that occur in nature. We have not been able to prove this with chemotactic experiments (Figure 3.3). However, a recent study by Yurkiw et al. (Yurkiw et al., 2012) has shown that ability to colonize microaerobic environments and microaerobic survival are related. Also we do not know how a strain that has lost the GEI can re-acquire it, i.e. the mechanism of horizontal transfer is unknown.

We have shown evidence here that the physiological function of the *D. vulgaris* Hcps is in preventing inhibition by S and PS, which can form when SRB-produced sulfide reacts chemically or microbiologically with a high potential electron acceptor (oxygen, nitrate, nitrite, tetrathionate). For instance, exposure of cultures of *D. vulgaris* Hildenborough in tubes filled with soft agar to an air headspace causes formation of a band of sulfur globules (Fu and Voordouw, 1997). Although we have not yet determined the extent to which this inhibition prevention can be credited to Hcp1 or Hcp2, we speculate that the GEI(Hcp1)$^+$-strain is better equipped to counter inhibition presented by partially oxidized sulfur compounds, that may occur

in the upper regions of soil and sediment gradients. In conclusion, it appears that we have discovered an interesting GEI in *D. vulgaris* Hildenborough, which like the pathogenicity islands, extends the range of environments which the organism can occupy. However, the ability of accessing this extended environmental range comes at a cost to the organism of being a poorer anaerobe. This important subtlety may indicate that the quest for an SRB that does well in both aerobic and anaerobic environments is bound to fail.

Chapter Four: Gene expression under conditions of S and PS formation

4.1 Introduction

While sulfide is known to be toxic to all living organisms, even SRB (Caffrey and Voordouw, 2010), S and PS alone are not. This is demonstrated by the wide variety of sulfur cycle bacteria that are able to obtain energy by oxidizing or reducing S and/or PS. For example, the anaerobic *Desulfuromonas acetoxidans* directly reduces S and/or PS to sulfide, coupled with the oxidation of acetate to CO_2 (Finster et al., 1994). Numerous other bacteria oxidize sulfide to sulfate, via an S intermediate, which may be sequestered and stored for later use. Common examples are species of *Beggiatoa*, *Thioploca*, *Thiobacillus* and *Sulfurimonas* (Sorokin et al., 2007, Ghosh and Dam, 2009, Beller et al., 2006, Hogslund et al., 2009, Sievert et al., 2008).

However, it was shown in Chapter 3 that PS is inhibitory to *D. vulgaris*, (Johnston et al., 2009, Haveman et al., 2005), and that the Hcp's function to help overcome this inhibition. This poses an interesting problem: if SRB reside at the oxic-anoxic interface (Pereira et al., 2008), these are conditions where S and PS are likely to be present. Why, then, and how, do they inhibit SRB? This question is investigated here by microarray experiments, as little work has been done on the effects of S and PS on SRB at the genomic level.

4.1.1 Tetrathionate and S/PS

As mentioned, S and PS can form through chemical reaction of sulfide with either nitrite and/or oxygen. Additionally, as seen in Table 1-2, S and PS can also be formed through chemical reaction of sulfide with tetrathionate. Tetrathionate on its own is not inhibitory to *D. vulgaris*, however it can react with sulfide to form inhibitory S and PS (Chapter 3). Numerous species do utilize tetrathionate as an electron acceptor, and recently a newly isolated species of

Methylophaga thiooxidans was found to be able to oxidize dimethylsulfide back to tetrathionate via a thiosulfate intermediate (Park et al., 2011b, Shiers et al., 2011, Boden et al., 2010). The effects of tetrathionate on gene expression in SRB have not been studied. Some data are available for other bacteria such as *Salmonella* sp. and *Acidothiobacillus* sp. (Kanao et al., 2007, Hensel et al., 1999). Tetrathionate was used here in microarray experiments to produce S and PS in *D. vulgaris* cultures without the additional effects of nitrite interfering in gene expression.

4.2 Methods

Methods used were described in Chapter 2. Cultures were grown on lactate-sulfate WP-LS media and S and PS production was induced using nitrite or tetrathionate. All strains used were GEI^{+}. For qPCR, primers of less than 200 base pairs were designed for *hcp1* and *hcp2* (p350f and p351r; p352f and p353r, respectively Table 2-6). Changes greater than 2 fold (log2 scale) were considered significant.

As gene expression studies with *D. vulgaris* and nitrite have been done previously (Haveman et al., 2004), qPCR was performed to verify the effects of nitrite on *hcp1* and *hcp2* and to further elucidate their function. Wild type *D. vulgaris* was exposed to 2 mM nitrite or tetrathionate for 30 minutes before RNA extraction and subsequent qPCR or microarrays.

4.3 Results

4.3.1 Nitrite addition

It was found that *hcp2* was strongly upregulated with nitrite (128 fold), while *hcp1* was slightly downregulated (2 fold) compared to 16S rRNA controls as seen in Figure 4.1. This data confirms

previous macroarray data in which *hcp2* was upregulated in the presence of nitrite (Haveman et al., 2004) and in co-cultures with NR-SOB where nitrite formed (Haveman et al., 2005).

4.3.2 Tetrathionate addition

From the qPCR results, it was found that *hcp2* was slightly upregulated (2 fold), while *hcp1* was downregulated 3 fold (Figure 4.1).

Based on the microarray results, *hcp2* was upregulated approximately 2 fold and *hcp1* downregulated approximately 2 fold, consistent with the qPCR results (Figure 4.1). The expression level of *nrf* did not change significantly.

The top up- and downregulated genes are listed in Table 4-1. General stress response genes such as heat shock proteins (e.g. DVU2643), flagellar synthesis (e.g. DVU2893), drug resistance proteins (e.g. DVU0576), along with genes encoding enzymes involved in synthesis of sulfur-containing amino acids and proteins (e.g. DVU3371) were upregulated 21, 20, 28 and 24-fold, respectively (Table 4-1). The most upregulated gene was *msrB* (DVU0576), which was upregulated 55 fold.

Genes encoding ATP synthases (e.g. DVU0920) and ribosomal synthesis genes (e.g. DVU1669) were downregulated by 9 and 6 fold, and were the majority of categories of downregulated genes (Table 4-1).

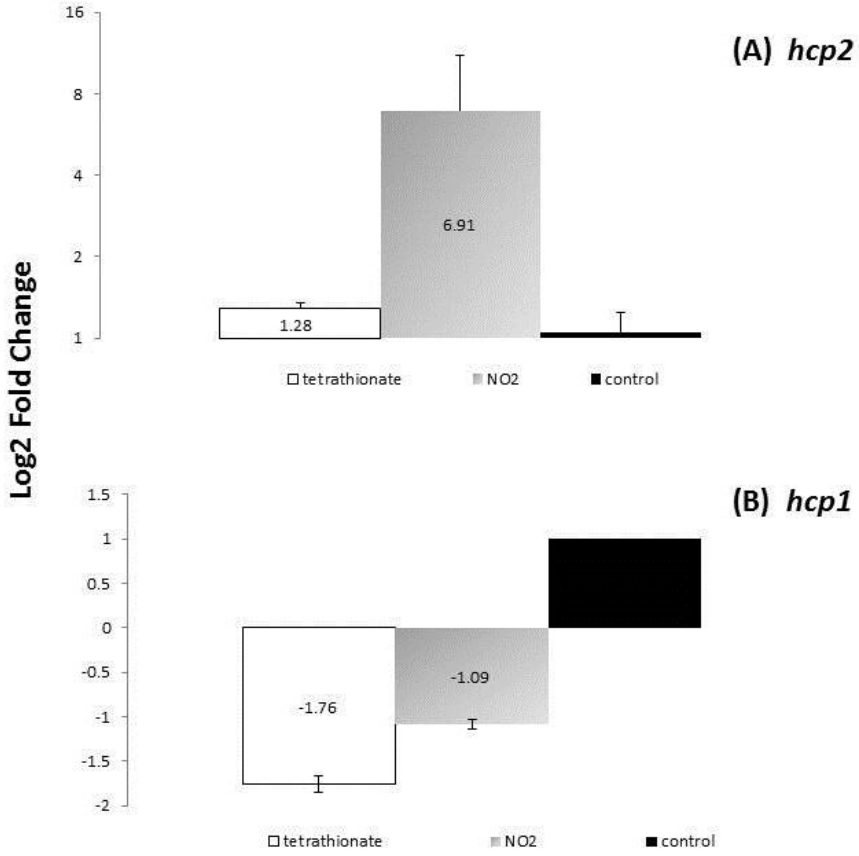

Figure 4.1 Results of qPCR comparing expression levels of the *hcp* genes in cells exposed to either 2 mM tetrathionate (white) or nitrite (grey) to untreated control cells (black). (A) *hcp2* expression levels (B) *hcp1* expression levels. Data shown are normalised to the untreated control (+1 fold change).

Table 4-1 Top up and down regulated genes in wild type *D. vulgaris* with 2mM tetrathionate.

Gene ID	***Gene Name***	***log2***
DVU0576	peptide methionine sulfoxide reductase MsrB	5.78
DVU3136	nitroreductase family protein	5.65
DVU0525	"transcriptional regulator, MarR family"	5.45
DVU2978	"hydrolase, haloacid dehalogenase-like family"	5.36
DVU0298	hypothetical protein	5.11
DVU3135	flavodoxin-like fold domain protein	5.07
DVU2324	copper-translocating P-type ATPase	4.99
DVU2103	iron-sulfur cluster-binding/ATPase domain protein	4.95
DVU0759	"peptidase, M29 family"	4.94
DVU2282	hypothetical protein	4.88
DVU0526	"drug resistance transporter, putative"	4.79
DVU1645	"transcriptional regulator, ArsR family"	4.67
DVU2310	metallo-beta-lactamase family protein	4.66
DVU3371	5-methyltetrahydropteroyltriglutamate-homocysteine S-methyltransferase	4.61
DVU2109	MTH1175-like domain family protein	4.52
DVU1212	fxsA protein	4.52
DVU0865	"membrane-associated zinc metalloprotease, putative"	4.48
DVU0150	"membrane protein, putative"	4.42
DVU0865	"membrane-associated zinc metalloprotease, putative"	4.42
DVU2643	heat shock protein HtpG	4.41
DVU3171	cytochrome c3	4.39
DVU2893	"flagellar basal-body rod protein, putative"	4.38
DVU0149	"membrane protein, putative"	4.28
DVU2754	quinone oxidoreductase	4.28
DVU1170	hypothetical protein	4.24
DVU2573	hypothetical protein	4.19
DVU2494	"peptidase, M48 family"	4.17
DVU1213	rhomboid family protein	4.15
DVU1430	"peptidase, M16 family"	4.13
DVU1193	DNA repair protein RadC	3.95
DVU0147	"lipoprotein, putative"	3.93
DVU2572	"ferrous iron transport protein A, putative"	3.91
DVU1984	peptide methionine sulfoxide reductase MsrA	3.88
DVU2497	"lipoprotein, putative"	3.83
DVU0819	"FMN reductase, NADPH-dependent"	3.76
DVU2548	acyl carrier protein phosphodiesterase	3.72

DVU2817	multidrug resistance protein	3.71
DVU2422	nitroreductase family protein	3.67
DVU3062	sensor histidine kinase/response regulator	3.64
DVU1457	"thioredoxin reductase, putative"	3.62

Gene ID	*Gene Name*	*log2*
DVU2839	conserved hypothetical protein	-3.31
DVU0242	SEC-C motif domain protein	-3.29
DVU0920	ATP synthase protein I	-3.23
DVU0694_0697	"molybdopterin oxidoreductase, molybdopterin-binding subunit, putative"	-3.20
DVU0434	"Ech hydrogenase, subunit EchA, putative"	-2.86
DVU0919	hypothetical protein	-2.84
DVU1425	"glycine cleavage system P protein, subunit 1"	-2.65
DVU1423	"dihydrolipoamide dehydrogenase, glycine cleavage system"	-2.65
DVU0671	conserved hypothetical protein	-2.61
DVU1657	hypothetical protein	-2.59
DVU1669	ribosomal large subunit pseudouridine synthase B	-2.57
DVU2226	"acetyl-CoA carboxylase, biotin carboxylase, putative"	-2.55
DVU2227	hypothetical protein	-2.54
DVU2838	conserved hypothetical protein	-2.53
DVU2947	"anaerobic ribonucleoside-triphosphate reductase, putative"	-2.47
DVU1934	"phosphonate ABC transporter, permease protein"	-2.46
DVU2220	conserved hypothetical protein	-2.34
DVU2328	"hydrogenase nickel insertion protein HypA, putative"	-2.33
DVU2892	conserved hypothetical protein	-2.29
DVU2402	"heterodisulfide reductase, A subunit"	-2.27
DVU1289	"reductase, iron-sulfur binding subunit, putative"	-2.26
DVU1935	"phosphonate ABC transporter, permease protein"	-2.26
DVU1426	glycine cleavage system H protein	-2.25
DVU1260	"outer membrane protein P1, putative"	-2.23
DVU1051	cytochrome c-type biogenesis protein CcmE	-2.23
DVU0300	radical SAM domain protein	-2.23
DVU0918	"ATP synthase F0, A subunit"	-2.22
DVU0848	"heterodisulfide reductase, putative"	-2.21
DVU1089	alanyl-tRNA synthetase	-2.19
DVU1655	"aminotransferase, classes I and II"	-2.18
DVU1882	HDIG domain protein	-2.18
DVU1424	"glycine cleavage system P protein, subunit 2"	-2.15
DVU1842	"lipoprotein, putative"	-2.15

DVU1090	recA protein	-2.15
DVU0753	"amino acid ABC transporter, ATP-binding protein"	-2.13
DVU2531	ribulose-phosphate 3-epimerase	-2.12
DVU2891	nickel responsive regulator	-2.11
DVU0778	"ATP synthase, F1 delta subunit"	-2.07
DVU1075	ribonuclease P protein component	-2.06
DVU0281	"exopolysaccharide biosynthesis protein, putative"	-2.05
DVU1064	"aconitate hydratase, putative"	-2.02

4.4 Discussion

4.4.1 S and PS inhibition

It is clear that S and PS are inhibitory to SRB (Haveman et al., 2005, Johnston et al., 2009). Microarray analysis conducted here indicated that several genes involved in sulfur-amino acid synthesis were strongly upregulated when tetrathionate was added to MLP cells causing S and PS formation, along with general stress response genes, while protein and ATP synthesis were downregulated.

The most highly upregulated gene was *msrB* (DVU0576), which catalyzes the reduction of the R epimer of methionine sulfoxide back to methionine. Methionine sulfoxide arises from the reaction of methionine with oxygen or reactive oxygen species. Therefore, all Eukarya and Bacteria, along with some Archaea possess *msrB* to protect against oxidative damage (Zhang and Weissbach, 2008). *msrB* has also been shown to be upregulated during heat shock, peroxide and low pH stress, and when *D. vulgaris* is grown using thiosulfate as an electron acceptor instead of sulfate (VIMSS). In addition, cytochrome c_3 and several oxidoreductases which are involved in oxygen reduction pathways in various species of *D. vulgaris* and *D. desulfuricans* G20 (Brioukhanov et al., 2010) were also significantly upregulated during exposure to tetrathionate (Table 4-1). These results would suggest that *D. vulgaris* increased assimilation of the excess sulfur, possibly to replace proteins with oxidized cysteine or methionine, while eliciting a general oxidative stress response.

A recent study noted that similar changes in gene expression were seen in *D. vulgaris* during both H_2O_2 stress and exposure to an increased redox potential (Zhou et al., 2010, Wildschut et al., 2012). This included an increase in expression of ROS detoxification and DNA and protein repair genes, and a decrease in expression of genes related to protein synthesis and central

metabolic pathways (Zhou et al., 2010, Brioukhanov et al., 2010). *msrB* and some cytochromes are also upregulated during both oxidative stress and in the presence of tetrathionate (Table 4-1). This is interesting, as it suggests that tetrathionate and subsequent S and PS formation may be causing an oxidative stress to *D. vulgaris*. This concept is supported if we look at a Pourbaix diagram for sulfur and water (Figure 4.2), which is a plot of potential against pH and the sulfur species stable at each potential and pH. SRB typically grow at neutral pH and at a low potential (approximately -0.8V vs SHE). From Figure 4.2 it can be seen that in this range, H_2S and HS^- are the predominant sulfur species. However, we can see that elemental sulfur is only stable in a very narrow window, from pH -2 to 0, and a potential of about 0.4. This redox potential is too high for SRB, supporting the idea that sulfur poses an oxidative stress to *D. vulgaris*. Based on the similarities in gene expression observed with both oxidative stress and tetrathionate, it is likely that the inhibition caused by S and PS is due to an increase in redox potential to values too high for anaerobic growth and subsequent oxidative stress response.

4.4.2 Function of Hcp's

The hybrid cluster proteins have been identified in a wide range of Bacteria, Archaea and Eukarya. They are unusual as they contain two different types of Fe-S clusters; one present as either a [2Fe-2S] or [4Fe-4S] cluster, and the other being a 'hybrid' cluster of [4Fe-2S-3O] (Aragao et al., 2008). Studies with pathogens suggest that Hcps contribute to survival in stressful environments such as macrophages (Flatley et al., 2005), and they have also been suggested to function in hydroxylamine reduction and oxygen defense in *E. coli* (Wolfe et al., 2002).

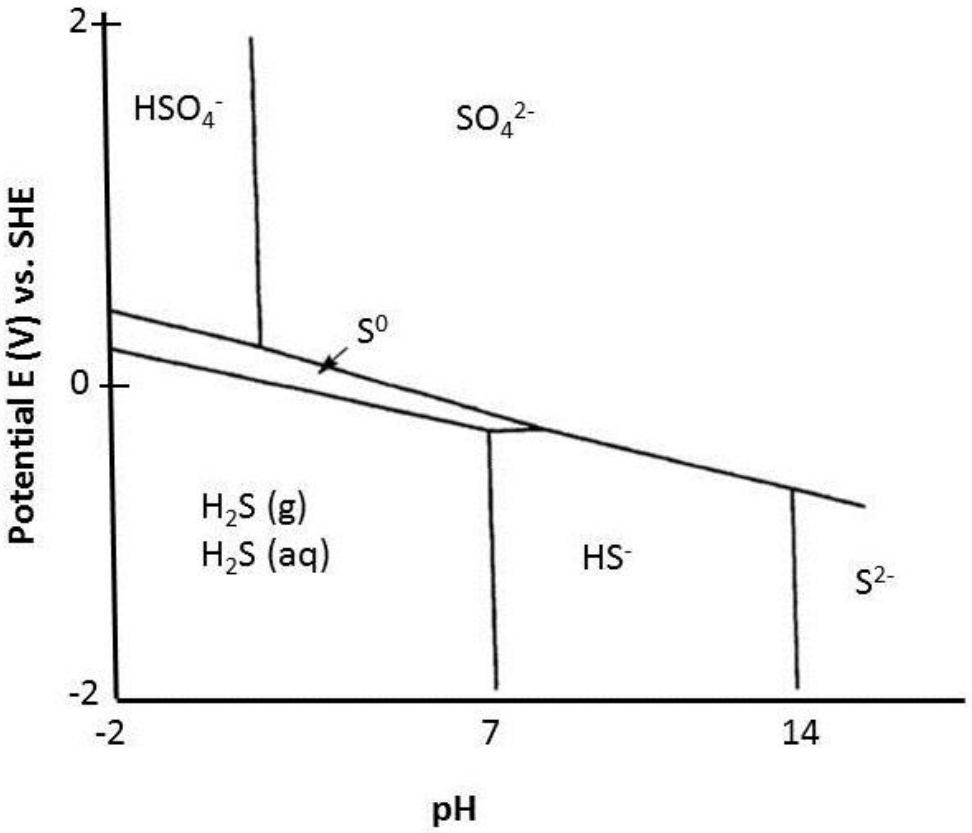

Figure 4.2 Pourbaix diagram showing the most thermodynamically stable species of sulfur in water at varying pH and potential. It can be seen that at pH > 7, HS^- is the most stable from of sulfur. It can also be seen that elemental sulfur is present at pH 7 between about -100 and 100 mV, which is too oxidized to support anaerobic growth. Adapted from Jones, 1996.

Among the multiple interpretations of the function of the Hcp's, there is a general consensus that they are upregulated during nitrite exposure.

It has been previously shown and again verified here that nitrite strongly upregulates *hcp2* (VIMSS, Haveman et al., 2004). This indicated that nitrite presents a stress that induces *hcp2*, but the function of *hcp2* is not to directly cope with nitrite.

Gene expression studies with *D. vulgaris* when exposed to oxygen and oxidative stress have been carried out previously (Mukhopadhyay et al., 2007, Zhou et al., 2010, Pereira et al., 2008, Wildschut et al., 2006). Whole genome microarray studies carried out at VIMSS showed that neither *hcp1* nor *hcp2* were significantly affected by oxygen, although *hcp2* was slightly downregulated (-2.5 fold) after exposure to 500 ppm oxygen for 240 minutes (VIMSS).
The qPCR and microarray data were in agreement for *hcp1* and *hcp2*, showing that *hcp1* was downregulated about 2 fold, and *hcp2* was upregulated about 2 fold.
The gene expression and previous experimental data from Chapter 3 further suggest that *hcp2* is the dominant player in S and PS reduction, and that nitrite may be an 'early warning' of impending S and PS formation for *hcp2*. Thus it is upregulated only with nitrite, not when S and PS are formed by addition of tetrathionate or oxygen. This suggests that *D. vulgaris* typically encounters S and PS formed by reaction with nitrite, not oxygen in the natural environment. Overall, the gene expression data shown here and experimental evidence from Chapter 3 suggest that *hcp2* is the dominant gene for dealing with S and PS formed specifically through reaction of nitrite with sulfide.

A recent study by Yurkiw and colleagues (Yurkiw et al., 2012) has shown that the Hcp-like proteins found in *D. vulgaris* and other organisms have multiple roles in both oxygen and nitrite mediated oxidative stresses, as observed in previous investigations into the function of

Hcp's (Gardner et al., 2002, Overeijnder et al., 2009). Studies with a variety of mutants of *hcp, nrf* and GEI^+ or GEI^- strains of *D. vulgaris* indicated that *hcp1,* which is located on the GEI, is constitutively expressed and functions during nitrite stress when lactate is present as an electron donor. On the other hand, *hcp2* alleviated nitrite stress when hydrogen was present as an electron donor. This work demonstrated that both copies of *hcp* aid in the maintenance of high nitrite reduction rates by *nrf*; thus maintaining the integrity of electron transport chains from lactate or hydrogen to *nrf*. This, in turn resulted in less polysulfide forming through chemical reaction of sulfide and nitrite, allowing *D. vulgaris* to survive in environments with frequent nitrite and S and PS stresses (Yurkiw et al., 2012).

Chapter Five: Sulfur and Polysulfide Metabolism by *D. vulgaris* sp. Hildenborough

5.1 Introduction

In the previous chapters, the effects of S and PS on *D. vulgaris* were investigated by adding nitrite and tetrathionate to wild type and mutant strains. The function of the discovered GEI was investigated, and evidence was shown for the role of the Hcp's, especially Hcp2, in S and PS metabolism and detoxification. The genetic basis for S and PS inhibition was also investigated. However, the effects of S and PS formed through reaction of sulfide with oxygen had not been researched, nor the capacity of *D. vulgaris* to metabolize S and PS.

Here, the effects of S and PS formed via reaction with sulfide and oxygen and their metabolism by *D. vulgaris* are investigated in greater detail. The aim was to verify the inhibitory effects of S and PS, and how these compounds form through reaction of sulfide with oxygen, and see what tolerance *D. vulgaris* has to these compounds. Polysulfide is specifically investigated here.

5.2 Methods

All methods used are described in Chapter 2. *D. vulgaris* was grown on lactate-sulfate containing WP-LS medium at pH 8 and exposed to different oxygen: sulfide ratios (Ros) at both stationary and mid log phase (MLP) to generate S and PS. Cultures were also grown to MLP and then autoclaved and cooled before oxygen addition as abiotic controls. This ensured that biogenic sulfide was present in each condition. Also note that in this study any *hcp1* mutants are by default GEI^- strains.

It should be noted that polysulfide concentrations are represented as the OD_{410} or OD_{360} value, not as a concentration in mM, as these were determined before the HPLC and GC-MS methods

were established. Some polysulfide data was obtained using the methyltriflate derivization method (2.5.6). Sulfur was not analyzed as the analysis techniques were still being developed at that time. Oxygen concentrations were calculated and added as described in Equation 2-4. Iron corrosion coupons were added to the last set of abiotic incubations, and the data will be discussed in the following chapter.

5.3 Results

5.3.1 Growth at pH 8

Cultures were grown at pH 8, as polysulfides are more stable at slightly basic pH, where sulfide (including HS^-) is the stable form of sulfur (Figure 4.2; (Jones, 1996)). Previously, PS formation was examined at neutral pH, where HS^- is the prevalent form of sulfur at low redox potentials. As a result, the PS that was formed was transient, even in abiotic studies. *D. vulgaris* showed no adverse effects to these growth conditions (data not shown).

5.3.2 Biotic incubation with oxygen

5.3.2.1 Stationary phase

To investigate S and PS formation from sulfide and oxygen, stationary phase cultures of *D. vulgaris* containing 18 mM sulfide were exposed to varying amounts of pure oxygen, ranging from 0.72 to 5.62 mM (R_{OS} ranging from 0.04:1 to 0.31:1). Within 24 hours, the cultures developed a bright yellow colour, with increasing intensity and turbidity (sulfur precipitation) with increasing oxygen (Figure 5.1).

In a second experiment, increasing concentrations of oxygen produced increasing concentrations of PS up to about 20 mM oxygen (with 18 mM sulfide, i.e. close to a 1:1 Ros), where PS

$$2\ H_2S + O_2 \rightarrow 2S^0 + 2H_2O$$

Figure 5.1 Increasing amounts of oxygen added to stationary phase *D. vulgaris* cultures containing 18 mM sulfide generated increasing amounts of PS. The cultures became visibly more turbid with more oxygen due to increased sulfur precipitate, which can be seen adhering to the bottom of the serum bottles (bottom panel). The R_{OS} from left to right are: 0.04:1, 0.0625:1, 0.125:1, 0.1875:1, 0.25:1, 0.31:1.

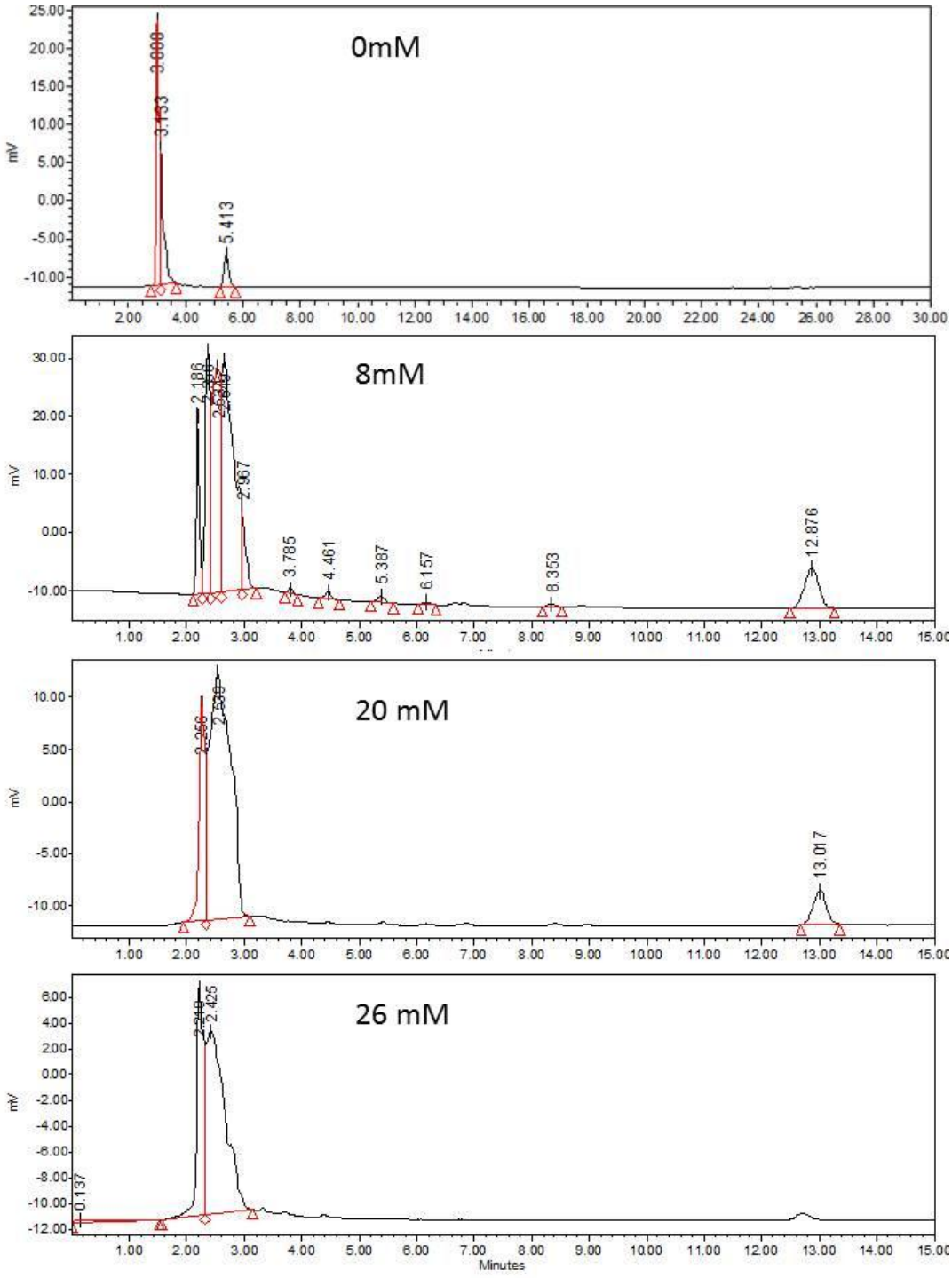

Figure 5.2 HPLC chromatograms showing increasing PS formation with increasing oxygen when added to stationary phase *D. vulgaris* cultures. Amounts of PS formed increased up to approximately 20 mM oxygen. After this point, PS production decreases, and no PS is detected at 26 mM oxygen. The R_{OS} from top to bottom are: 0:1, 0.45:1, 1.0:1, and 1.5:1. The large peak around 2 minutes is the injection peak. The remaining peaks represent different PS chain lengths.

production reached a plateau (Figure 5.2). Also, as more oxygen was added, the last peak at about 12 minutes, thought to be Me_2S_8 or Me_2S_9 became more prevalent. At higher than 20 mM oxygen, the PS peaks began to decrease, and no PS was detected with 26 mM oxygen. Small peaks began to appear again around 38 mM oxygen (R_{OS} = 2:1), as PS chains grew longer and broke off into smaller chains that could be detected using HPLC (data not shown).

5.3.2.2 Mid log phase

Pure oxygen, 0, 0.9, 1.8 or 2.7 mM (R_{OS}= 0:1, 0.09:1, 0.18:1 and 0.27:1), was added to MLP cultures of wild type, *nrf* and *hcp1-hcp2* mutants and PS formation was monitored by OD_{360}, along with sulfate and sulfide. No S precipitate or PS was seen in the controls with no oxygen added, nor with 0.9 mM oxygen (Figure 5.3, Figure 5.4, Figure 5.5; A and B), likely because the strains have intact oxygen defense systems and can easily remove small amounts of oxygen (Wildschut et al., 2006). Similar amounts of PS (maximum OD_{360} = 0.319 wild type; 0.356 *nrf*; 0.221 *hcp1-hcp2*) were formed in all three strains when 1.8 mM oxygen was added (Figure 5.3, Figure 5.4, Figure 5.5; C). PS formation varied greatly with 2.7 mM oxygen, with OD_{360} = 0.445 (WT), 0.595 (*nrf*) and 0.299 (*hcp1-hcp2*). All maximum OD_{360} values were reached after 24 hours (Figure 5.3, Figure 5.4, Figure 5.5; D). Experiments were performed in duplicate.

5.3.3 Abiotic experiments with oxygen

5.3.3.1 Autoclaved wild type cultures with 0 to 2.7 mM oxygen added

Wild type cultures were grown to MLP (10 – 12 mM sulfide, OD_{600} = 0.350) and autoclaved. Once cooled, 0, 0.45, 0.90, 1.8, or 2.7 mM of pure oxygen was added (R_{OS}= 0:1, 0.045:1, 0.090:1, 0.18:1 and 0.27:1) to triplicate bottles. Concentrations of sulfate, sulfide, PS OD_{360} and OD_{600} were monitored (Figure 5.6). No PS formed with 0 mM oxygen (maximum OD_{360} = 0.01

± 0.001).

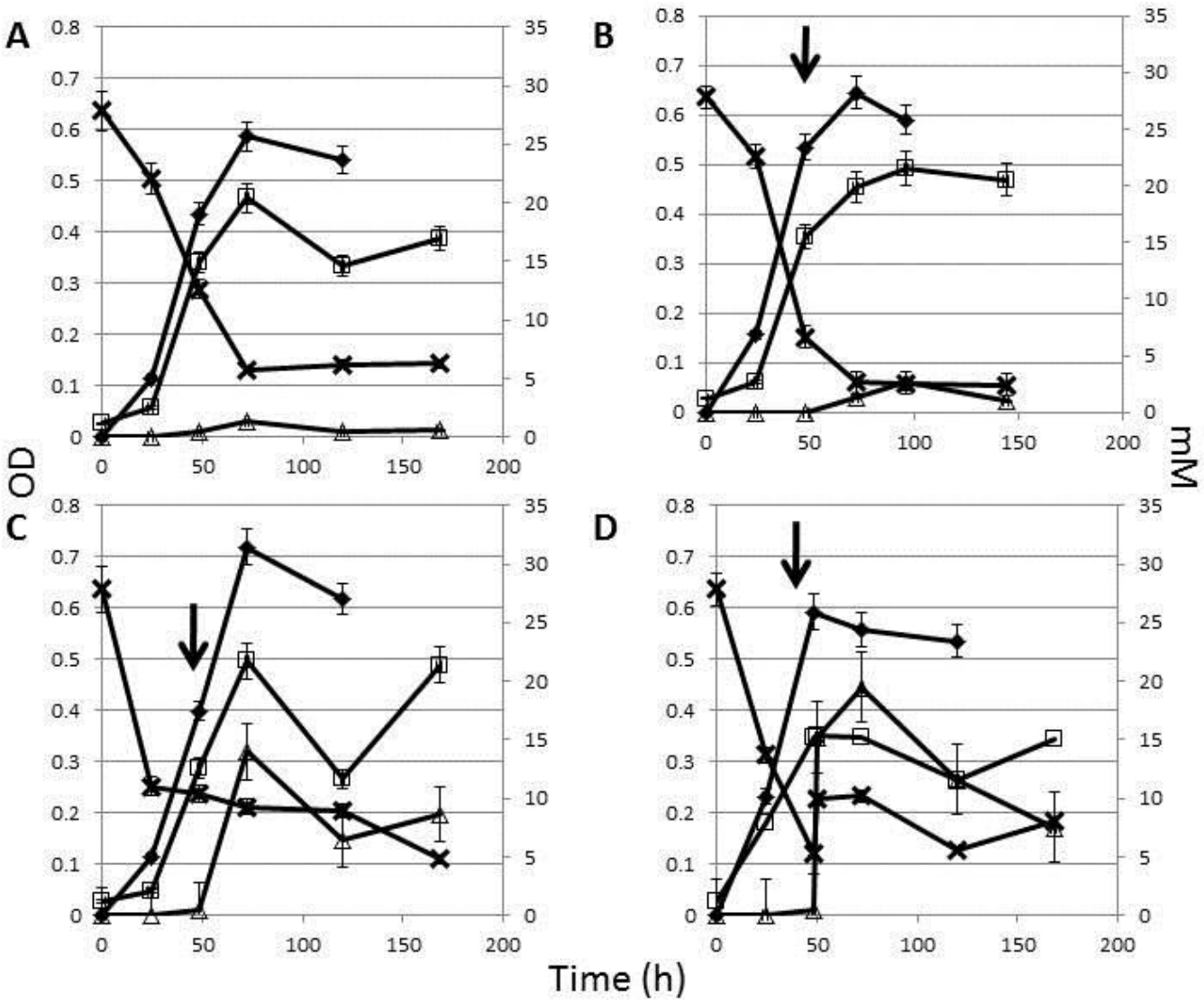

Figure 5.3 Mid log phase biotic experiments with wild type *D. vulgaris.* Varying amounts of oxygen were added at the time indicated by the arrow. A) No oxygen control B) 0.9 mM oxygen C) 1.8 mM oxygen, and D) 2.7 mM oxygen. OD_{600} (◆), sulfide (□), sulfate (✖) and OD_{360} (△) are shown. Results shown are for duplicate experiments, error bars represent standard deviation.

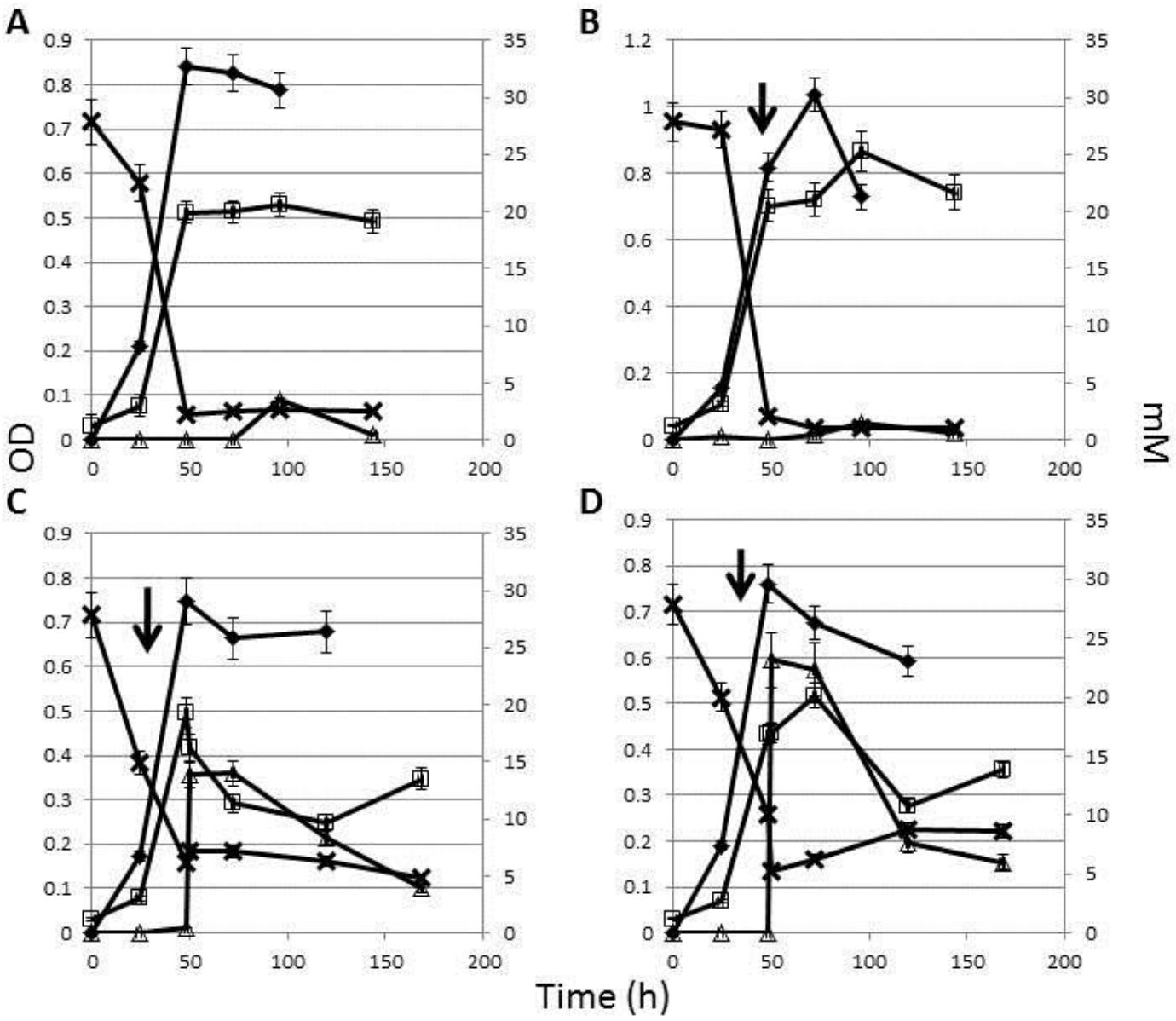

Figure 5.4 Mid log phase biotic experiments with the *nrf* mutant of *D. vulgaris.* Varying amounts of oxygen were added at the time indicated by the arrow. A) No oxygen control B) 0.9 mM oxygen C) 1.8 mM oxygen, and D) 2.7 mM oxygen. OD_{600} (◆), sulfide (□), sulfate (✖) and OD_{360} (△) are shown. Results shown are for duplicate experiments, error bars represent standard deviation.

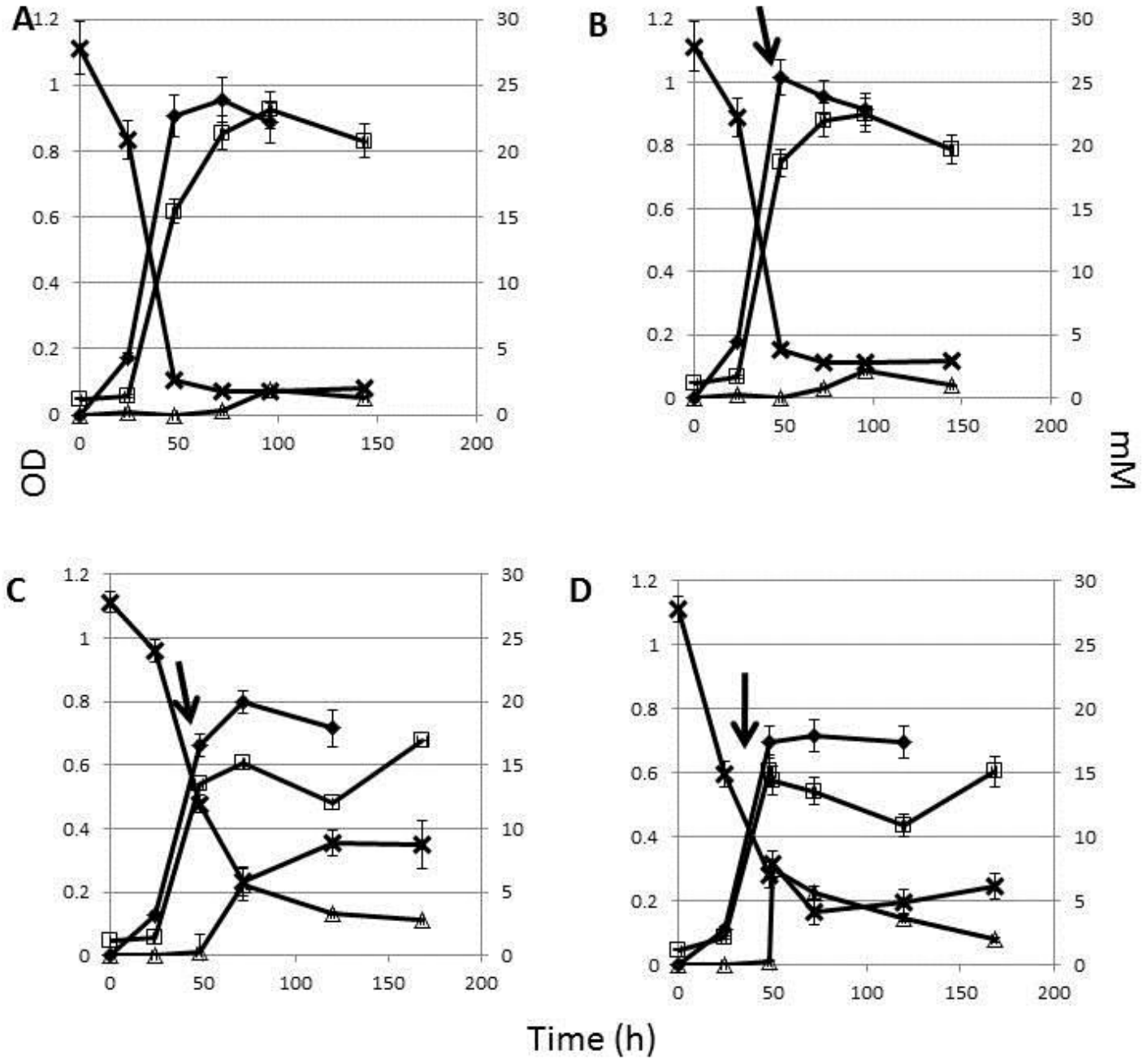

Figure 5.5 Mid log phase biotic experiments with the *hcp1-hcp2* mutant of *D. vulgaris.* Varying amounts of oxygen were added at the time indicated by the arrow. A) No oxygen control B) 0.9 mM oxygen C) 1.8 mM oxygen, and D) 2.7 mM oxygen. OD_{600} (◆), sulfide (□), sulfate (✖) and OD_{360} (△) are shown. Results shown are for duplicate experiments, error bars represent standard deviation.

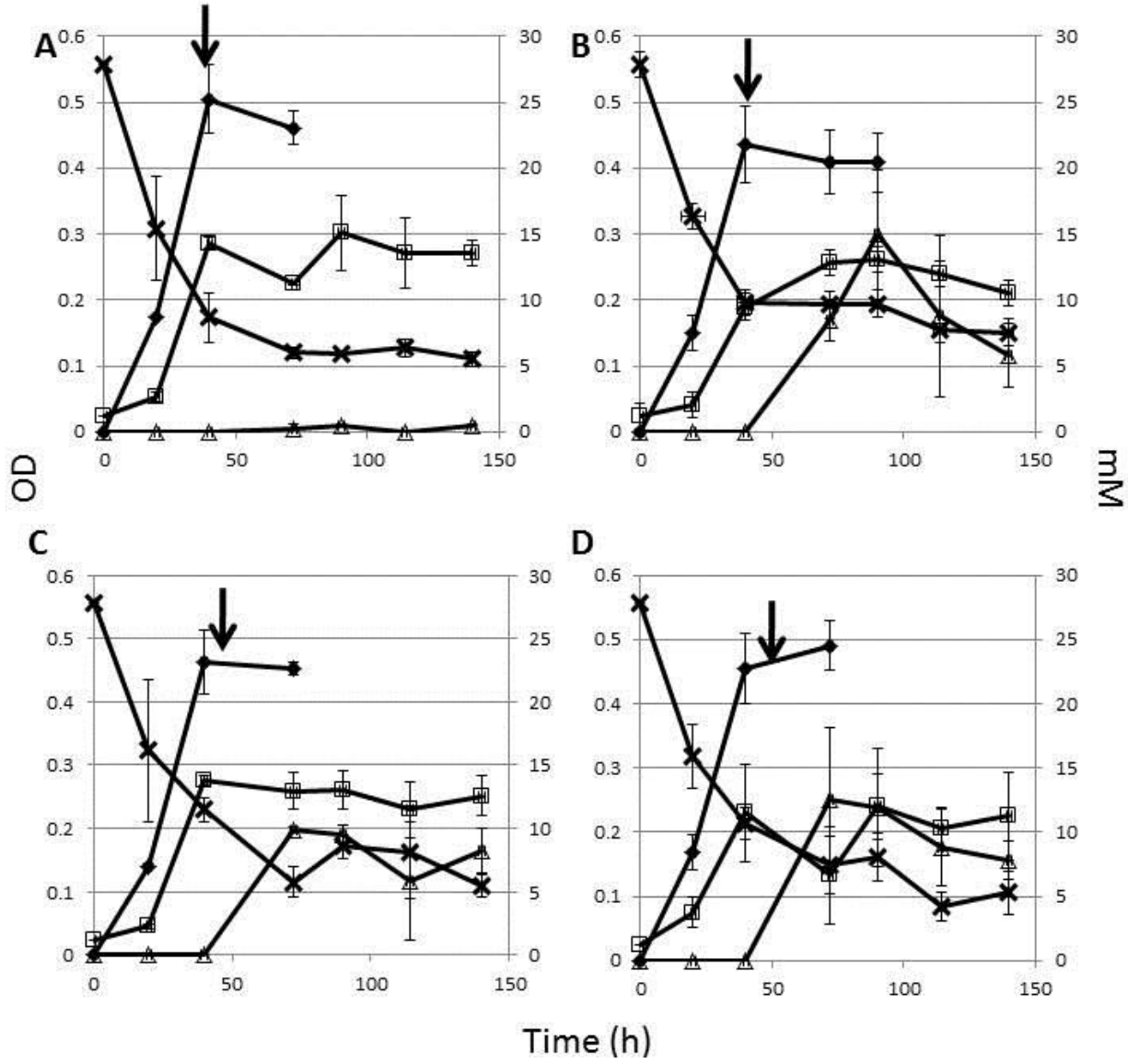

Figure 5.6 Abiotic experiments with wild type *D. vulgaris.* Cultures were autoclaved and/or oxygen added at the time indicated by the arrow. A) No oxygen control B) 0.45 mM oxygen C) 0.90 mM oxygen D) 2.7 mM oxygen. OD_{600} (◆), sulfide (□), sulfate (✖) and OD_{360} (△) are shown. Triplicate data is shown, error bars represent standard deviation.

While similar amounts of PS formed in each experiment, the rate of PS formation differed. For 0.45 mM oxygen, the maximum OD_{360} (0.299 ± 0.098) was reached 24 hours after oxygen addition; for 0.90 mM oxygen, OD_{360} = 0.244 ± 0.093 after 48 hours; for 1.8 mM oxygen, OD_{360} = 0.226 ± 0.050 after 6 hours; and for 2.7 mM oxygen, OD_{360} = 0.251 ± 0.111 was again reached after 6 hours.

5.3.3.2 Autoclaved wild type cultures with Ros of 0.5:1, 1:1 and 2:1

Wild type cultures were again grown to MLP (10 -12 mM sulfide, OD_{600} = 0.350) and autoclaved. Pure oxygen was added to generate Ros of 0.5:1, 1:1 and 2:1. Each ratio was done in triplicate. Concentrations of sulfide and sulfate were followed along with the OD_{600}. With Ros = 0.5:1, approximately 25% sulfide oxidation was observed, and the cultures had a heavy black precipitate with a yellowish undertone, indicating the presence of FeS and polysulfides (Figure 5.8; A). With the 1:1 ratio, an 86% oxidation of sulfide was observed, and the cultures had an opaque blackish-grey precipitate throughout, indicating the presence of FeS and elemental sulfur (Figure 5.8; B). When Ros = 2:1, 100% sulfide oxidation was observed, and the cultures had an opaque, pink-white precipitate, suggesting that only elemental sulfur formed, no FeS was likely present (Figure 5.8; C).

5.4 Discussion

5.4.1 Biotic incubations

In the biotic stationary incubations, the plateau in S and PS formation at an approximate Ros of 1:1 again verifies that oxidation past sulfur requires an enzymatic catalyst (Figures 5.1 and 5.2). From the mid log experiments, it is interesting to note that the *hcp1-hcp2* strain had the lowest amount of PS formation, while *nrf* had the highest. It was hypothesized that the *hcp1-hcp2*

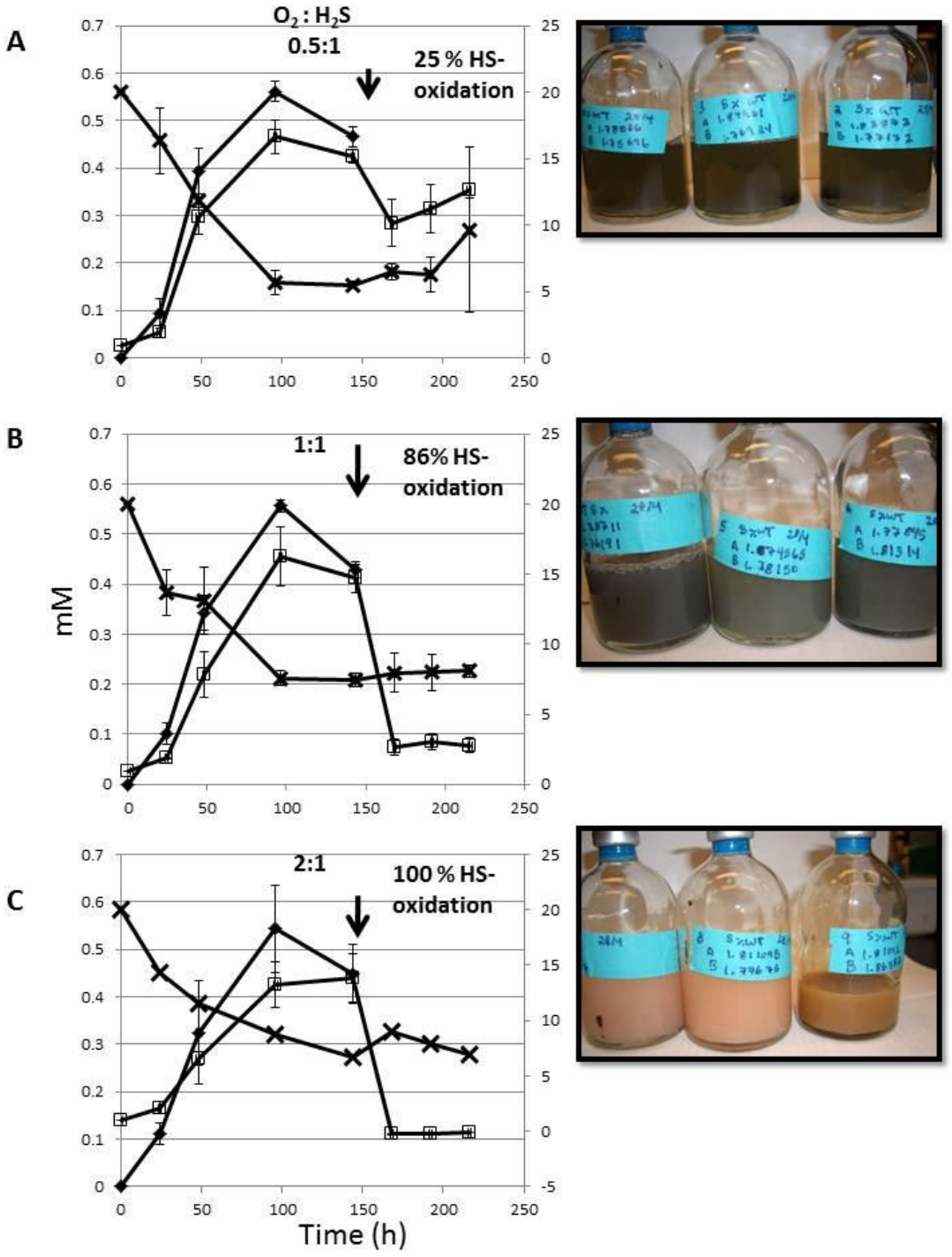

Figure 5.7 Abiotic experiments with wild type *D. vulgaris.* Cultures were autoclaved and oxygen added at the time indicated by the arrow. A) 0.5:1 sulfide: oxygen ratio B) 1:1 ratio C) 1:2 ratio. OD_{600} (◆), sulfide (□), sulfate (✖). Data shown is for triplicate experiments, error bars represent standard deviation.

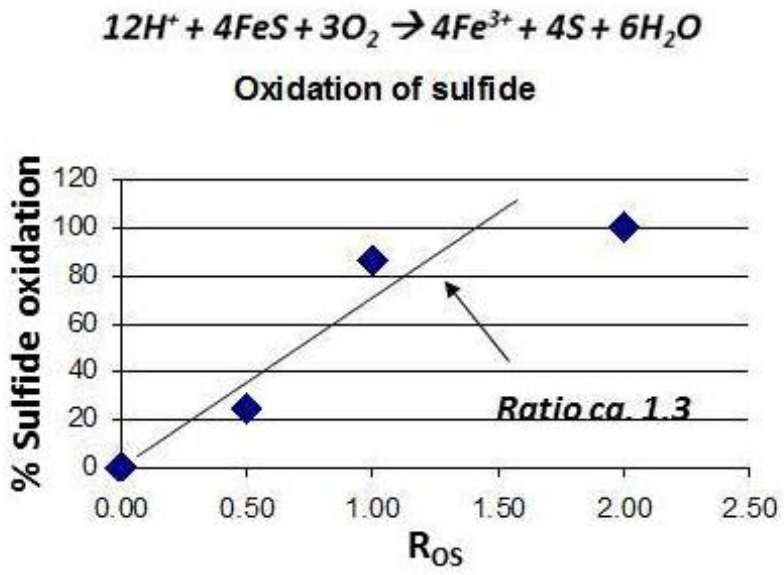

Figure 5.8 Proposed chemical reaction for the experiments shown in Figure 5.7.

mutant should have the greatest amount of PS as it supposedly is unable to reduce S and PS back to sulfide efficiently. This apparent discrepancy could be an artifact of the OD_{360} method, or perhaps is a result of the fact that S and PS were not separately measured, which was done in future experiments.

The amount of PS removal can be qualitatively inferred from the OD_{360} data. The ΔOD_{360} for wild type with 1.8 mM and 2.7 mM oxygen, respectively, was 0.122 and 0.175 (Figure 5.3; C, D: average ΔOD_{360} = 0.149); for *nrf* 1.8 mM and 2.7 mM oxygen was 0.256 and 0.441 (Figure 5.4; C, D: average ΔOD_{360} = 0.349); for *hcp1-hcp2* 1.8 mM and 2.7 mM oxygen was 0.109 and 0.219, respectively (Figure 5.5; C, D average ΔOD_{360} = 0.164). It is again interesting to note that the wild type and *hcp1-hcp2* mutant strains were able to reduce similar amounts of PS, while the *nrf* mutant strain was able to reduce approximately 45% more PS. This is somewhat puzzling as it was proposed in the previous chapters that nitrite may be an 'early warning' for PS as seen with nitrite treatment. However, it was also shown that neither the *nrf*, *hcp1* nor *hcp2* mutants were significantly affected by oxygen (Chapter 4). This observation does support the idea suggested in Chapter 4, that *hcp2* functions in S and PS removal only when formed through reaction of sulfide and nitrite. Apparently, *D. vulgaris* more frequently encounters S and PS stress in environments with nitrite instead of oxygen, which makes some degree of sense given the elaborate oxygen defense systems of *D. vulgaris* (Chapter 4). It is still curious as to why S and PS metabolism is more efficient when *nrf* is lacking, suggesting that *nrf* expression may not be beneficial during oxygen stress. Apparently, *D. vulgaris* is better able to respond to oxygen mediated S and PS stress when periplasmic Nrf, which is a c-type cytochrome, is absent.

5.4.2 Abiotic experiments

From the initial set of abiotic incubations (0 to 2.7 mM oxygen added), it is clear that there is a chemical as well as a biological aspect to oxygen removal. In the biotic MLP incubations, PS formation was delayed until 24 hours after oxygen addition, whereas in the abiotic experiment, PS formation was more rapid, with maximum PS forming 6 hours after oxygen addition. This shows that metabolically active SRB are able to remove small amounts of oxygen and PS, both of which are toxic to them, from their environment.

Looking at the comparable data from the abiotic and biotic experiments (wild type, with 1.8 mM and 2.7 mM oxygen), some interesting trends in PS reduction rates can be observed. In the abiotic incubation, PS was relatively stable following addition of 1.8 mM oxygen showing a decline of Δ OD_{360}=0.066; whereas following addition of 2.7 mM the decline was Δ OD_{360} = 0.096 (average abiotic Δ OD_{360} =0.081). This can be compared to the biotic experiments, in which PS was more transient. In these experiments, addition of 1.8 mM gave a decline of Δ OD_{360} = 0.122; whereas addition of 2.7 mM oxygen gave a decline of Δ OD_{360} = 0.175 (average Δ OD_{360} = 0.149). Thus, a 55% increase in PS removal was observed with live *D. vulgaris* as compared to the abiotic control.

From the abiotic incubations with Ros = 0.5:1, 1:1 and 2:1, we can again observe chemical oxidation of sulfide to sulfur, whereas oxidation to sulfate is not seen, even though there is sufficient O_2 to form sulfate at an R_{OS} of 2:1 ratio (Table 1-2). FeS and sulfur precipitate also formed; a possible reaction suggested by these observations is:

$$12H^+ + 4FeS + 3O_2 \rightarrow 4Fe^{3+} + 4S^0 + 6H_2O \qquad \textbf{(Equation 5-1)}$$

Here the FeS, which readily forms on the iron coupons in un-inoculated media, reacts with the added oxygen to form S and PS. This would produce sulfur at a 4/3 (1.3) ratio of sulfur to

oxygen. Plotting the percent sulfide oxidation against the ratios of sulfide to oxygen produces a fairly linear graph with a slope of 1.3, supporting this idea (Figure 5.8).

Chapter Six: Corrosivity of sulfur and polysulfide and mechanisms of removal

6.1 Introduction

6.1.1 S-PS and microbially influenced corrosion

With an understanding of the effects of S and PS on *D. vulgaris*, and the capacity of *D. vulgaris* to metabolize these compounds, we can begin to look at more applied aspects. In Chapter 5, we observed something quite interesting: live SRB can metabolize some S and PS and delay its formation during oxygen exposure. So, what does this mean in terms of iron corrosion?

The corrosive nature of reduced sulfur compounds (e.g. sulfur, polysulfide, sulfide) has been well-documented (Dowling, 1992, Heck, 1940). Sulfide, for example, is known to promote the entry of hydrogen into steel, leading to hydrogen blistering and cracking (Alekseev et al., 1990). Sulfide can also react rapidly with any oxygen or nitrite present to form S and PS as shown in Table 1-2. Sulfur in direct contact with iron and moisture can result in corrosion rates of 1.5 – 2.0 mm/yr (Dowling, 1992).

However, the corrosivity of polysulfides is less studied. Like sulfur, polysulfide is an oxidizer that receives electrons from steel surfaces to form sulfide (Ramo et al., 2003). Polysulfides are also soluble and are thus able to disperse more widely than sulfur or iron sulfide. Schutt and Rhodes (1996) examined corrosion rates in solutions with sulfide (1 mM) and oxygen (8 ppm, 0.25 mM). Corrosion rates of 15.2 mm/yr were reported for this solution at neutral pH, which would have contained some sulfur and polysulfides. This is compared to corrosion rates of 6.1 mm/yr with oxygen alone, and 1.1 mm/yr for sulfide alone (Schutt and Rhodes, 1996). Hence, like sulfur, polysulfides also pose a corrosion problem.

The measurement of corrosion rates by sulfide or polysulfide can be impeded by the ability of FeS to form a passivating film on a clean steel surface in the absence of other corrosion products. However, depending on their nature, these films are not stable indefinitely and may not offer permanent protection of the underlying steel surface (Mara and Williams, 1975).

SRB contribute to corrosion via several mechanisms (Dinh et al., 2004, Hardy and Brown, 1984), though their most significant contribution is their ability to produce sulfide, which is rapidly chemically converted to corrosive species, like iron sulfides (Equation 1-8) or partially oxidized compounds like S and PS (Table 1-2). It was observed in earlier experiments that reaction of biogenic sulfide with nitrite produced primarily a bright yellow solution, indicative of polysulfides; while reaction of sulfide with oxygen produced primarily a white precipitate, indicative of sulfur.

One case of S and PS mediated corrosion involved a brand new 7 mm thick pipe designed for sour service, which failed within 2 months of commencing operation. Inspection revealed deep pits at the gas–oil interface (3 and 9 o'clock positions) of the pipe. Localized FeS and sulfur precipitates resulting from periodic air exposure, which settled on the metal surface where this was contacted by the gas-liquid interface, were suggested as the cause of failure.

As mentioned, S and PS are also formed by chemical reaction of nitrite and sulfide (Table 1-2) and may be formed during nitrate treatment, and this is discussed in detail in Chapter 8. Thus, there may be an increased corrosion risk associated with nitrate treatment due to the formation of these sulfur compounds (Lin et al., 2008).

6.1.2 Control and removal of S and PS

S and PS formation can be proactively avoided with careful monitoring and control of system chemistry. However, once formed, S and PS can be removed by either of two alternative routes,

which may reduce the corrosion risk presented by these compounds. In the presence of (i) excess electron acceptor (e.g. nitrate), NRB may further oxidize the S and PS to sulfate (Figure 6.1); whereas in the presence of (ii) excess electron donor (oil organics, e.g. acetate) the S and PS may be reduced back to sulfide. A specialized group of sulfur-reducing bacteria (sulfur-RB) catalyzes this reaction. A representative of this group, *Desulfuromonas acetoxidans* (*Dsm. acetoxidans*), uses elemental sulfur and disulfide bonds as electron acceptors (Pfennig and Biebl, 1976) and derives energy for growth from the reaction (Pfennig and Biebl, 1976):

$4\ S^0 + \text{acetate} \rightarrow 4\ H_2S + 2\ CO_2$ **(Equation 6-1,** Figure 6.2 -a5)

As oil field waters are typically electron donor rich and electron acceptor poor, one would expect S and PS removal by the second route. A 16S rRNA survey of the microbial community in produced waters from the Medicine Hat Glauconitic C field (MHGC), with a low bottomhole temperature indicated that *Desulfuromonas* species were the most commonly found delta-proteobacterium (the group to which most SRB also belong) during nitrate treatment (Shartau et al., 2010).

S and PS can also be microbially removed by *Sulfurovum* species, which couple the reduction of nitrate to the oxidation of either sulfur or thiosulfate to sulfate (Figure 6.2-c3, (Inagaki et al., 2004)). These species were only found in enrichment cultures from the MHGC field (Shartau et al., 2010) but are likely present in the reservoirs. In addition, aerobic sulfur-oxidizing bacteria, such as *Thiobacillus* species can oxidize sulfide and sulfur to sulfate (Figure 6.2-c6, (Madigan et al., 2003)).

SRB are also able to remove limited amounts of S and PS (Figure 6.2-a5, (Johnston et al., 2009, Takahashi et al., 2005)). Some sulfate reducers, such as *Desulfobulbus propionicus*, are able to disproportionate elemental sulfur to sulfide and sulfate in the presence of manganese (IV) (Phillips and Lovley, 1994), presenting another potential means of S and PS removal.

This chapter investigates the corrosivity of S and PS, and looks at the potential of SRB and other sulfur cycle bacteria which are commonly found in pipelines to remove these corrosive products.

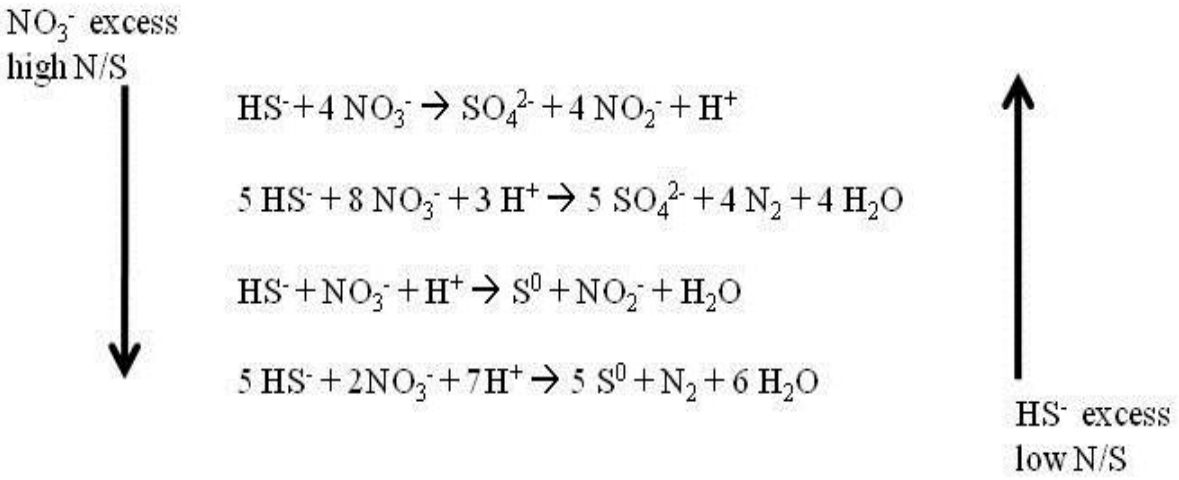

Figure 6.1 The NRB *Sulfurimonas denitrificans* strain CVO carries out different reactions according to the nitrate: sulfide ratio, forming S and PS at low ratios and sulfate at higher ratios. For simplicity S and PS are both represented as sulfur (S^0).

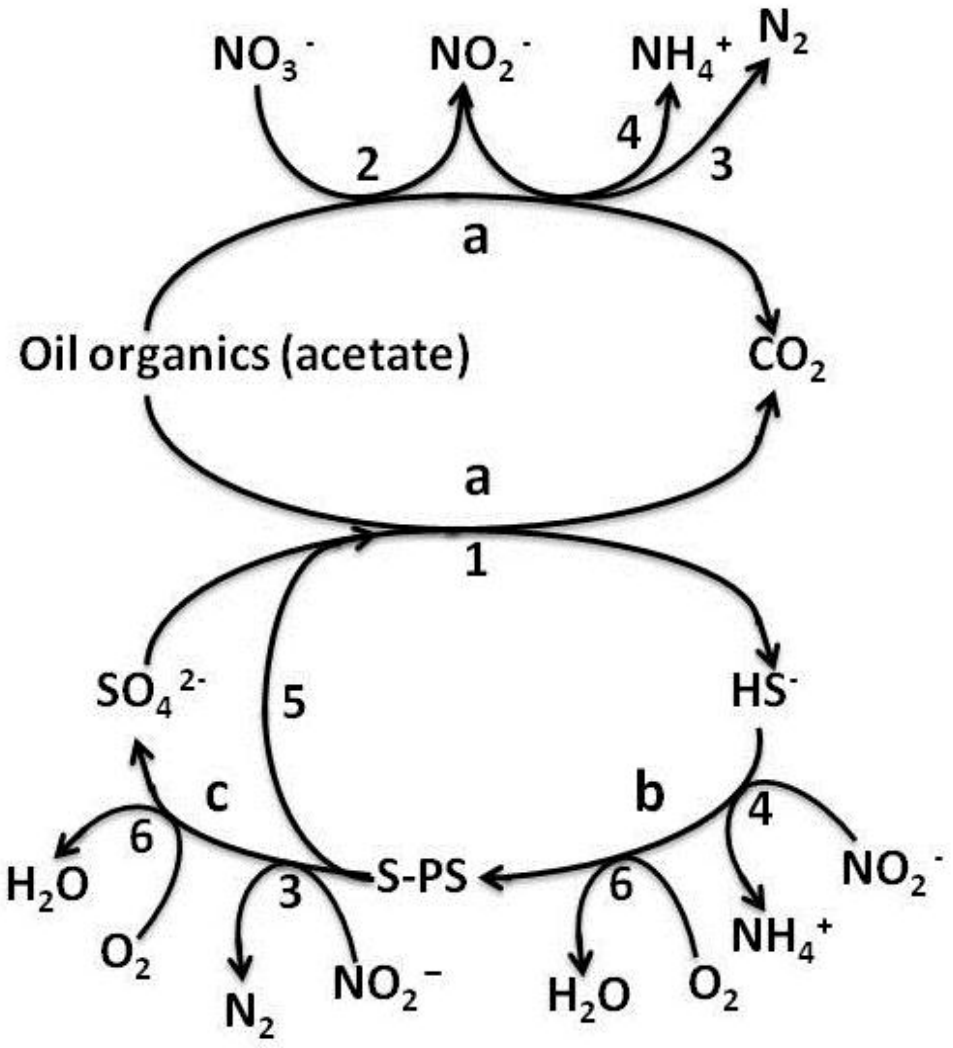

Figure 6.2 Formation and removal of sulfur-polysulfide (S-PS) by chemical and microbially-mediated reactions in oil fields. Oxidations are (a) oil organics, which includes acetate, to CO_2, (b) sulfide to S-PS and (c) S-PS to sulfate. Reductions are (1) sulfate to sulfide, (2) nitrate to nitrite, (3) nitrite to dinitrogen, (4) nitrite to ammonium, (5) S-PS to sulfide, and (6) oxygen to water. Chemical reactions are b4 and b6. Microbially catalyzed reactions are a1-a5, b4, b6, c3 and c6. Some possible microbially-catalyzed reactions (e.g. a6, b2, b3, c2, c4) are not shown in the diagram. As an example, SRB catalyze a1; *Desulfuromonas* sp. catalyze a5; *Sulfurovum* sp. catalyze c2 and c3.

6.2 Methods

The methods for culturing and preparing and analysis of corrosion coupons are described in Chapter 2. Wild type and the *hcp1-hcp2* mutant strain of *D. vulgaris* were cultured in WP-LS medium, and *D. acetoxidans* was cultured in MMS medium. For the corrosion experiments, the biotic and abiotic incubations were set up as described in Chapter 5. For the sulfur accumulation experiments, oxygen was added to stationary phase cultures of *D. vulgaris* containing approximately 18 mM of sulfide to oxidize the sulfide to S and PS. S and PS were monitored using HPLC and OD_{360}, respectively. Approximately 4 days after oxygen addition, 5% of *Desulfuromonas acetoxidans* was inoculated into the serum bottles. Measurements of sulfide, PS and acetate were then recorded every 24 hours.

6.3 Results and Discussion

6.3.1 Corrosion with oxygen

The corrosion data is summarized in Table 6-1. An observation seen with all retrieved coupons was that they had a black, slimy non-adherent film covering them. This black material is likely FeS combined with bacterial biomass.

What is of interest from Table 6-1 is that for both 1.8 mM and 2.7 mM oxygen the *hcp1-hcp2* mutant strain showed the highest corrosion rates, despite having the lowest amount of PS present as discussed above in Chapter 5. This supports the theory that the Hcp's function to reduce S and PS back to sulfide, as it was predicted that this mutant strain would show the highest corrosion rates as it is unable to effectively remove S and PS, which was observed.

The abiotic incubations were performed in triplicate with two corrosion coupons per bottle.

In the first abiotic experiment (Table 6-1), the corrosion rates for the no oxygen control were (0.03719 ± 4 E -5 mm/yr) and with 1.8 mM oxygen (0.0416 ± 0.0004mm/yr) were similar. However, with 2.7 mM oxygen the corrosion rate increased nearly 5-fold to 0.2202 ± 0.01321. Looking at the comparable data from the biotic and abiotic incubations, the effect of the ability of SRB to interconvert various sulfur species can be seen in the associated corrosion rates, which are lower with active SRB, because *D. vulgaris* is able to reduce some oxygen and polysulfide (Table 6-1; (Johnston et al., 2009, Takahashi et al., 2005, Wildschut et al., 2006)). Thus it seems that *D. vulgaris* is actually playing a protective role against PS corrosion.

In the second abiotic experiment with the Ros of 0.5:1, 1:1 and 2:1, the data followed the expected trend of increased corrosion rates with increasing oxygen (Figure 6.3) though it is peculiar that the corrosion rates were not substantially higher than those seen in the first abiotic experiment, with the highest corrosion rate being 0.212 ± 0.0181 mm/yr as seen in the 0.5:1 ratio, which is very similar to the 0.220 ± 0.0132 seen with 2.7 mM oxygen.

Table 6-1 Corrosion rates of wild type *D. vulgaris* under biotic and abiotic conditions, and the *hcp1-hcp2* mutant when exposed to oxygen. NA means data not available.

Treatment	***Strain***	***Biotic CR (mm/yr)***	***Abiotic CR (mm/yr)***
No O_2	Wild type	0.00	0.037 ± 4 E -5
1.8 mM O_2	Wild type	0.00	0.041 ± 0.0004
	hcp1-hcp2	0.334	NA
2.7 mM O_2	Wild type	0.064	0.220 ± 0.013
	hcp1-hcp2	0.149	NA

However, upon visual inspection, the coupons from the second abiotic incubation were more severely damaged, with damage increasing notably with more oxygen (Figure 6.3a, b, c), again highlighting the corrosive nature of S and PS.

Another unusual observation from the 2:1 ratio set was that the coupons had patches that were very blue in colour (Figure 6.3d) after the black FeS film had been initially wiped off. The blue colour went away after cleansing in the acid bath as per NACE protocol (NACE, 2005). This likely indicates the presence of vivianite, $Fe_3(PO_4)_2 \cdot 8(H_2O)$, which forms by reaction of iron with phosphate already present in the medium. The presence of vivianite is of interest as it means that Fe^{2+} is being oxidized to Fe^{3+} by the added oxygen.

6.3.2 Prevention of sulfur accumulation

Initial experiments with the sulfur reducer *Desulfuromonas acetoxidans* were set up to achieve a better understanding of whether this organism is able to use both sulfur and polysulfide as electron acceptors.

A late-stationary phase culture of *D. vulgaris* with 18 mM sulfide and 35 mM acetate was exposed to a total of 35 mM oxygen to chemically form sulfur. A 5% inoculum of *Dsm. acetoxidans* was then added, and concentrations of acetate and sulfide were monitored (Figure 6.4) Previous experiments were done with less oxidation of sulfide; however *D. acetoxidans* was unable to grow when sulfide concentrations were above 5 mM (data not shown (Pfennig and Biebl, 1976)). It is presumed that all 18 mM sulfide was oxidized to sulfur, as the cultures were completely white; and according to the reaction shown in Table 1-2, 9 mM of oxygen should have been sufficient to convert 18 mM sulfide to sulfur. The overall reaction carried out by *Dsm. acetoxidans* is shown in Equation 6-1, with one acetate being able to reduce four sulfurs back to four sulfides.

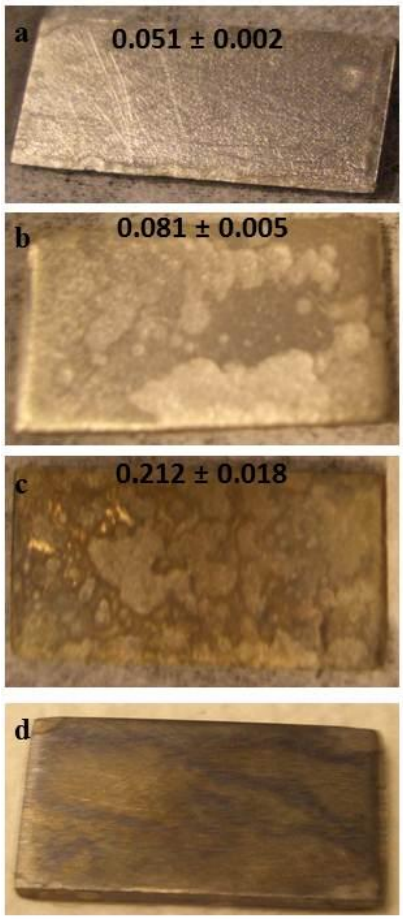

Figure 6.3 Increasing corrosion damage with increasing sulfide oxidation with oxygen .in abiotic *D.vulgaris* cultures with 15 mM sulfide. See Figure 5.8. (a): Oxygen was added to generate an R_{OS} of 0.5:1. The associated corrosion rate, in mm/yr is shown in bold on the right with a picture of the corrosion coupon after 8 weeks incubation. (b): R_{OS} of 1:1. Corrosion rate is shown with the resulting corrosion coupon. (c): R_{OS} of 2:1. The resulting corrosion coupon and corrosion rate are shown to the right. (d): blue colour, potentially vivianite can be seen on a coupon from the 2:1 ratio experiment. The blue colour was not present after acid cleansing.

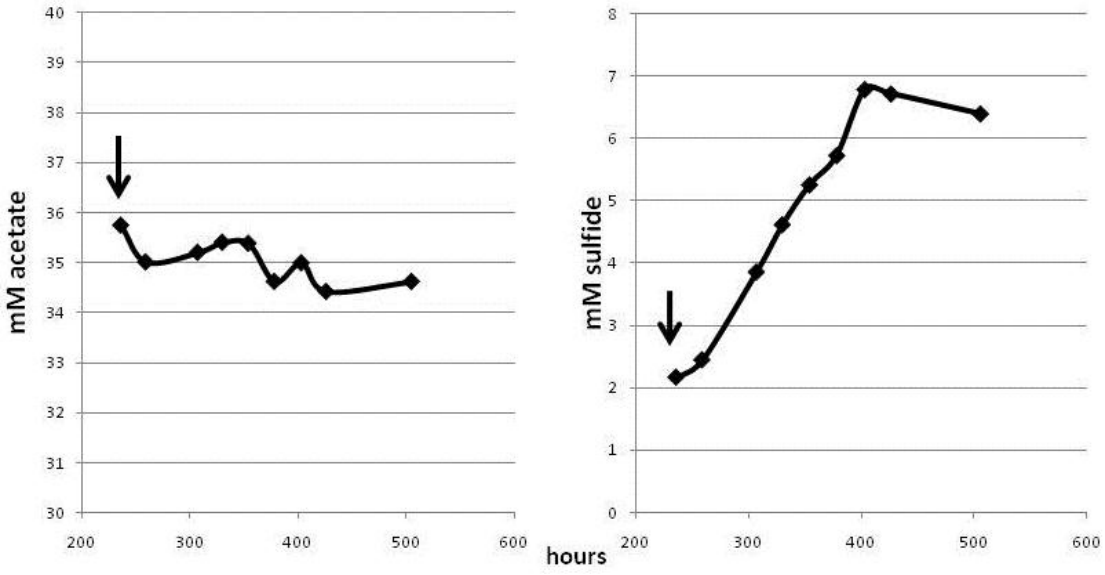

Figure 6.4 *Dsm. acetoxidans* uses sulfur produced by chemical reaction of biogenic sulfide with oxygen. A 5% inoculum of *Dsm. acetoxidans* was added to a completely oxidized stationary phase *D. vulgaris* culture at the time indicated by the arrow. The concentrations of acetate (left panel) and sulfide (right panel) were monitored with time.

When *Dsm. acetoxidans* was added to the oxidized culture, acetate oxidation was observed (1.1 mM, Figure 6.4 left panel), along with the production of 4.2 mM sulfide (Figure 6.4, right panel), indicating that 4.2 mM of sulfur was reduced as anticipated.

The data suggests that *D. acetoxidans* is able to grow under these conditions and that its growth reduces the amount of sulfur produced through chemical oxidation of sulfide.

6.4 Conclusions

The corrosive nature of reduced sulfur compounds, such as S and PS is known (Dowling, 1992, Heck, 1940). The reaction of sulfide with oxygen to form S and PS, and its effects on corrosion rates were explored in both biotic and abiotic experiments. There was a notable increase in corrosion rates and surface damage to the coupons in abiotic experiments where S and PS readily formed and could not be removed. This was also reflected in the higher corrosion rates observed with the *hcp1-hcp2* mutant, as *D. vulgaris* was unable to efficiently remove the S and PS, verifying the role of the Hcp's here. The corrosion data also clearly demonstrate the corrosive nature of PS.

While S and PS formation can be prevented, once formed, however, microbial action is required to remove it. This can be achieved either by use of additional nitrate which will allow the NRB to completely oxidize S and PS to sulfate (Figure 6.1), or by the action of other microorganisms summarized in Figure 6.2.

As such, the formation of S and PS during nitrate treatment may not be as much of a concern as initially thought (Lin et al., 2008), as it can be removed by a variety of resident sulfur cycle microbes.

Chapter Seven: Role of *D. vulgaris* in sulfur-mediated pitting corrosion under conditions of oxygen ingress

7.1 Introduction

As has been discussed, and demonstrated in Chapter 6, S and PS are very corrosive compounds and their formation in pipelines is undesirable. These compounds can readily form through reaction of sulfide with nitrite and oxygen as shown in Table 1-2. Here, the corrosion implications of oxygen ingress on the function of *D. vulgaris* are discussed.

Sources of oxygen ingress into pipelines include leaky valves and dissolved oxygen in methanol added for hydrate control. Another common point of oxygen entry is the vapour recovery unit, which is used to collect hydrocarbon vapours from oil tanks (Haveman et al., 2004). As discussed previously, nitrite can be formed when nitrate is added for souring control (Haveman et al., 2004). S and PS can also form, and are aggressive corrosion agents and their formation is undesirable. The presence of S and PS is toxic to SRB as shown in Chapters 3 and 4, as their presence indicates an environment with a redox potential too high to support anaerobic sulfate reduction (Jones, 1996). If S and PS form, *D. vulgaris* can reduce these back to sulfide through an electron transport chain that involves hybrid cluster proteins Hcp1 and Hcp2 (Johnston et al., 2009, Yurkiw et al., 2012).

This information raises an interesting question: if SRB are able to remove S and PS or prevent their formation, can they actually reduce the corrosion risk in situations where these might form? Can the presence of SRB be beneficial in certain circumstances, in terms of corrosion? The work presented in this chapter explores corrosion by S and PS formed by adding oxygen to sulfide-

containing cultures of live *D. vulgaris*, autoclaved *D. vulgaris* and to media containing added sulfide, representing biotic, abiotic and chemical conditions, respectively.

7.2 Methods

All methods used are described in Chapter 2. Elemental sulfur (S) was quantified using the perchloroethylene extraction and HPLC method, while sulfur as polysulfide (PS) was derivatized with TPP and measured with GC-MS. Again, note that this method measures both S and PS, or total sulfur, and will be referred to as TPP-S in this chapter. Oxygen addition and the establishment of biotic and abiotic incubations were performed as described in Chapter 2 and Chapter 5. Briefly, biotic and abiotic incubations were exposed to Ros of 0. 0.25, 0.50, 1.0, 1.6 and 2.4:1. The same Ros were also set up under chemical conditions, in high sulfide (12 mM) WP-LS medium. Corrosion rates were first monitored using LPR and weight loss coupons, however subsequent experiments used only weight loss coupons. Corrosion coupons were included in all incubations.

7.3 Results

7.3.1 LPR

LPR was used in initial biotic and abiotic incubations, which produced some unclear results. The general trend observed was a rapid spike in corrosion rates immediately after oxygen was added, followed by a gradual decrease in both biotic and abiotic incubations, as seen in Figure 7.1. A three-fold difference in corrosion rates between biotic and abiotic incubations was observed with LPR, although this is not believed to be accurate. Additional anomalies were also observed when comparing results with and without the presence of the LPR electrodes. When the LPR

electrodes were present, a substantial decrease in sulfide oxidation rates was observed, up to 50% in the biotic incubations (Figure 7.2 A, B). Also, nearly 50% less S and TPP-S were formed in the presence of the LPR electrodes (Figure 7.2 C, D). Weight loss corrosion rates were also 10% lower in the LPR system than when used alone (data not shown). Due to these discrepancies, subsequent experiments were carried out using only weight loss coupons and no LPR.

7.3.2 Biotic incubations

Complete oxidation of lactate was seen at all values of R_{OS} (Figure 7.3). In the absence of added oxygen ($R_{OS} = 0$), aqueous sulfide was produced to its maximum observed value of 15 mM (Figure 7.3A). Likewise, the reduction of sulfate to sulfide was not affected at $R_{OS}= 0.25$ (Figure 7.3B). Sulfate reduction slowed slightly and the sulfide concentration reached only 12 mM at $R_{OS}= 0.5$ (Figure 7.3C). In contrast, half of the sulfide was removed after oxygen addition to $R_{OS} = 1.0$ and no subsequent increase in sulfide concentration was seen (Figure 7.3D). At R_{OS} values of 1.6 and 2.4 near complete sulfide oxidation (98%) was seen. Sulfate reduction slowed and then ceased after oxygen addition (Figure 7.3E and F). The continued use of lactate following oxygen addition (Figure 7.3D, E and F) indicates that *D. vulgaris* redirected electrons from lactate oxidation to oxygen reduction, instead of to sulfate reduction. Highly oxidized conditions will eventually kill *D. vulgaris*, when these persist (Wildschut et al., 2006). Apparently, cells survived the single oxygen pulses administered here as indicated by the continued lactate oxidation.

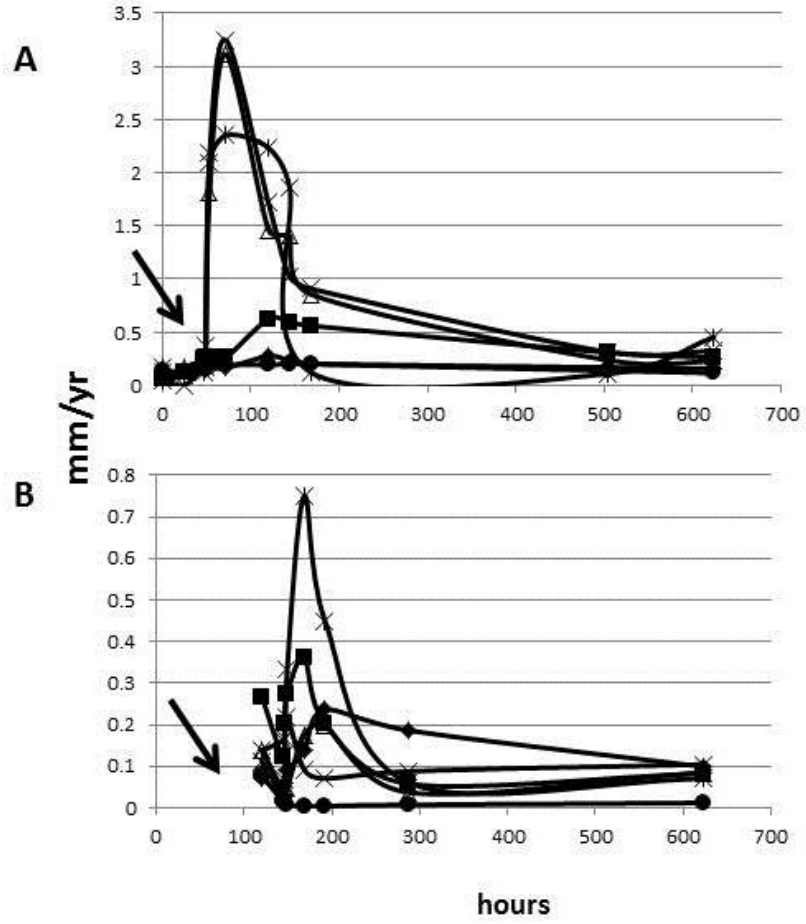

Figure 7.1 LPR results of the (A) biotic and (B) abiotic incubations. Oxygen was added as indicated by the arrows. R_{OS} = (◆) 0.25:1, (■) 0.5:1, (△) 1.0:1, (**X**) 1.6:1, (∗) 2.4:1, (•) control. Oxygen was added as indicated by the arrows.

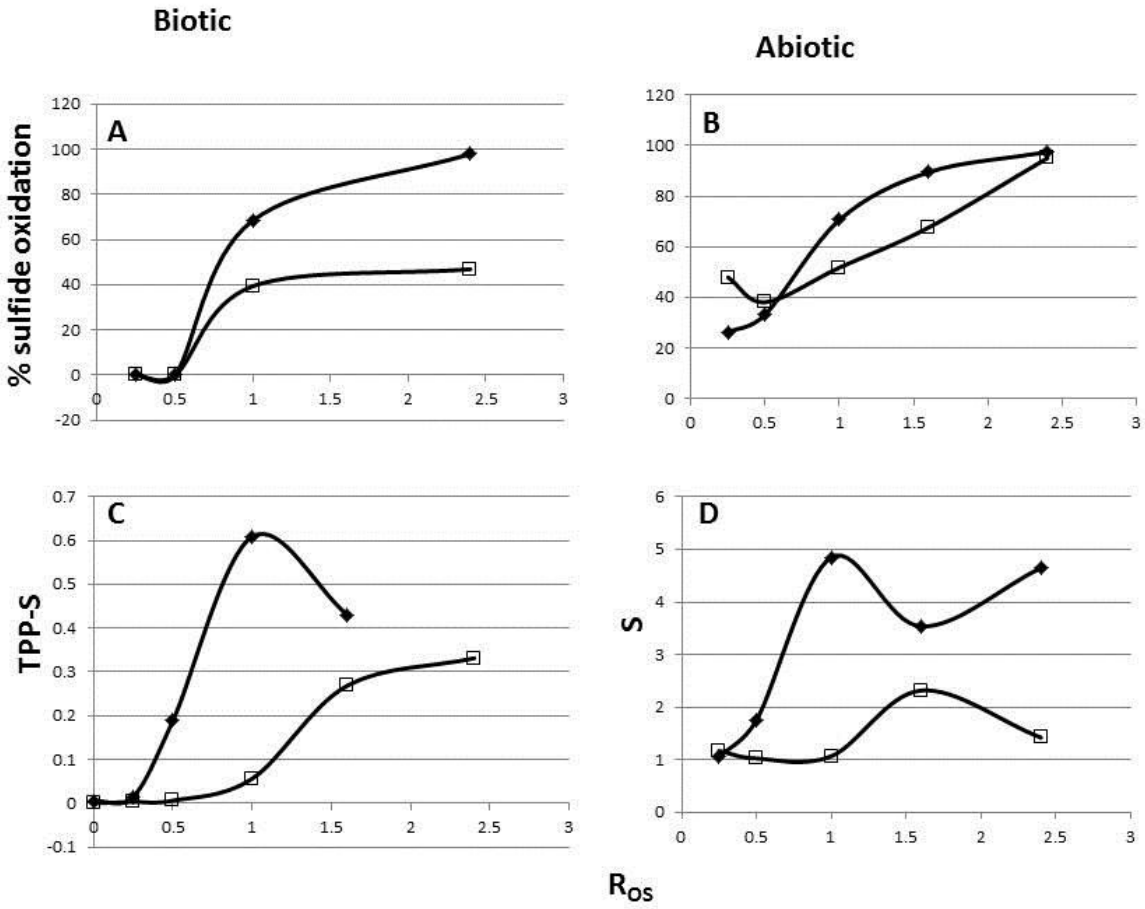

Figure 7.2 Differences observed in the presence (□) or absence (◆) of LPR electrodes. (A) sulfide oxidation in the biotic and (B) abiotic incubations; (C) TPP-S formation in biotic incubations and (D) S formation in abiotic incubations.

Increasing concentrations of S were formed with increasing oxygen (Figure 7.3A to F). Maximum S concentrations formed were 0.02, 0.47, 0.17, 0.90, 1.86 and 3.35 mM for R_{OS} values of 0 to 2.4, respectively. S was transient in the experiments with R_{OS} = 0.25 and R_{OS} = 0.50. For R_{OS} values of 1.0, 1.6 and 2.4 the maximal observed concentration of TPP-S increased to 2.9, 6.2 and 14.5 mM, respectively (Figure 7.3D, E, and F).

The equation $2H_2S + O_2 \rightarrow 2S^0 + 2H_2O$ (Table 1-2) indicates that all sulfide can be converted to sulfur at R_{OS} values of 0.5 or higher. The fact that only small concentrations of S were observed at R_{OS} values up to 1.0, suggested that *D. vulgaris* was able to prevent the formation of sulfur under these conditions.

Formation of the maximal TPP-S concentrations, that were observed, required 13, 20 and 35% of added oxygen for R_{OS} values of 1.0, 1.6 and 2.4, respectively (Table 7-1). The remaining oxygen was likely used for lactate oxidation. Alternatively, concentrations of S and TPP-S may have been underestimated because these are insoluble (S) or may have bound to or reacted with the iron coupons. The data presented for S and TPP-S are therefore only semi-quantitative.

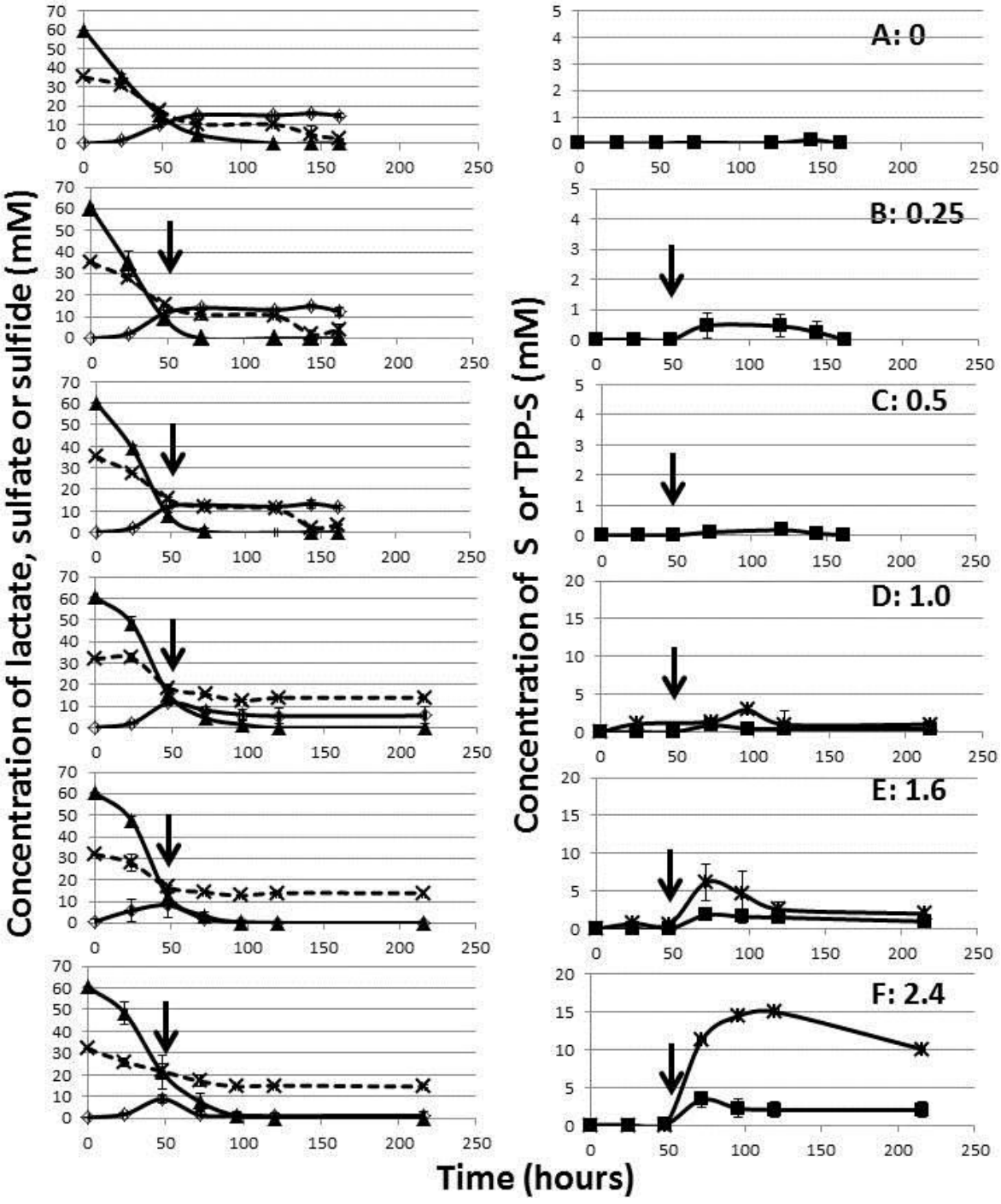

Figure 7.3 Concentrations of lactate (▲), sulfate (x) and sulfide (◊) (left panels) and of S (■) and TPP-S (✱) (right panels) as a function of time for biotic incubations at R_{OS} of 0 to 2.4, as indicated. Oxygen was added at the indicated time (↓). No TPP-S was measured in panels A to C. Error bars calculated as standard deviation among the triplicates.

Table 7-1 Sulfur balance for the biotic experiment.

A	***B***	***C***	***D***	***E***	***F***	***G***
Sulfide (mM)	**O_2 added (mM)**	**R_{OS}**	**Maximum S formed (mM)**	**Maximum TPP-S formed (mM)**	**O_2 required for TPP-S formation (mM)**	**(F/B)*100 (%)**
0	0	0	0.016	ND[1)]	0.01	NA [3)]
12.1	3.03	0.25	0.469	ND[1)]	0.23[2)]	7.7
11.9	5.95	0.50	0.169	ND[1)]	0.08[2)]	1.4
11.5	11.5	1.00	0.903	2.95	1.48	12.8
10.2	16.3	1.60	1.86	6.16	3.08	18.9
8.9	21.3	2.40	3.35	14.3	7.15	33.6

[1)]Not determined
[2)]Value is based on determined S, as TPP-S was not determined
[3)]Not applicable, as no O_2 was added (C=0).

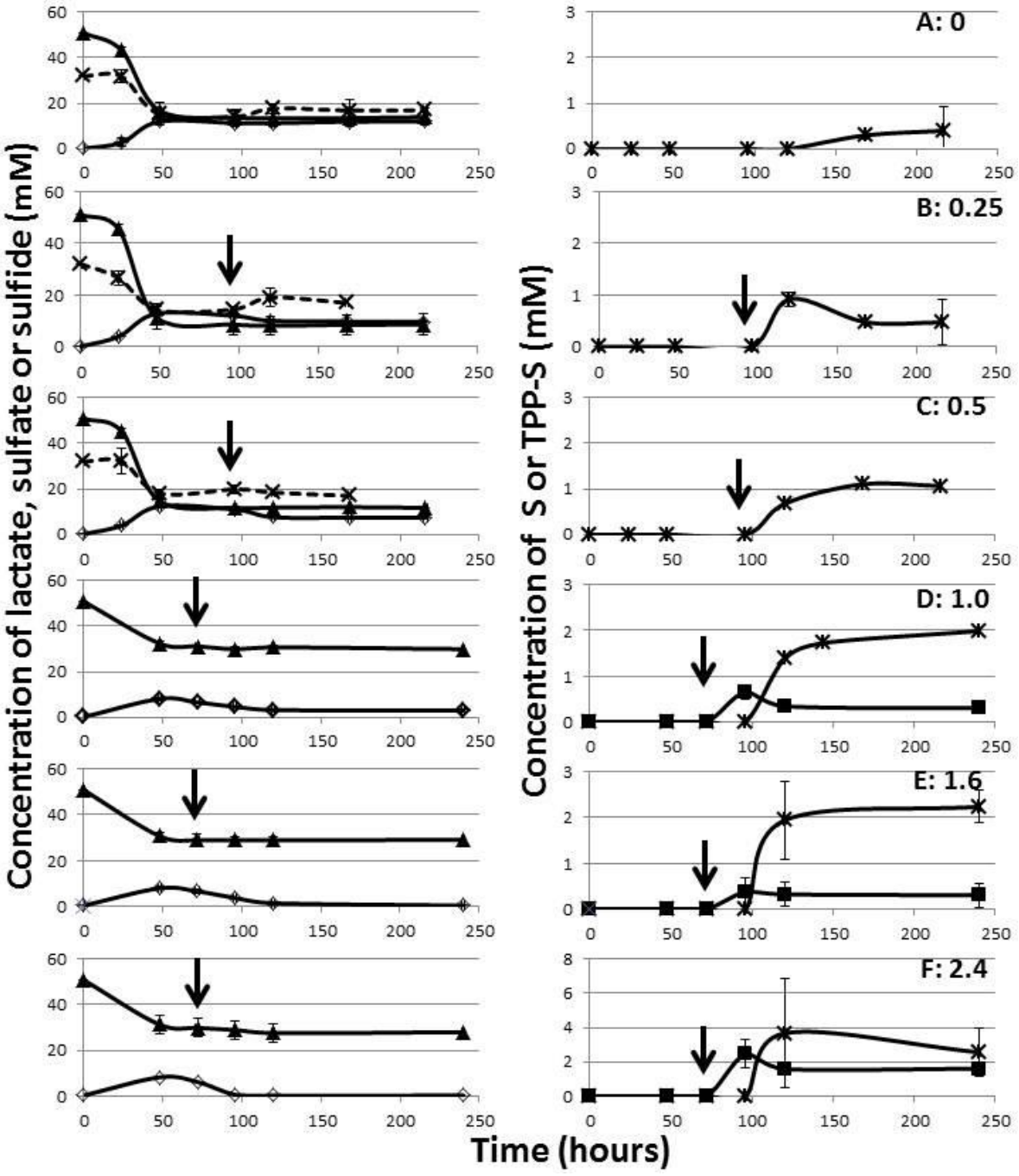

Figure 7.4 (A-F) Abiotic incubation at R_{OS} of 0 to 2.4 as indicated. Cultures were autoclaved at 48 hours and oxygen added at either 72 or 96 hours as indicated (↓). Left panels: concentrations of lactate (▲), sulfate (x) and sulfide (◇). Right panels: concentrations of and of S (■) and TPP-S (✳). Note change of scale on the right panels. No sulfate was measured in panels E to F and no S was measured in panels A to C. Error bars calculated as standard deviation among the triplicates.

7.3.3 Abiotic incubations

Lactate oxidation and sulfate reduction stopped after autoclaving at which point 10 to 15 mM sulfide was present (Figure 7.4A-F). No sulfide was oxidized without oxygen addition (Figure 7.4A: $R_{OS} = 0$). With R_{OS} values of 0.25, 0.5 and 1.0, partial sulfide oxidation was observed of 18, 32 and 60%, respectively. Complete sulfide oxidation was observed with R_{OS} values of 1.6 and 2.4.

TPP-S reached maximum values of 0.49, 0.90, 1.1, 1.7, 2.3 and 3.7 mM for R_{OS} of 0 to 2.4, respectively (Figure 7.4A-F). TPP-S was formed immediately at $R_{OS} = 0.25$ and higher and remained for the duration of the experiment. For R_{OS} values of 1.0, 1.6 and 2.4 the maximum S concentrations formed were 0.65, 0.40 and 2.45 mM, respectively (Figure 7.4, E, F). S and TPP-S were formed to maximum values and then decreased in some cases. As no concurrent increase in sulfide was observed, the observed decrease was likely due to reaction with the iron coupons to form FeS or due to precipitation of S. A good sulfur balance was not obtained, i.e. maximally 40% of the approximately 10 mM sulfide oxidized was recovered as TPP-S (Figure 7.4).

7.3.4 Chemical incubation

Increasing oxidation of the 10-12 mM of added sulfide was observed with increasing oxygen addition (Figure 7.5). Near complete sulfide oxidation occurred at R_{OS} values of 1.0, 1.6 and 2.4. Increased sulfide oxidation corresponded to increased TPP-S formation to maximum values of 0.40, 2.78, 2.81, 4.55 and 4.33 mM, respectively (Figure 7.5B). The TPP-S concentration formed was constant with time, except at $R_{OS} = 1.6$ (Figure 7.5E), where it declined possibly for the same reasons as explained above. Figure 7.5 indicates that maximally only 25-30% of the sulfide oxidized was recovered as TPP-S. S was not measured.

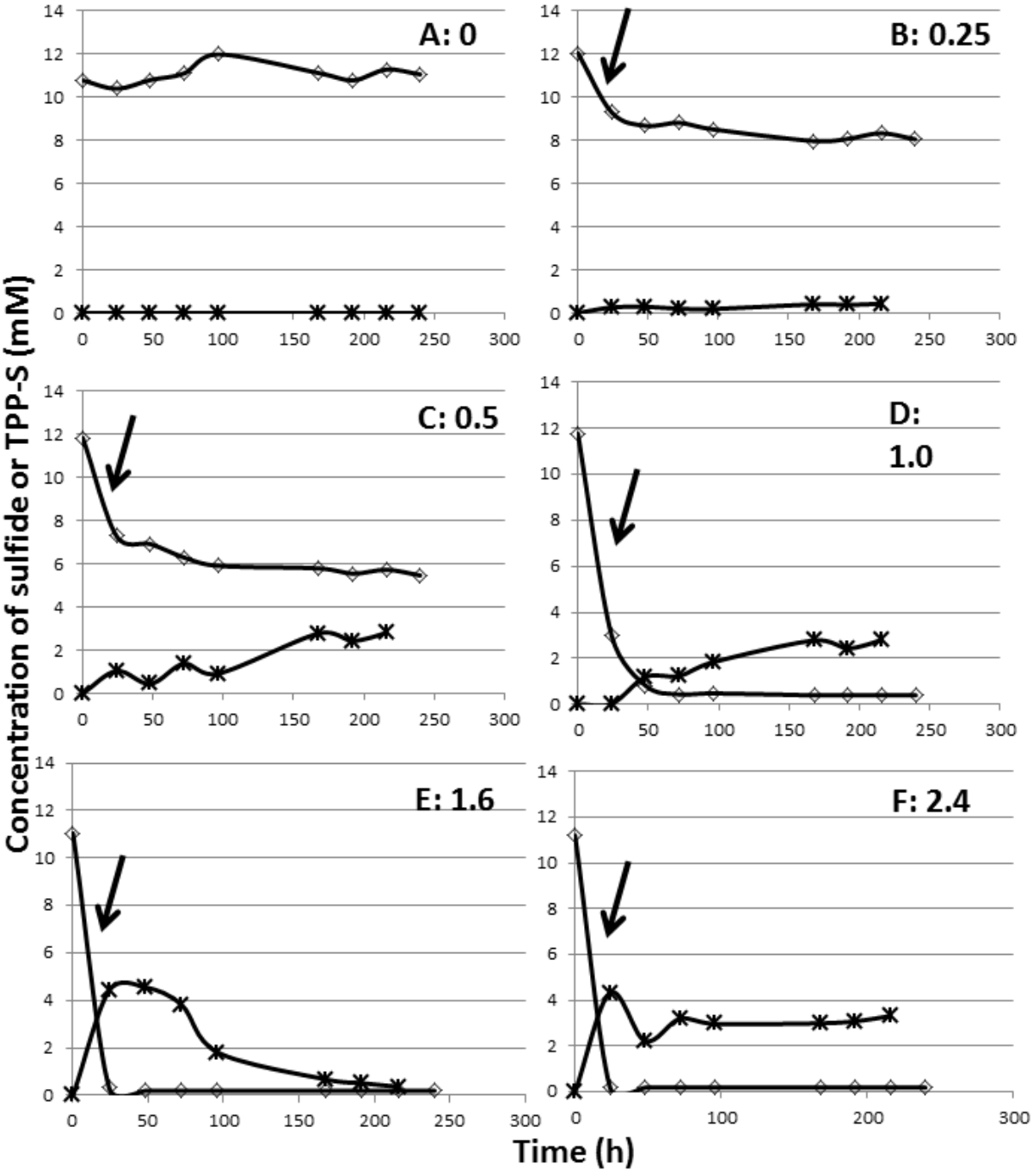

Figure 7.5 Concentrations of sulfide (◇) and TPP-S (∗) as a function of time for chemical incubations at R_{OS} of 0 to 2.4, as indicated. Oxygen was added at the indicated time (↓).

7.3.5 Comparison of biotic, abiotic and chemical conditions

Figure 7.6A shows a comparison of the percent sulfide oxidation in the three experiments. Under biotic conditions no net sulfide oxidation was observed until R_{OS} = 1.0, giving rise to an S-shaped curve. Under chemical and abiotic conditions sulfide oxidation increased linearly and was higher than under biotic conditions up to R_{OS} = 1.6 (Figure 7.6A). At R_{OS} = 1.0 the percentage of sulfide oxidation was 6-fold and 10-fold higher under abiotic and chemical conditions than under biotic conditions. Complete sulfide oxidation occurred for all three conditions at R_{OS} = 1.6 and R_{OS} = 2.4. The differences between R_{OS} values for 100% sulfide oxidation in the chemical and abiotic incubations indicates the presence of reduced, oxygen-reactive targets other than sulfide in the latter. The results show that live *D. vulgaris* was able to prevent sulfide oxidation up to R_{OS} = 0.5, presumably through direct oxygen reduction with lactate as the electron donor.

Low concentrations of TPP-S were found under all three conditions until R_{OS} = 1.0 (Figure 7.6B). More TPP-S was detected under biotic conditions at R_{OS} > 1. Similar concentrations of S were detected under biotic and abiotic conditions throughout (Figure 7.6C). No firm conclusions can be drawn whether live *D. vulgaris* forms more TPP-S than is formed under abiotic or chemical conditions at R_{OS} > 1 in view of the incomplete sulfur balances.

7.3.6 General and pitting corrosion

The general corrosion rates for the three incubations are compared in Figure 7.6D. The WP-LS medium alone was not corrosive (0.006 mm/yr, data not shown). Under biotic conditions with R_{OS} values of 0 to 0.5, the general corrosion rates were below 0.02 mm/yr. However, for R_{OS} of 1.0, 1.6 and 2.4 these increased to 0.050, 0.090 and 0.095 mm/yr, respectively. For the abiotic

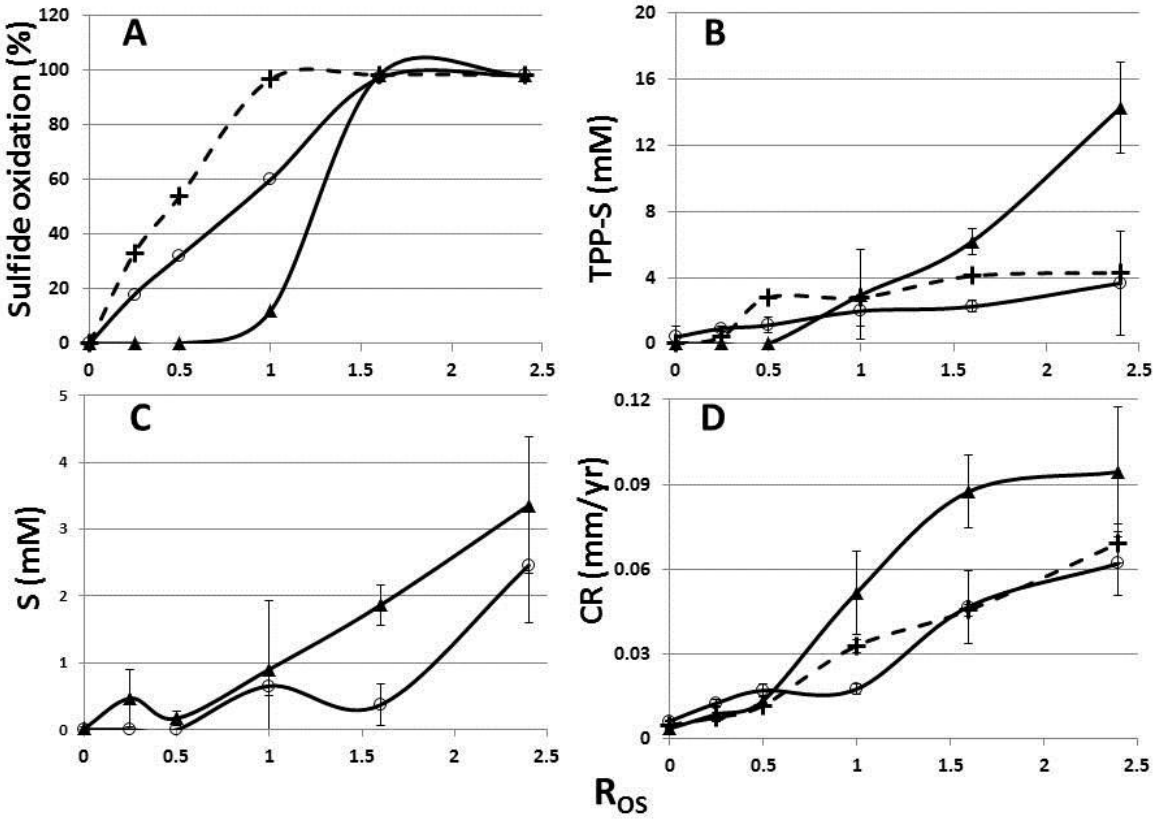

Figure 7.6 Comparison of biotic (▲), abiotic (○) and chemical (✚) conditions with respect to: (A) percent sulfide oxidation, (B) formation of TPP-S, (C) formation of S and (D) general corrosion rate as determined by weight loss. Maximum values of S and TPP-S are shown. R_{OS} values are shown on the x-axis. Error bars calculated as standard deviation. Triplicate data is shown for biotic and abiotic conditions.

incubations, the general corrosion rates increased continuously with increasing oxygen addition, although these remained quite low (0.006, 0.013, 0.017, 0.017, 0.046 and 0.061 mm/yr for R_{OS} values of 0 to 2.4, respectively). A similar trend was observed in the chemical incubations with corrosion rates of 0.005, 0.008, 0.012, 0.033, 0.045 and 0.069 mm/yr for R_{OS} values of 0 to 2.4, respectively. Overall, the corrosion rates appeared to depend more linearly on R_{OS} under abiotic and chemical conditions than under biotic conditions (Figure 7.6D). For R_{OS} values of 0 to 0.5 similar general corrosion rates were observed for all three conditions, whereas these were higher for biotic than for abiotic and chemical conditions for R_{OS} values of 1.0 or higher.

Examination of the surface of the corrosion coupons showed most pitting corrosion for the chemical incubation (Figure 7.7). At R_{OS} = 2.4, surface damage appeared to be similar for the three conditions, but the maximum observed pit depth was highest in the chemical incubation (Figure 7.8). Moreover, maximum pit depth increased with R_{OS} for chemical and abiotic incubations but not for biotic incubations (Figure 7.8).

7.3.7 Properties of sulfur formed

Sulfur particles were observed as highly refractive bodies in light microscopy images (Figure 7.9). Sulfur particles in the biotic incubation and its concentrate consisted of similarly-sized globules of 0.5 to 1.0 µm, which formed large aggregates (Figure 7.9A, B). Isolated sulfur globules were not found. Large, round single globules, as well as stick-shaped sulfur crystals, ranging in size from 1 µm to greater than 10 µm, were observed under abiotic conditions (Figure 7.9C, D). Sulfur formed under chemical conditions by dissolution in PCE and precipitation with water consisted of globules, sticks and other irregular shapes, ranging in size from 1 µm to greater than 10 µm (Figure 7.9E, F). No aggregates as in Figure 7.9B were observed. Overall, a variety of shapes and sizes of sulfur were formed under abiotic and chemical conditions, with

particles remaining separate from each other. The sulfur formed under biotic conditions always consisted of uniformly-sized globules which aggregated together.

For the partition tests with water and hexadecane, the sulfur from both the biotic and abiotic incubations dispersed into the bottom water layer; chemical sulfur flour remained in the hexadecane phase. When chemical sulfur flour was added to uninoculated WP-LS medium, the sulfur remained on the surface; when added to a stationary phase *D. vulgaris* culture, the sulfur sank to the bottom of the serum bottle after a few hours. This indicates that both the biotic and abiotically produced sulfur are hydrophilic, in contrast to sulfur flour which is hydrophobic.

7.4 Discussion

Corrosion due to sulfur formation from oxygen ingress has been reported previously (Boivin and Oliphant, 2011, Soylemezoglu and Harper, 1982, Fang et al., 2011, Boivin, 2010). In one case study, pipeline failure occurred when warm, wet gas came into contact with cold, slightly sour gas, resulting in water condensation. Oxygen in the water reacted with sulfide present to form S, which led to pitting and failure. XRD analysis revealed that 10% S was present in the pit deposits (Boivin and Oliphant, 2011). Failures have also been reported in systems with both low (trace) and high (25%) sulfide where oxygen-containing methanol was added for hydrate control. Analysis of deposits showed 25% and 16% S in each system, respectively (Boivin and Oliphant, 2011).

Sulfur formation has also been reported during oxygen ingress into geothermal systems with high-sulfide steam (Soylemezoglu and Harper, 1982).

Experiments with LPR suggest that it may not be the most effective corrosion monitoring technique in these conditions, as it posed several problems. Firstly, the LPR electrodes cannot be

autoclaved, so to establish the abiotic incubations the cultures were first grown with regular stoppers and then autoclaved. Then, the bottles had to be opened and refitted with the LPR electrodes, which allowed oxygen and other particles to enter the system. Secondly, there was less overall activity when the LPR electrodes were present; including a decrease in sulfide oxidation, S and TPP-S formation, and weight loss corrosion rates (Figure 7.2). A likely explanation for the decreased S and TPP-S formation is that the platinum counter electrode was acting as a catalyst for sulfur oxidation. To test this, a small piece of platinum wire was embedded in a soft agar plate with elemental sulfur. Within 24 hours, a clearing was observed around the wire, indicating that sulfur oxidation had occurred (data not shown). In addition, platinum and the added oxygen can react to form platinum oxide (ΔH = -32kcal/mol) as:

$Pt + O_2 \rightarrow PtO_2$ **Equation 7-1**

which would decrease the overall amount of oxygen available to react with aqueous sulfide. Overall, the presence of additional iron surfaces, as well as platinum and silver (reference electrode) create very complex chemistry in the small serum bottles, and is likely the source of the unusual results observed. Based on these results, it was decided that LPR is not a good tool to use in the presence of elemental sulfur.

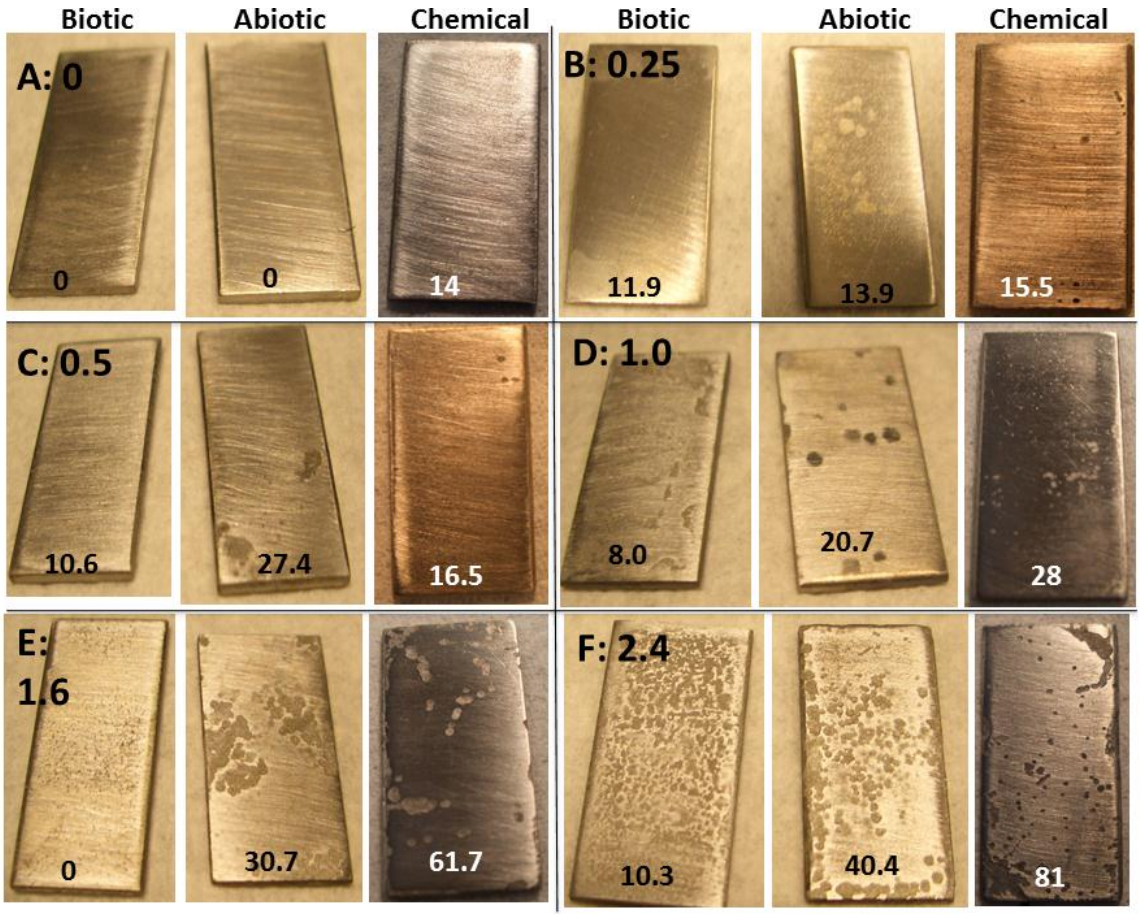

Figure 7.7 Visible surface damage of corrosion coupons from biotic, abiotic, and chemical incubations incubated for 1 month at 30 ^{o}C with (A-F) R_{OS} values of 0, 0.25, 0.5, 1.0, 1.6 and 2.4, as indicated. The measured maximum pit depth (μm) is indicated for each coupon.

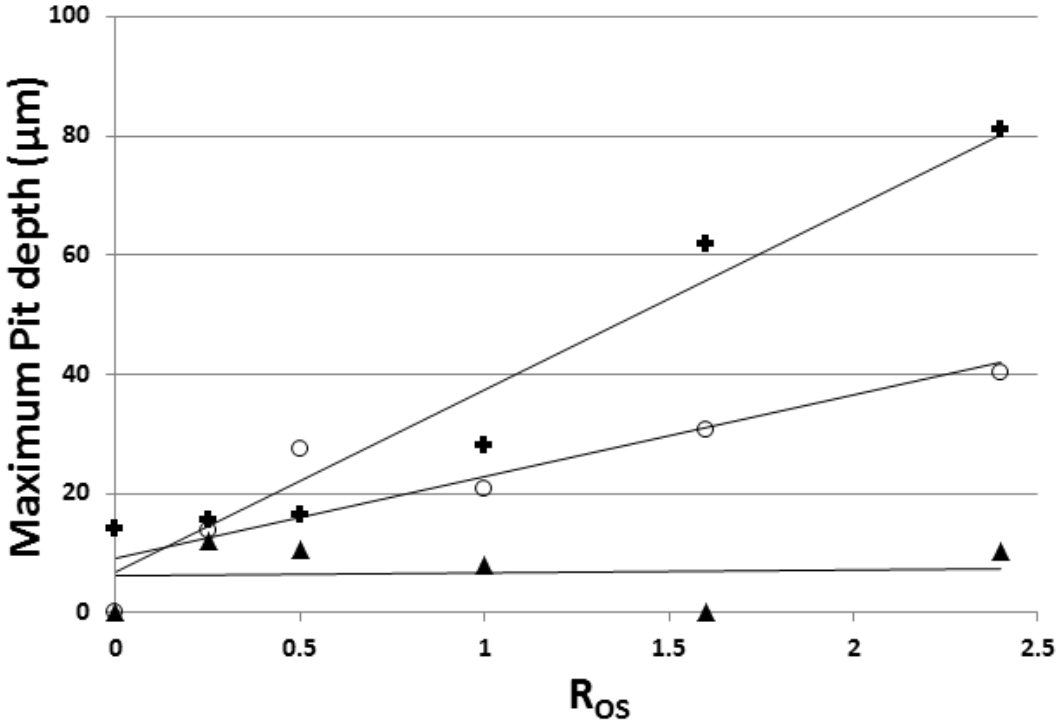

Figure 7.8 Maximum pit depth (µm) as a function of R_{OS} for biotic (▲), abiotic (○) and chemical (✚) incubations.

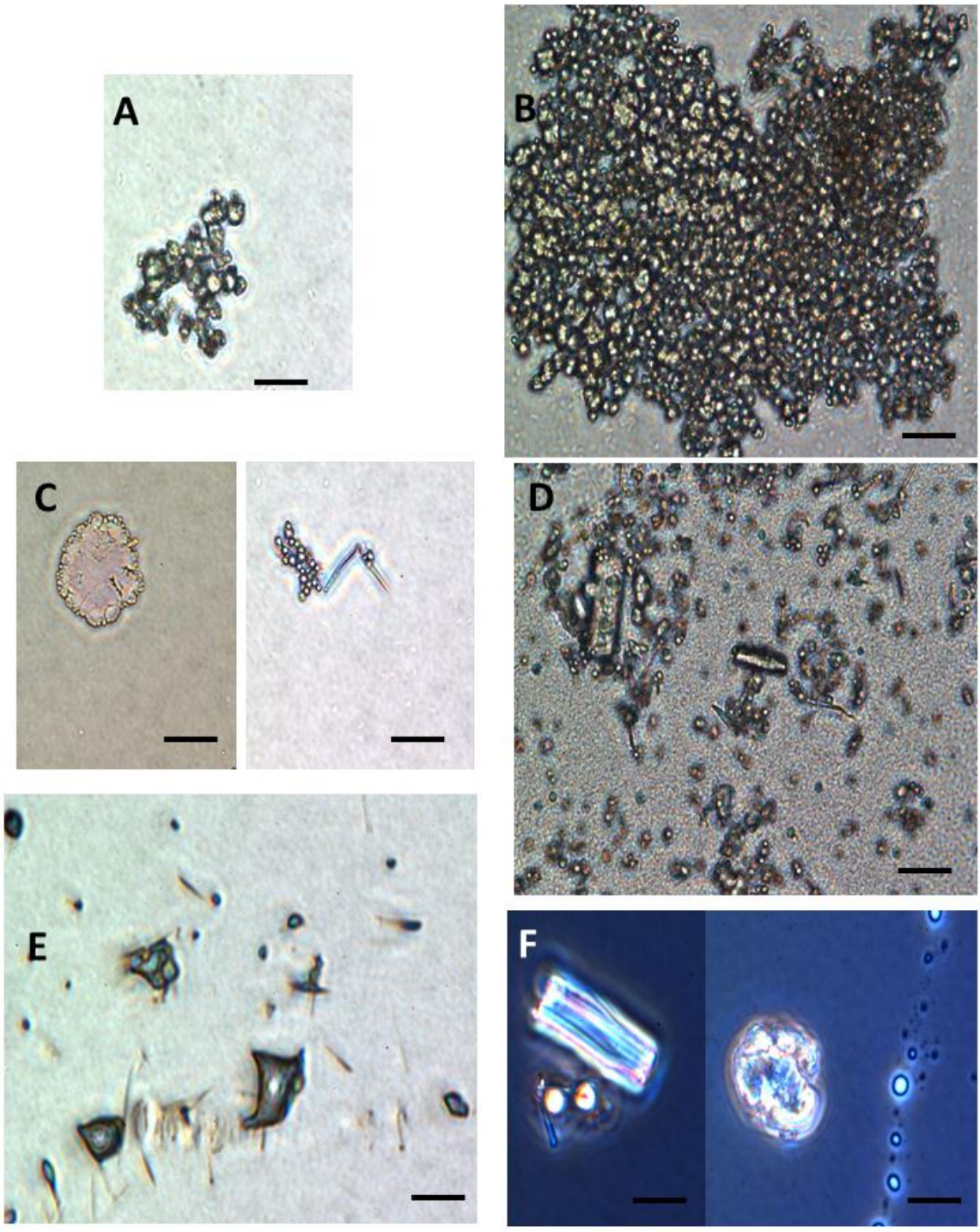

Figure 7.9 Light microscope images of sulfur formed under (A, B) biotic, (C, D) abiotic and (E, F) chemical conditions, generated as described in the text. Samples used for (B), (D) and (F) were concentrated by centrifugation. The bar is 10 μm in all cases.

We have shown here that *D. vulgaris* cells prevent sulfide oxidation up to R_{OS} = 0.5. At R_{OS} = 1.0, sulfide oxidation was less complete under biotic conditions, than under abiotic or chemical conditions (Figure 7.6A). Complete sulfide oxidation was observed for all conditions at R_{OS} = 1.6 and R_{OS} = 2.4. Live *D. vulgaris* used lactate completely at every R_{OS}. These observations suggest that at $R_{OS} < 1$, live *D. vulgaris* may form less S and TPP-S than is formed under abiotic or chemical conditions. This is not easily confirmed by direct measurement (Figure 7.6B, C), possibly because abiotic and chemical sulfur are less dispersed in the aqueous phase and were, therefore, less completely measured. At $R_{OS} > 1$ significant S and TPP-S was formed by live cells, which caused a higher general but a lower pitting corrosion rate (Figure 7.6, Figure 7.8). Increased dispersal of biotic sulfur may make it more prone to attack generally, but less prone to attack locally. Increased pitting corrosion is worse from a perspective of system integrity. Most pipeline failures are due to localized pitting, while few result from general corrosion (Jones, 1996). Therefore, reducing the rate of pit penetration is crucial. It should also be noted that during typical cases of oxygen ingress into pipelines, R_{OS} may be below 0.5 (Boivin and Oliphant, 2011, Soylemezoglu and Harper, 1982, Boivin, 2010, Fang et al., 2011). Additional experiments at low R_{OS} values of 0.2, 0.4, 0.6, and 0.8 indicated nearly identical general corrosion rates for biotic and abiotic conditions, but more severe pitting depth in the abiotic experiments (data not shown). Collectively, these data indicate that live *D. vulgaris* offers protection from pitting corrosion under conditions of oxygen ingress, because it can remove oxygen by respiration and therefore less corrosive sulfur products form.

The increased pitting under chemical and abiotic conditions (Figure 7.7, Figure 7.8) is thus likely caused by differences in the properties of the sulfur formed. Elemental sulfur is hydrophobic and remains as crystals in aqueous solution. Crystalline sulfur has a density of 1.9-

2.2 g cm^{-3} and a solubility in water of 5 μg/L (Kleinjan, 2005) . In contrast, biologically-formed sulfur is hydrophilic and can be dispersed in water. In sulfur-oxidizing bacteria, such as *Acidithiobacillus thiooxidans*, the hydrophilicity is thought to be due to interactions with phosphotidyl glycerol, which coats the sulfur and allows it to wet and disperse in water (Jones and Benson, 1965b, Jones and Starkey, 1961). *Allochromatium vinosum* oxidizes sulfide to sulfate with sulfur as an intermediate, which can be stored. The size of stored sulfur globules is limited by sulfur-binding proteins, which have so far only been found in *Allochromatium* species (Prange et al., 2004). Sulfur globules isolated from *Allochromatium* species had a density of only 1.31 g cm^{-3}, suggesting the presence of protein (Starkey, 1936, Hageage et al., 1970b, Truper, 2008). These hydrophilic sulfur globules turn into crystalline sulfur when the bacteria are killed or when the sulfur is extracted (Starkey, 1936, Truper, 2008, Hageage et al., 1970a). Likewise, we observed that biotic sulfur was present as aggregated globules of 0.5-1.0 μm, whereas abiotic and chemical sulfur were present as individual globules or as large crystals (Figure 7.9). The hexadecane-water partition test suggests that a metabolic product in *D. vulgaris* cultures (e.g. a phospholipid, as for *Thiobacillus thiooxidans* (Jones and Benson, 1965a)) may cause the wetting of biotic sulfur, allowing it to disperse in water. This coating may decrease contact between the sulfur and metal surfaces, decreasing pitting corrosion. This coating could be disrupted in abiotic incubations, where less biomass and thus less surfactant is available. Thus abiotic sulfur may make better direct contact with the metal surface than biotic sulfur. However, the presence of autoclaved biomass still confers significant protection, as pitting was less severe in the abiotic than in the chemical incubations. In increasing order of corrosion severity, biotic sulfur was clearly the least destructive, followed by abiotic and by chemical sulfur (Figure 7.8).

In conclusion, although programs to control bacteria in pipelines are routine and contribute to containment of biofouling and MIC, these may be counterproductive under conditions of sulfur formation due to oxygen ingress. The increased pitting corrosion under these conditions may be further enhanced by using biocides, because of the beneficial ability of microbes to respire oxygen with organic carbon as an electron donor and because sulfur formed by microbes is less corrosive. Biocide programs to eliminate fouling and MIC should, therefore, be restarted only after oxygen-free conditions have been restored.

Chapter Eight: Sulfur formation during nitrate injection

8.1 Introduction

The role of *D. vulgaris* in sulfur mediated corrosion during oxygen ingress was investigated in Chapter 7. But what about during nitrate injection, when nitrite and sulfide can potentially react to form S and PS? In a previous paper, sulfur formation in a reservoir under nitrate injection was modelled using the STARS program (Lin et al., 2008). It was predicted that sulfur production would increase as the nitrate: sulfide ratio decreased (Figure 6.1); in other words sulfur would increase in the zones between injectors and producers as the amount of nitrate dropped over space and time. This would suggest that sulfur mediated corrosion may then be a serious issue in the areas between injectors and producers (Lin et al., 2008). However, as discussed in Chapter 6, there are many sulfur cycle bacteria present in oilfields which may function to either oxidize or reduce sulfur once it forms (Figure 6.2). In addition, in Chapter 7 it was shown that live *D. vulgaris,* and perhaps other live bacteria, can alter the properties of sulfur that is produced to become a less aggressive form. This chapter investigates whether sulfur formation during nitrate injection actually occurs.

To do this, the sulfur content of oil and water samples taken from a field currently undergoing nitrate treatment was determined. The field, described in detail by Agrawal and colleagues (Agrawal et al., 2012), is the Medicine Hat Glauconitic C (MHGC) field, located in Medicine Hat, Alberta. It is a shallow (850 m), low-temperature (30 °C) field from which heavy oil with an American Petroleum Institute (API) gravity of 12–18° is produced by water reinjection (PWRI). During PWRI, water is injected into a reservoir to maintain or increase reservoir pressure,

thereby pushing oil towards a producing well. A schematic of a PWRI system is shown in Figure 8.1.

Souring in the MHGC field is currently being controlled via nitrate injection. Typically, water soluble volatile fatty acids are used as electron donors for both sulfate and nitrate reduction; however in this particular field, toluene and *m*- and *p*- xylene were shown to be the electron donors for nitrate reduction. The electron donors for sulfate reduction in the MHGC field are more diverse, encompassing a wide range of alkanes and alkyl benzenes (Agrawal et al., 2012). The MHGC field has been subject to 2 mM field wide nitrate injection (45% w/w calcium nitrate) at three water plants (WP): 1 WP and 17 WP since May 2007, and 20 WP since September 2008. A map of the field is shown in Figure 8.2.

Nitrate injection resulted in a 70% decrease in sulfide concentrations during the first 8 weeks of treatment, followed by a subsequent recovery to pre-nitrate injection sulfide concentrations. This is because sulfate reduction is possible in every part of the reservoir, and is not limited to the area around the injection well in low temperature oil fields (Agrawal et al., 2012). The injection water contains approximately 0.8 mM sulfate, meaning that SRB will grow in areas close to the injection well (IW). As nitrate is added and NRB are stimulated, SRB activity will be inhibited in this area, pushing the SRB further into the reservoir to nitrate free areas, thereby leading to a recovery of sulfide levels (Agrawal et al., 2012). It is critical to know whether sulfur formation takes place during nitrate injection so the corrosion risk of nitrate injection can be more accurately determined.

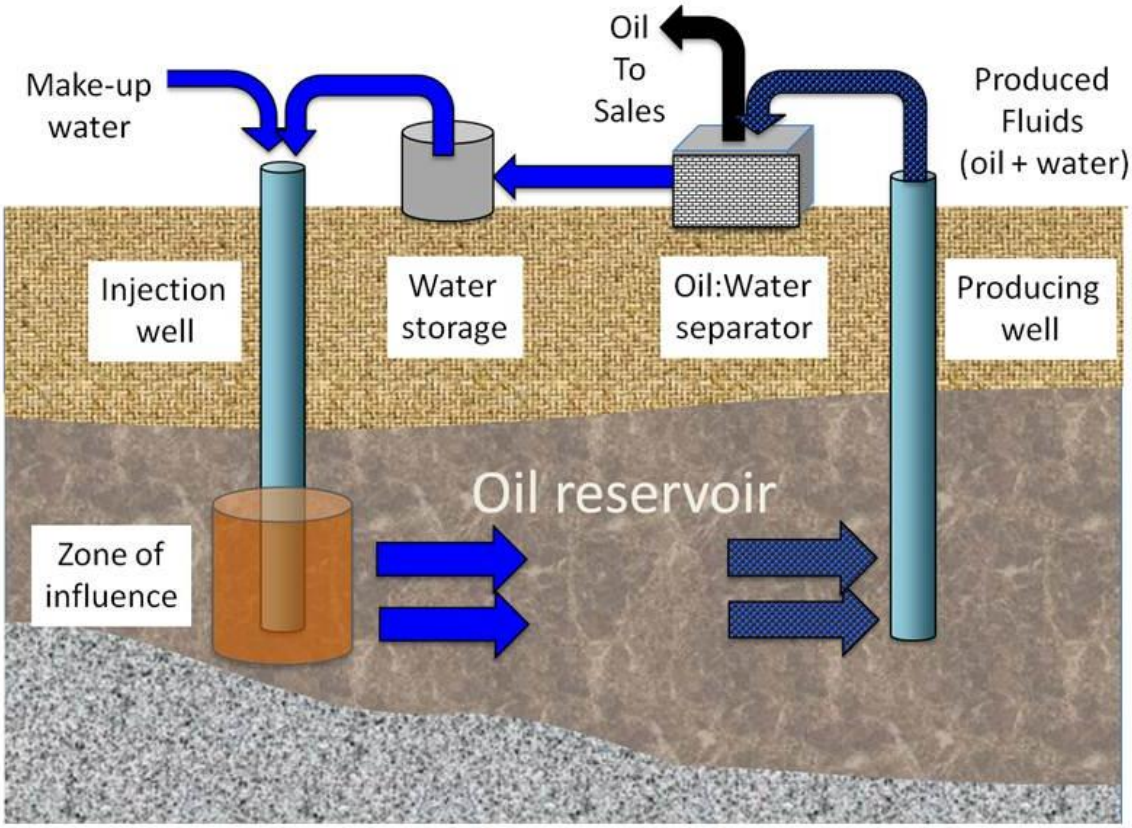

Figure 8.1 Schematic representation of oil production through PWRI. The oil-water mixture is pumped to the surface at producing wells (PW) and the oil and water separated. The water is piped to a water plant (WP) where it is mixed with make-up water, also known as source water (SW) to account for the lost volume. The water is then injected at injection wells (IW) (Gieg et al., 2011).

Sampling sites list as of Sept 2011

MHGC Field Site	Sampling Site List UWI	Unit
1-WP	04-02	Battery Waterplant
2-PW	03/03-35-12-05W4	producer
3-PW	0/02-03-13-05W4	producer
4-PW	02/02-10-13-05W4	producer
5-PW	02/07-09-13-05W4	producer
6-PW	02/13-16-13-05W4	producer
7-PW	02/12-09-13-05W4	producer
8-IW	00/12-09-13-05W4	Injector
9-PW	02/11-34-12-05W4	producer
10-PW	0/07-33-12-05W4	producer
11-PW	02/16-33-12-05W	producer
12-PW	03/05-34-12-05W4	producer
13-PW	03/15-04-13-05W4	producer
14-IW	00/15-04-13-05W4	Injector
15-PW	8D-08-13-05W4	producer
16-PW	04/14-04-13-05W4	producer
17-WP	06-16	Battery Waterplant
18-PW	02/02-09-13-05W4	producer
19-PW	05/15-04-13-05W4	producer
20-WP	15-07-13-05W4M	Battery Waterplant
21-SW	1F1/14-07-13-05W4	Source water
22-SW	04-04-13-05W4	Source water
23-SW	1F1/04-18-13-05W4	Source water

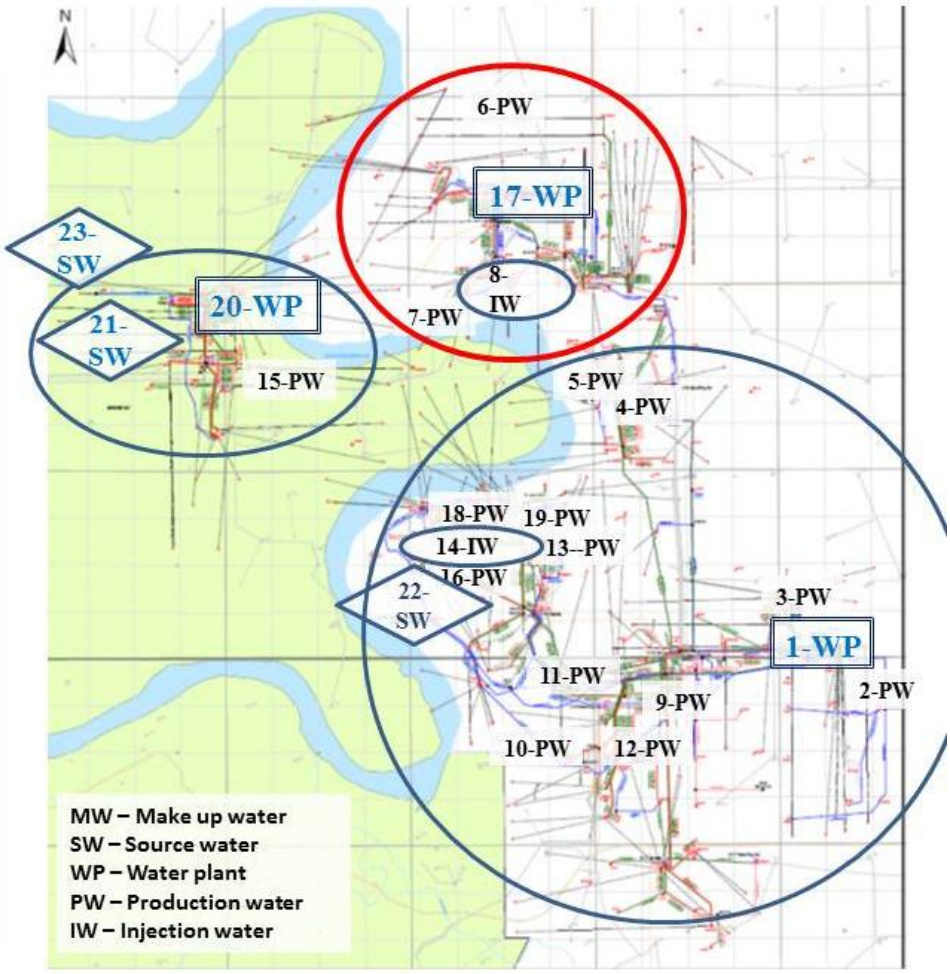

Figure 8.2 Map of the MHGC field in Medicine Hat, Alberta, showing the locations of sampling points (right) and the descriptions and coordinates of each site (left) (Voordouw et al., 2009).

8.2 Methods

All methods used were described in Chapter 2. Details of sample collection and hydrocarbon analysis are described by Agrawal and colleagues (Agrawal et al., 2012). Briefly, oil and water samples from three water plants, two injection wells, 14 production wells and three source waters were collected monthly for five years and stored in an anaerobic hood. Samples were collected in 1 L sterile Nalgene bottles filled completely to maintain anaerobic conditions. Concentrations of sulfide, sulfate, nitrite and nitrate were determined immediately. Hydrocarbon analysis was performed by GC-MS as previously described (Gieg et al., 2008). The oil (O) and water (W) from each sample was separated, and the samples prepared for sulfur (TPP-S) analysis in the anaerobic hood, and analyzed by GC-MS as described in Chapter 2. Both the oil and water phases were analyzed. Samples from July and August 2012 were analyzed.

8.3 Results

Nitrate, nitrite, sulfide and sulfate concentrations for 12-PW are shown in Figure 8.3. After 250 weeks, nitrate, nitrite and sulfate breakthrough were observed with a decrease in sulfide. Nitrate breakthrough in 12-PWcorresponded to a decrease in toluene concentrations, as seen in Figure 8.4

Toluene has been shown to serve as an electron donor for nitrate reduction in the MHGC field, and the toluene concentrations over time for all of the producing wells (PW) are shown in Figure 8.4. Toluene depleted oils were found in 2, 3, 4, 5, 9 and 12-PW, which corresponded with

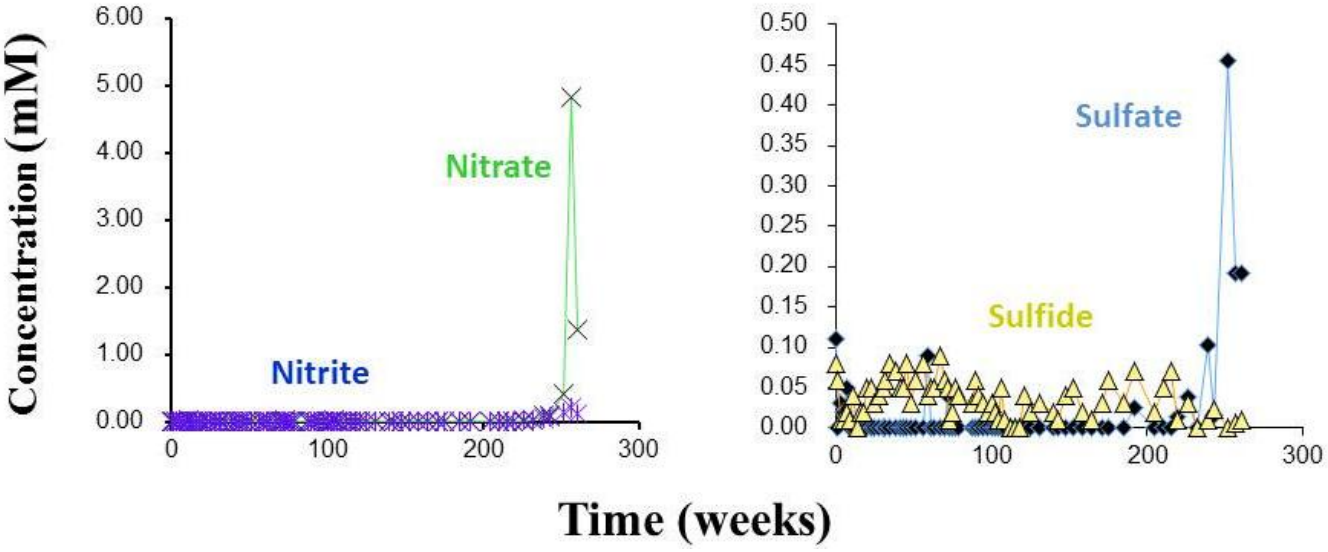

Figure 8.3 Left: breakthrough of nitrate and nitrite. Right: breakthrough of sulfate and decrease of sulfide from 12-PW following more than five years of nitrate injection.

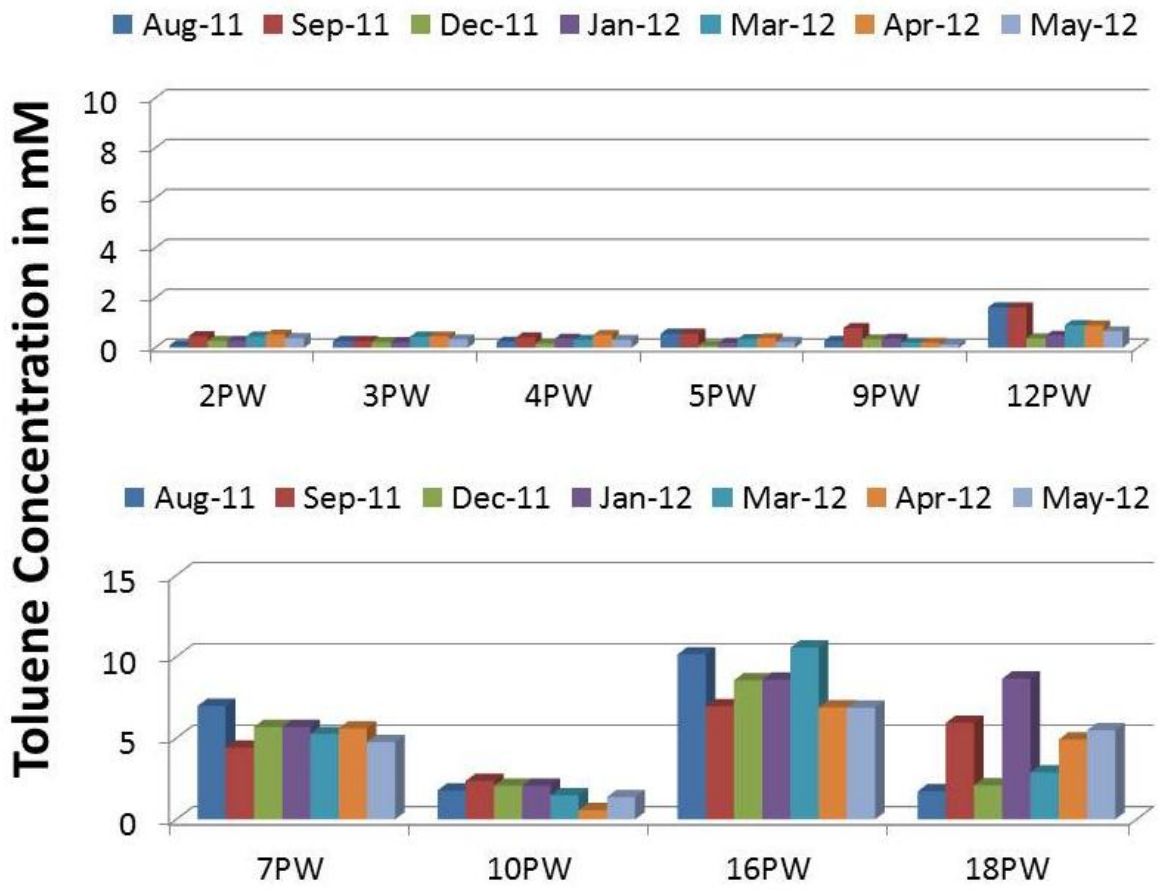

Figure 8.4 Toluene concentrations in oil from ten different PW's from August 2011 to May 2012.

sulfide concentrations that dropped to near zero (sulfide data not shown). Oils with higher toluene concentrations were found in 7-PW, 10-PW, 16-PW and 18-PW **(**Figure 8.4)

and the sulfide concentrations of these wells has fluctuated; but generally remained constant over time (sulfide data not shown).

The TPP-S content of the July and August 2012 samples was analyzed, and the results are shown in Figure 8.5. It can be seen in Figure 8.5 that TPP-S was detected only in the water phase, so in future analysis only the water phase needs to be analyzed. TPP-S was detected, from highest to lowest concentrations, respectively, in 5-PW, 12-PW, 19-PW, 29-PW, 13-PW, 18-PW, 4-PW, 25-PW, 9-PW and 30-PW. In 4-PW, 5-PW, 14-PW and 16-PW, TPP-S was detected only in the July samples. In 13-PW, 25-PW and 30-PW, TPP-S was detected only in August samples. In 9-PW and 29-PW, similar amounts of TPP-S were found in both months. With PW's 12 and 19, TPP-S increased from July to August (Figure 8.5).

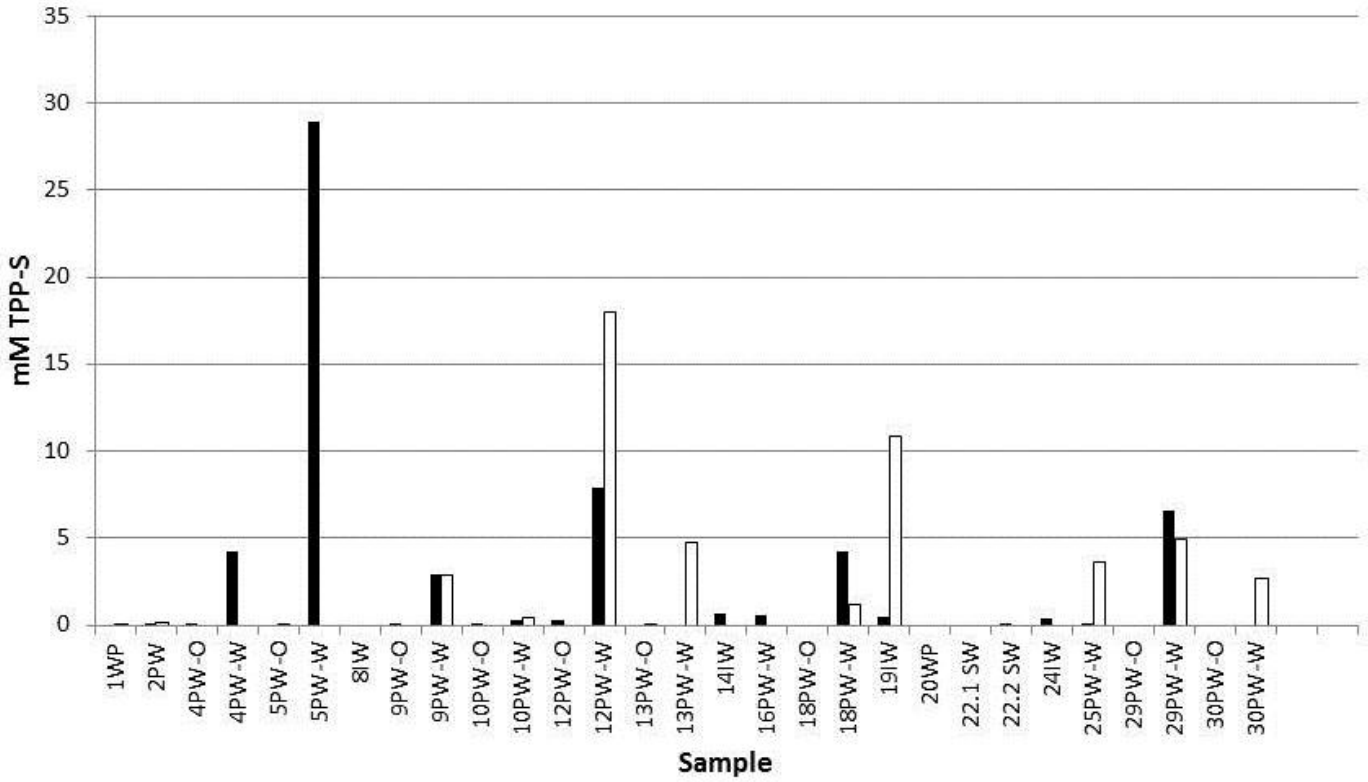

Figure 8.5 Sulfur formation (as TPP-S) from samples from the MHGC field from July (black) and August (white) 2012. Each sample was separated into oil (O) and water (W) phases. The numbers correspond to the wells as shown in Figure 8.2. WP- water plant; PW- produced water; IW-injection well; and SW – source water (make-up water).

8.4 Discussion

It has been recently shown that decreased toluene concentrations are indicative of nitrate breakthrough, as toluene is the preferred electron donor for NRB in the MHGC field (Agrawal et al., 2012). Therefore, wells with a low toluene concentration would have active populations of NRB reducing nitrate to nitrite. The nitrite produced would inhibit SRB activity (sulfide production), but would also react chemically with sulfide that was already present, to form S and PS as shown in Table 1-2 and Figure 6.1.

PW's 2, 3, 4, 5, 9 and 12 all have low toluene content, and nearly zero sulfide (toluene data Figure 8.4), and sulfur as TPP-S was detected in PW's 4, 5, 9 and 12 (Figure 8.5). Data for 3-PW was not available, and the water phase could not be separated from 2-PW to get an accurate reading. PW's 7, 10, 16 and 18 have higher toluene content and a relatively constant sulfide concentration (toluene data, Figure 8.4) which corresponds to low or no TPP-S detected. In other words, wells with demonstrated nitrate breakthrough show increased sulfur formation, which presents a potential corrosion risk.

As TPP-S concentrations varied in each well between July and August, it is difficult to state whether the sulfur that forms is a temporary side effect of the initial reaction of nitrite with residual sulfide, and if it will decrease or increase with time. Continued monitoring of the sulfur content of the samples and further corrosion tests are necessary to determine whether this sulfur formation truly represents a corrosion risk. As discussed in Chapters 6 and 7, the presence of other sulfur cycle bacteria and the presence of live bacteria can potentially remove and/or alter the sulfur formed to become less corrosive. How nitrate injection affects the populations of

sulfur reducing bacteria such as *Desulfuromonas acetoxidans* is currently being investigated, and is beyond the scope of this thesis. It is also not clear exactly whether the presence of live SRB makes the sulfur less corrosive, if it is some type of leaked metabolite or extrapolymeric substance (EPS), or other type of biosurfactant. Once this substance has been identified, it could be possible in the future to inject EPS along with nitrate to decrease the corrosivity of any sulfur that may form.

Chapter Nine: Conclusions

The experiments presented here have demonstrated that live SRB actually confer some degree of protection against corrosion caused by S and PS, which can form through chemical reaction of oxygen or nitrite with the SRB produced sulfide. These reactions are important as nitrite is used to control souring, and oxygen ingress into pipelines is a common occurrence.

Previously, when investigating the inhibitory mechanisms of nitrite on *D. vulgaris*, it was observed that the hybrid cluster protein, Hcp2 was upregulated 255 fold in the presence of nitrite (Haveman et al., 2004). It was also demonstrated that Hcp2 functions in polysulfide metabolism, and is part of an S and PS detoxification pathway involving Nrf. While investigating the role of *hcp2*, it was found that *hcp1* is part of a genomic island that confers resistance to oxygen and may allow for *D. vulgaris* to be a better anaerobe in the natural environment, as discussed in Chapter 3.

By adding oxygen or nitrite to live and autoclaved cultures of *D. vulgaris*, it was observed that both S and PS can easily form through chemical reaction with SRB produced sulfide and either oxygen or nitrite. It was demonstrated that both S and PS are inhibitory to *D. vulgaris*, and the mode of this inhibition is discussed in Chapter 4. Genome wide microarrays using tetrathionate were carried out, as tetrathionate reacts with sulfide to produce S and PS without the side effects of nitrite. It was observed from the microarray results that S and PS trigger an oxidative stress response in *D. vulgaris*, as many oxidative stress pathways were upregulated, along with an increase in expression of sulfur based amino acids. General growth and metabolism genes were downregulated, a similar trend observed as during oxygen exposure (Chapter 4). Therefore, S and PS are inhibitory to *D. vulgaris* due to the resultant increase in redox potential, as seen in Figure 4.2.

The ability of *D. vulgaris* to metabolize S and PS was investigated in Chapter 5. S and PS were formed through reaction of oxygen and biogenic sulfide in the presence of live or autoclaved cells. It was found that live cells could prevent the formation of, and remove small amounts of S and PS.

With an understanding of how S and PS can form, how they inhibit *D. vulgaris*, and how in turn *D. vulgaris* is able to cope with these compounds, we focused on the implications of S and PS on iron corrosion and how it can be removed in oilfield facilities once it is formed. Chapter 6 investigated the corrosivity of S and PS, and determined the potential of SRB and other sulfur cycle bacteria which are commonly found in pipelines to remove these corrosive products.

The reaction of sulfide with oxygen to form S and PS, and its effects on corrosion rates were explored in both biotic and abiotic conditions. Under conditions in which S and PS could not be removed, such as the abiotic experiments and with various mutants of *hcp2*, there was a notable increase in corrosion rates and surface damage to the corrosion coupons. However, if S and PS do form in an oilfield, microbial action is required to remove them. *Desulfuromonas acetoxidans*, a sulfur reducer commonly found in oilfields, was able to reduce sulfur formed through reaction of sulfide and oxygen back to sulfide, and is one potential source of sulfur removal in oilfields. Additionally, S and PS removal can be achieved either by use of additional nitrate which will allow the NRB to completely oxidize S and PS to sulfate (Figure 6.1), or by the action of other microorganisms summarized in Figure 6.2.

In this view, the formation of S and PS during nitrate treatment may not be as much of a concern as initially thought (Lin et al., 2008), as it can potentially be removed by a variety of resident sulfur cycle microbes.

Corrosion scenarios during oxygen ingress were then investigated. It was hypothesized that the experiments with live *D. vulgaris* would have substantially higher corrosion rates than the abiotic experiments. Oxygen was added to bottles with live or autoclaved *D. vulgaris*, or to high sulfide WP-LS medium, and it was observed that live cells could delay the formation of S and PS up to an oxygen: sulfide ratio of 1:1, which should reduce corrosion rates up to this point. Surprisingly, similar weight loss corrosion rates were seen in all conditions. However, upon closer inspection of the corrosion coupons, it was found that the surface damage and pitting type corrosion increased in severity as biotic<abiotic<chemical incubations (Figure 7.6). This was a curious observation, and the types of sulfur formed under each condition were examined to see if this was causing the differing pitting severity.

It was found that there was a striking difference in the properties of sulfur formed under each condition, as shown in Figure 7.7. It is apparent that some type of bacterial metabolite or excreted substance is acting to reduce the rates of pitting corrosion by altering the properties of the sulfur formed, as the highest rates of pitting were observed when no bacteria at all were present.

Finally, sulfur formation in an oilfield under nitrate injection was investigated. The sulfur content of oil and water samples from the MHGC field, described in the previous chapter, was determined. It was found that sulfur was only found in produced waters with low toluene content, which is indicative of nitrate breakthrough, and therefore the presence of nitrite. This is potentially worrisome as it suggests that sulfur formation does occur as a result of nitrate injection despite the presence of sulfur-removing microbes, meaning that nitrate injection can control souring at the cost of a potentially higher corrosion risk.

The experiments and data presented here allow for more informed decisions to be made regarding souring and corrosion control in pipelines. The formation of S and PS can occur quite easily, and can be exacerbated by souring control methods (nitrate injection) or oxygen ingress. However, with careful monitoring of system chemistry, their formation can be prevented; but, if formed, they can potentially be removed through the action of a variety of oilfield microbes, including *D. vulgaris.*

Hence, SRB present a complex case when it comes to souring and corrosion: they are the cause of souring and a major player in MIC, but are also able to prevent the formation of and remove corrosive sulfur species and alter the properties of sulfur to be less corrosive in terms of pitting. Therefore, it may actually be detrimental to attempt to completely eradicate SRB and other microbes from a system, and the aim should be more towards controlling their activity and preventing the formation of S and PS. The research presented here again highlights the great importance of having a clear understanding of not only system chemistry, but biology as well, before biocides and other treatment programs are implemented. As we learn more about petroleum microbiology, it becomes increasingly clear that industry can no longer ignore the biological aspects; we need to bridge the gaps between chemistry, biology and engineering as problems such as souring and corrosion are multidisciplinary. In particular, with regards to oxygen ingress, biocide programs should only be restarted after oxygen-free conditions have been restored. These findings also open the door to the potential development of biosurfactants or other bacterial substances as a means of controlling sulfur corrosion by converting any sulfur present in a pipeline to a less aggressive form, potentially providing a "green" and low cost alternative to corrosion control.

References

www.corrosionsource.com/.../galv_series.gif [Online]. [Accessed February 8, 2010.

www.gordonengland.co.uk/img/corr5.gif [Online]. [Accessed February 9, 2010.

VIMSS, Virtual Institute for Microbial Stress and Survival. *Microbes Online* [Online]. Available: http://www.microbesonline.org/ [Accessed February20, 2010.

AGRAWAL, A., PARK, H. S., NATHOO, S., GIEG, L. M., JACK, T. R., MINER, K., ERTMOED, R., BENKO, A. & VOORDOUW, G. 2012. Toluene depletion in produced oil contributes to souring control in a field subjected to nitrate injection. *Environmental Science & Technology,* 46**,** 1285-1292.

ALEKSEEV, V. I., KISELEV, O. A. & LEVSHINA, I. V. 1990. Role of the high-pressure of hydrogen in the phenomenon of hydrogen-sulfide corrosion cracking of steel. *Soviet Materials Science,* 26**,** 149-152.

ARAGAO, D., MITCHELL, E. P., FRAZAO, C. F., CARRONDO, M. A. & LINDLEY, P. F. 2008. Structural and functional relationships in the hybrid cluster protein family: structure of the anaerobically purified hybrid cluster protein from *Desulfovibrio vulgaris* at 1.35 angstrom resolution. *Acta Crystallographica Section D-Biological Crystallography,* 64**,** 665-674.

ANTHONY, A., OSEME, I. & ADESINA, F. 2009. Possible sources of hydrogen sulfide in petroleum reservoirs – challenges and implications. *Biotechnologies for Improved Oil and Gas Production in the Gulf of Guinea (BIOPOG3).* Abuja, Nigeria.

BELLER, H. R., CHAIN, P. S. G., LETAIN, T. E., CHAKICHERLA, A., LARIMER, F. W., RICHARDSON, P. M., COLEMAN, M. A., WOOD, A. P. & KELLY, D. P. 2006. The genome sequence of the obligately chemolithoautotrophic, facultatively anaerobic bacterium *Thiobacillus denitrificans. Journal of Bacteriology,* 188**,** 1473-1488.

BOARD: Alberta Energies and Utilities Board, 2007. Report 2007-A: Pipeline performance in Alberta, 1990-2005.

BODEN, R., KELLY, D. P., MURRELL, J. C. & SCHAFER, H. 2010. Oxidation of dimethylsulfide to tetrathionate by *Methylophaga thiooxidans* sp. nov.: a new link in the sulfur cycle. *Environmental Microbiology,* 12**,** 2688-2699.

BOIVIN, J. Sulfur Failures in Low H_2S Systems. From NACE Calgary Northern Area Elemental Sulfur Corrosion Mini Symposium, 2010 Calgary, Alberta, October 8, 2010

BOIVIN, J. & OLIPHANT, S. 2011. Sulfur Corrosion due to Oxygen Ingress. In: *NACE International, Corrosion 2011 Conference and Expo.* Houston, Texas: NACE International.

BRIOUKHANOV, A., PIEULLE, L. & DOLLA, A. 2010. Antioxidative defense systems of anaerobic sulfate-reducing microorganisms *Current Research, Technology and Education Topics in Applied Microbiology and Microbial Biotechnology.* [Online]. Available: http://www.formatex.info/microbiology2/148-159.pdf.

CAFFREY, S. A., PARK, H. S., VOORDOUW, J. K., HE, Z., ZHOU, J. & VOORDOUW, G. 2007. Function of periplasmic hydrogenases in the sulfate-reducing bacterium *Desulfovibrio vulgaris* Hildenborough. *Journal of Bacteriology,* 189**,** 6159-6167.

CAFFREY, S. M., PARK, H. S., BEEN, J., GORDON, P., SENSEN, C. W. & VOORDOUW, G. 2008. Gene expression by the sulfate-reducing bacterium *Desulfovibrio vulgaris* Hildenborough grown on an iron electrode under cathodic protection conditions. *Applied and Environmental Microbiology,* 74**,** 2404-2413.

CAFFREY, S. M. & VOORDOUW, G. 2010. Effect of sulfide on growth physiology and gene expression of *Desulfovibrio vulgaris* Hildenborough. *Antonie Van Leeuwenhoek International Journal of General and Molecular Microbiology,* 97**,** 11-20.

CHHABRA, S. R., HE, Q., HUANG, K. H., GAUCHER, S. P., ALM, E. J., HE, Z., HADI, M. Z., HAZEN, T. C., WALL, J. D., ZHOU, J., ARKIN, A. P. & SINGH, A. K. 2006. Global analysis of heat shock response in *Desulfovibrio vulgaris* Hildenborough. *Journal of Bacteriology,* 188**,** 1817-1828.

CORD-UWISCH, R. 1985. A quick method for the determination of dissolved and precipitated sulfides in cultures of sulfate-reducing bacteria. *Journal of Microbiological Methods,* 4**,** 33-36.

CORREA, L. A., BAPTISTA, W. & FERREIRA, L. A. Wet H_2S and CN^- corrosion control through on-site polysulfide generation. *6th Annual International Conference on Equipment Technologies*. 2002 Salvador-Bahia, Brazil.

DECKERS, H. M. & VOORDOUW, G. 1994. Membrane topology of the methyl-accepting chemotaxis protein DcrA from *Desulfovibrio vulgaris* Hildenborough. *Antonie Van Leeuwenhoek International Journal of General and Molecular Microbiology,* 65**,** 7-12.

DEXTER, S. C. & LAFONTAINE, J. P. 1998. Effect of natural marine biofilms on galvanic corrosion. *Corrosion,* 54**,** 851.

DINH, H. T., KUEVER, J., MUSSMANN, M., HASSEL, A. W., STRATMANN, M. & WIDDEL, F. 2004. Iron corrosion by novel anaerobic microorganisms. *Nature,* 427**,** 829-832.

DOBRINDT, U., HOCHHUT, B., HENTSCHEL, U. & HACKER, J. 2004. Genomic islands in pathogenic and environmental microorganisms. *Nature Reviews Microbiology,* 2**,** 414-424.

DOLLA, A., KURTZ, J. D. M., TEIXEIRA, M. & VOORDOUW, G. 2007. Biochemical, proteomic and genetic characterization of oxygen survival mechanisms in sulfate-reducing bacteria of the genus *Desulfovibrio*. *In:* BARTON, L. L. A. H., W. A. (ed.) *Sulphate-Reducing Bacteria: Environmental and Engineered Systems 1st Ed.* 1 ed. Cambridge, UK: Cambridge University Press.

DOWLING, N. I. 1992. Corrosion of materials used in storage and handling of solid elemental sulfur. *Materials Performance: Sulfur and Energy.*

DUNCAN, K. E., GIEG, L. M., PARISI, V. A., TANNER, R. S., TRINGE, S. G., BRISTOW, J. & SUFLITA, J. M. 2009. Biocorrosive thermophilic microbial communities in Alaskan North Slope oil facilities. *Environmental Science & Technology,* 43**,** 7977-7984.

EVANS, U. R. 1981. *An Introduction to Metallic Corrosion,* London.

FANG, H., BROWN, B., YOUNG, D. & NEŠIĆ, S. 2011. Investigation of Elemental Sulfur Corrosion Mechanisms. *In: NACE International Corrosion 2011 Conference and Expo.* Houston, Texas: NACE International.

FINSTER, K., BAK, F. & PFENNIG, N. 1994. *Desulfuromonas acetexigens* sp-nov, a dissimilatory sulfur-reducing eubacterium from anoxic fresh-water sediments. *Archives of Microbiology,* 161**,** 328-332.

FLATLEY, J., BARRETT, J., PULLAN, S. T., HUGHES, M. N., GREEN, J. & POOLE, R. K. 2005. Transcriptional responses of *Escherichia coli* to S-nitrosoglutathione under defined chemostat conditions reveal major changes in methionine biosynthesis. *Journal of Biological Chemistry,* 280**,** 10065-10072.

FU, R. D. & VOORDOUW, G. 1997. Targeted gene-replacement mutagenesis of DcrA, encoding an oxygen sensor of the sulfate-reducing bacterium *Desulfovibrio vulgaris* Hildenborough. *Microbiology-Uk,* 143**,** 1815-1826.

FU, R. D., WALL, J. D. & VOORDOUW, G. 1994. DcrA, a c-type heme-containing methyl-accepting proten from *Desulfovibrio vulgaris* Hildenborough, senses the oxygen concentration of the environment. *Journal of Bacteriology,* 176**,** 344-350.

GHOSH, W. & DAM, B. 2009. Biochemistry and molecular biology of lithotrophic sulfur oxidation by taxonomically and ecologically diverse bacteria and archaea. *Fems Microbiology Reviews,* 33**,** 999-1043.

GREENE, E. A., HUBERT, C., NEMATI, M., JENNEMAN, G. E. & VOORDOUW, G. 2003. Nitrite reductase activity of sulphate-reducing bacteria prevents their inhibition by nitrate-reducing, sulphide-oxidizing bacteria. *Environmental Microbiology,* 5**,** 607-617.

HAGEAGE, G. J., EANES, E. D. & GHERNA, R. L. 1970b. X-ray diffraction studies of sulfur globules accumulated by *Chromatium* species. *Journal of Bacteriology,* 101**,** 464-469.

HAMILTON, W. A. 2003. Microbially influenced corrosion as a model system for the study of metal microbe interactions: A unifying electron transfer hypothesis. *Biofouling,* 19**,** 65-76.

HARDY, J. A. & BROWN, J. L. 1984. The corrosion of mild steel by biogenic sulfide films exposed to air. *Corrosion,* 40**,** 650-654.

HAVEMAN, S. A., BRUNELLE, V., VOORDOUW, J. K., VOORDOUW, G., HEIDELBERG, J. F. & RABUS, R. 2003. Gene expression analysis of energy metabolism mutants of *Desulfovibrio vulgaris* Hildenborough indicates an important role for alcohol dehydrogenase. *Journal of Bacteriology,* 185**,** 4345-4353.

HAVEMAN, S. A., GREENE, E. A., STILWELL, C. P., VOORDOUW, J. K. & VOORDOUW, G. 2004. Physiological and gene expression analysis of inhibition of *Desulfovibrio vulgaris* Hildenborough by nitrite. *Journal of Bacteriology,* 186**,** 7944-7950.

HAVEMAN, S. A., GREENE, E. A. & VOORDOUW, G. 2005. Gene expression analysis of the mechanism of inhibition of *Desulfovibrio vulgaris* Hildenborough by nitrate-reducing, sulfide-oxidizing bacteria. *Environmental Microbiology,* 7**,** 1461-1465.

HE, Q., HUANG, K. H., HE, Z. L., ALM, E. J., FIELDS, M. W., HAZEN, T. C., ARKIN, A. P., WALL, J. D. & ZHOU, J. Z. 2006. Energetic consequences of nitrite stress in *Desulfovibrio vulgaris* Hildenborough, inferred from global transcriptional analysis. *Applied and Environmental Microbiology,* 72**,** 4370-4381.

HECK, E. T. 1940. Hydrogenantion of oil: suggested natural source of hydrogen. *Bull. Amer. Assoc. Petr. Geol.,* 24, 1475-1497.

HEIDELBERG, J. F., SESHADRI, R., HAVEMAN, S. A., HEMME, C. L., PAULSEN, I. T., KOLONAY, J. F., EISEN, J. A., WARD, N., METHE, B., BRINKAC, L. M., DAUGHERTY, S. C., DEBOY, R. T., DODSON, R. J., DURKIN, A. S., MADUPU, R., NELSON, W. C., SULLIVAN, S. A., FOUTS, D., HAFT, D. H., SELENGUT, J., PETERSON, J. D., DAVIDSEN, T. M., ZAFAR, N., ZHOU, L. W., RADUNE, D., DIMITROV, G., HANCE, M., TRAN, K., KHOURI, H., GILL, J., UTTERBACK, T. R., FELDBLYUM, T. V., WALL, J. D., VOORDOUW, G. & FRASER, C. M. 2004. The genome sequence of the anaerobic, sulfate-reducing bacterium *Desulfovibrio vulgaris* Hildenborough. *Nature Biotechnology,* 22**,** 554-559.

HENSEL, M., HINSLEY, A. P., NIKOLAUS, T., SAWERS, G. & BERKS, B. C. 1999. The genetic basis of tetrathionate respiration in *Salmonella typhimurium*. *Molecular Microbiology,* 32**,** 275-287.

HERRERA, L. K. & VIDELA, H. A. 2009. Role of iron-reducing bacteria in corrosion and protection of carbon steel. *International Biodeterioration & Biodegradation,* 63**,** 891-895.

HOGSLUND, S., REVSBECH, N. P., KUENEN, J. G., JORGENSEN, B. B., GALLARDO, V. A., VAN DE VOSSENBERG, J. V., NIELSEN, J. L., HOLMKVIST, L., ARNING, E. T. & NIELSEN, L. P. 2009. Physiology and behaviour of marine *Thioploca*. *Isme Journal,* 3**,** 647-657.

HUBERT, C., NEMATI, M., JENNEMAN, G. & VOORDOUW, G. 2003. Containment of biogenic sulfide production in continuous up-flow packed-bed bioreactors with nitrate or nitrite. *Biotechnology Progress,* 19**,** 338-345.

HUBERT, C., NEMATI, M., JENNEMAN, G. & VOORDOUW, G. 2005. Corrosion risk associated with microbial souring control using nitrate or nitrite. *Applied Microbiology and Biotechnology,* 68**,** 272-282.

INAGAKI, F., TAKAI, K., NEALSON, K. H. & HORIKOSHI, K. 2004. *Sulfurovum lithotrophicum* gen. nov., sp nov., a novel sulfur-oxidizing chemolithoautotroph within the epsilon-Proteobacteria isolated from Okinawa Trough hydrothermal sediments. *International Journal of Systematic and Evolutionary Microbiology,* 54**,** 1477-1482.

JACK, T. 1990. Biological Corrosion Failures. In*:* Lampan, S. (ed.) *Failure analysis and prevention, ASM Handbook.* Materials Park, OH, USA: ASM International.

JACK, T. & WARD, V. 1983. Literature survey: Bacterially enhanced corrosion of pipelines. NOVA/Husky Research Corporation.

JOHNSTON, S., LIN, S. P., LEE, P., CAFFREY, S. M., WILDSCHUT, J., VOORDOUW, J. K., DA SILVA, S. M., PEREIRA, I. A. C. & VOORDOUW, G. 2009. A genomic island of the sulfate-reducing bacterium *Desulfovibrio vulgaris* Hildenborough promotes survival under stress conditions while decreasing the efficiency of anaerobic growth. *Environmental Microbiology,* 11**,** 981-991.

JONES, D. 1996. *Principles and prevention of corrosion,* Upper Saddle River, NJ, UDA, Prentice Hall.

JONES, G. E. & BENSON, A. A. 1965. Phosphatidyl glycerol in *Thiobacillus Thiooxidans. Journal of Bacteriology,* 89**,** 260-261.

JONES, G. E. & STARKEY, R. L. 1961. Surface-active substrates produced by *Thiobacillus Thiooxidans. Journal of Bacteriology,* 82**,** 788-789.

JORGENSEN, B. B. & BAK, F. 1991. Pathways and Microbiology of thiosulfate transformations and sulfate reduction in a marine sediment. *Applied and Environmental Microbiology,* 57**,** 847-856.

KAMYSHNY, A., GOIFMAN, A., GUN, J., RIZKOV, D. & LEV, O. 2004. Equilibrium distribution of polysulfide ions in aqueous solutions at 25 degrees C: A new approach for the study of polysulfides equilibria. *Environmental Science & Technology,* 38**,** 6633-6644.

KANAO, T., KAMIMURA, K. & SUGIO, T. 2007. Identification of a gene encoding a tetrathionate hydrolase in *Acidithiobacillus ferrooxidans. Journal of Biotechnology,* 132**,** 16-22.

KASTER, K. M., GRIGORIYAN, A., JENNEMAN, G. & VOORDOUW, G. 2007. Effect of nitrate and nitrite on sulfide production by two thermophilic, sulfate-reducing enrichments from an oil field in the North Sea. *Applied Microbiology and Biotechnology,* 75**,** 195-203.

KLEINJAN, W. 2005. *Biologically produced sulfur particles and polysulfide ions: Effects on a biotechnological process for the removal of hydrogen sulfide from gas streams.* Ph.D. dissertation, Wageningen University.

KLIMMEK, O., KROGER, A., STEUDEL, R. & HOLDT, G. 1991. GROWTH OF WOLINELLA-SUCCINOGENES WITH POLYSULFIDE AS TERMINAL ACCEPTOR OF PHOSPHORYLATIVE ELECTRON-TRANSPORT. *Archives of Microbiology,* 155**,** 177-182.
LIN, S., VOORDOUW, G. & COOMBE, D. Sulfur production associated with souring control by nitrate injection: a potential corrosion risk? NACE International 2008, 2008 Las Vegas, USA. Paper 08662.

MADIGAN, M. T., MARTINKO, J. M. & PARKER, J. 2003. *Brock Biology of Microorganisms,* Upper Saddle River, NJ, USA, Prentice Hall.

MARA, D. D. & WILLIAMS, D. J. A. The mechanism of sulphide corrosion by sulphate-reducing bacteria. Proceedings of the Second International Biodeterioration Symposium, 1975 Lunteren, Netherlands. 110-113.

MOHAPATRA, B. R., GOULD, W. D., DINARDO, O. & KOREN, D. W. 2008. An Overview of the Biochemical and Molecular Aspects of Microbial Oxidation of Inorganic Sulfur Compounds. *Clean-Soil Air Water,* 36**,** 823-829.

MUKHOPADHYAY, A., REDDING, A. M., JOACHIMIAK, M. P., ARKIN, A. P., BORGLIN, S. E., DEHAL, P. S., CHAKRABORTY, R., GELLER, J. T., HAZEN, T. C., HE, Q., JOYNER, D. C., MARTIN, V. J. J., WALL, J. D., YANG, Z. K., ZHOU, J. & KEASLING, J. D. 2007. Cell-wide responses to low-oxygen exposure in *Desulfovibrio vulgaris* Hildenborough. *Journal of Bacteriology,* 189**,** 5996-6010.

NACE 2005. NACE Standard Recommended Practice RP00775-2005. Preparation, installation, analysis and interpretation of corrosion coupons in oilfield operation. In: National Association of Corrosion Engineers.

NEMATI, M., JENNEMAN, G. E. & VOORDOUW, G. 2001. Impact of nitrate-mediated microbial control of souring in oil reservoirs on the extent of corrosion. *Biotechnology Progress,* 17**,** 852-859.

PARK, S. J., PHAM, V. H., JUNG, M. Y., KIM, S. J., KIM, J. G., ROH, D. H. & RHEE, S. K. 2011. *Thioalbus denitrificans* gen. nov., sp nov., a chemolithoautotrophic sulfur-oxidizing gammaproteobacterium, isolated from marine sediment. *International Journal of Systematic and Evolutionary Microbiology,* 61**,** 2045-2051.

PEREIRA, P. M., HE, Q., XAVIER, A. V., ZHOU, J. Z., PEREIRA, I. A. C. & LOURO, R. O. 2008. Transcriptional response of *Desulfovibrio vulgaris* Hildenborough to oxidative stress mimicking environmental conditions. *Archives of Microbiology,* 189**,** 451-461.

PFENNIG, N. & BIEBL, H. 1976. *Desulfuromonas acetoxidans* gen-nov. New anaerobic sulfur-reducing, acetate-oxidizing bacterium. *Archives of Microbiology,* 110**,** 3-12.

PHILLIPS, E. J. P. & LOVLEY, D. R. 1994. Oxidation of elemental sulfur coupled to manganese reduction by sulfate-reducing microorganisms.*Abstracts of Papers of the American Chemical Society,* 207**,** 80-88.

POOCK, S. R., LEACH, E. R., MOIR, J. W. B., COLE, J. A. & RICHARDSON, D. J. 2002. Respiratory detoxification of nitric oxide by the cytochrome c nitrite reductase of *Escherichia coli. Journal of Biological Chemistry,* 277**,** 23664-23669.

PRANGE, A., ENGELHARDT, H., TRUPER, H. G. & DAHL, C. 2004. The role of the sulfur globule proteins of *Allochromatium vinosum*: mutagenesis of the sulfur globule protein genes and expression studies by real-time RT-PCR. *Archives of Microbiology,* 182**,** 165-174.

RAMO, J., HYOKYVIRTA, O. & SILLANPAA, M. 2003. Interactions between polysulphides and stainless steel materials. *Materials and Corrosion-Werkstoffe Und Korrosion,* 54**,** 37-39.

RIZKOV, D., LEV, O., GUN, J., ANISIMOV, B. & KUSELMAN, I. 2004. Development of in-house reference materials for determination of inorganic polysulfides in water. *Accreditation and Quality Assurance,* 9**,** 399-403.

SAEED, A. I., SHAROV, V., WHITE, J., LI, J., LIANG, W., BHAGABATI, N., BRAISTED, J., KLAPA, M., CURRIER, T., THIAGARAJAN, M., STURN, A., SNUFFIN, M., REZANTSEV, A., POPOV, D., RYLTSOV, A., KOSTUKOVICH, E., BORISOVSKY, I., LIU, Z., VINSAVICH, A., TRUSH, V. & QUACKENBUSH, J. 2003. TM4: A free, open-source system for microarray data management and analysis. *Biotechniques,* 34**,** 374.

SANTANA, M. & GONZALEZ, L. 2009. *Desulfovibrio vulgaris* Hildenborough transcriptomic analysis by Restriction fragment functional display (RFFD). *Current Research Topics in Applied Microbiology and Microbial Biotechnology***,** 577-580.

SASS, H. & CYPIONKA, H. 2007. Response of sulfate reducing bacteria to oxygen. In: *Sulphate-Reducing Bacteria: Environmental and Engineered Systems 1st edn* 1ed. Cambridge, UK: eds Barton, L.L. and Hamilton, W.A.

SCHUTT, H. U. & RHODES, P. R. 1996. Corrosion in an aqueous hydrogen sulfide, ammonia, and oxygen system. *Corrosion,* 52**,** 947-952.

SCHWEIZER, H. P. 1992. Alleleic exchange in *Pseudomonas aeruginosa* using novel cole1-type vectors and a family of cassettes containing a portable orit and coutner-selectable *Bacillus-subtilis* SacB marker. *Molecular Microbiology,* 6**,** 1195-1204.

SHARTAU, S. L. C., YURKIW, M., LIN, S. P., GRIGORYAN, A. A., LAMBO, A., PARK, H. S., LOMANS, B. P., VAN DER BIEZEN, E., JETTEN, M. S. M. & VOORDOUW, G. 2010. Ammonium Concentrations in Produced Waters from a Mesothermic Oil Field Subjected to Nitrate Injection Decrease through Formation of Denitrifying Biomass and Anammox Activity. *Applied and Environmental Microbiology,* 76**,** 4977-4987.

SHIERS, D. W., RALPH, D. E. & WATLING, H. R. 2011. Batch culture of *Acidithiobacillus caldus* on tetrathionate. *Biochemical Engineering Journal,* 54**,** 185-191.

SIEVERT, S. M., SCOTT, K. A., KLOTZ, M. G., CHAIN, P. S. G., HAUSER, L. J., HEMP, J., HUGLER, M., LAND, M., LAPIDUS, A., LARIMER, F. W., LUCAS, S., MALFATTI, S. A., MEYER, F., PAULSEN, I. T., REN, Q., SIMON, J. & CLASS, U. S. F. G. 2008. Genome of the epsilonproteobacterial chemolithoautotroph *Sulfurimonas denitrificans*. *Applied and Environmental Microbiology,* 74**,** 1145-1156.

SIGALEVICH, P., MESHORER, E., HELMAN, Y. & COHEN, Y. 2000. Transition from anaerobic to aerobic growth conditions for the sulfate-reducing bacterium *Desulfovibrio oxyclinae* results in flocculation. *Applied and Environmental Microbiology,* 66**,** 5005-5010.

SMITH, J. S. & MILLER, J. D. A. 1975. Nature of sulfides and their corrosive effects on ferrous metals: A Review. *British Corrosion Journal,* 10**,** 136-143.

SOROKIN, D. Y., FOTI, M., TINDALL, B. J. & MUYZER, G. 2007. *Desulfurispirillum alkaliphilum* gen. nov sp nov., a novel obligately anaerobic sulfur- and dissimilatory nitrate-reducing bacterium from a full-scale sulfide-removing bioreactor. *Extremophiles,* 11**,** 363-370.

SOYLEMEZOGLU, S. & HARPER, R. 1982. Oxygen ingress into geothermal steam and its effect on corrosion of low carbon steel at Broadlands, New Zealand. *Geothermics,* 11**,** 31-42.

STARKEY, R. L. 1936. Formation of sulfide by some sulfur bacteria. *Proceedings of the Society for Experimental Biology and Medicine,* 35**,** 120-122.

TAKAHASHI, Y., SUTO, K., INOUE, C. & CHIDA, T. Phylogenetic characteristics of sulfate-reducing bacteria having ability to reduce polysulfide. 3rd International Workshop on Water Dynamics, Nov 16-17 2005 Sendai, JAPAN. 212-215.

TALAAT, A. M., HOWARD, S. T., HALE IV, W., LYONS, R., GARNER, H. & JOHNSTON, S. A. 2002. Genomic DNA standards for gene expression profiling in *Mycobacterium tuberculosis. Nucleic Acids Research,* 30.

TANG, K., BASKARAN, V. & NEMATI, M. 2009. Bacteria of the sulphur cycle: An overview of microbiology, biokinetics and their role in petroleum and mining industries. *Biochemical Engineering Journal,* 44**,** 73-94.

TATUSOV, R. L., KOONIN, E. V. & LIPMAN, D. J. 1997. A genomic perspective on protein families. *Science,* 278**,** 631-637.

TRUPER, H. G. 2008. Sulfur and light? History and "Thiology" of the phototrophic sulfur bacteria. *Microbial Sulfur Metabolism***,** 87-100.

TUSHER, V. G., TIBSHIRANI, R. & CHU, G. 2001. Significance analysis of microarrays applied to the ionizing radiation response. *Proceedings of the National Academy of Sciences of the United States of America,* 98**,** 5116-5121.

VON WOLZOGEN KUHR, C. A. H. & VLUGT, L. S. V. D. 1934. De grafiteering van Gietijzer als electrobiochemich Process inanaerobe Gronden. *Water,* 18**,** 147-165.

WALKER, C. B., STOLYAR, S. S., PINEL, N., YEN, H. C. B., HE, Z. L., ZHOU, J. Z., WALL, J. D. & STAHL, D. A. 2006. Recovery of temperate *Desulfovibrio vulgaris* bacteriophage using a novel host strain. *Environmental Microbiology,* 8**,** 1950-1959.

WHITE, D. 2000. The physiology and biochemistry of prokaryotes. 2 ed. New York, NY, USA: Oxford University Press.

WILDSCHUT, J. D., CAFFREY, S. M., VOORDOUW, J. K. & VOORDOUW, G. 2012. Oxygen exposure increases resistance of *Desulfovibrio vulgaris* Hildenborough to killing by hydrogen peroxide. *Antonie Van Leeuwenhoek International Journal of General and Molecular Microbiology,* 101**,** 303-311.

WILDSCHUT, J. D., LANG, R. M., VOORDOUW, J. K. & VOORDOUW, G. 2006. Rubredoxin: Oxygen oxidoreductase enhances survival of *Desulfovibrio vulgaris* Hildenborough under microaerophilic conditions. *Journal of Bacteriology,* 188**,** 6253-6260.

WOLFE, M. T., HEO, J., GARAVELLI, J. S. & LUDDEN, P. W. 2002. Hydroxylamine reductase activity of the hybrid cluster protein from *Escherichia coli*. *Journal of Bacteriology,* 184**,** 5898-5902.

XIONG, J. J., KURTZ, D. M., AI, J. Y. & SANDERS-LOEHR, J. 2000. A hemerythrin-like domain in a bacterial chemotaxis protein. *Biochemistry,* 39**,** 5117-5125.

ZHANG, X. H. & WEISSBACH, H. 2008. Origin and evolution of the protein-repairing enzymes methionine sulphoxide reductases. *Biological Reviews,* 83**,** 249-257.

ZHOU, A., HE, Z., REDDING-JOHANSON, A. M., MUKHOPADHYAY, A., HEMME, C. L., JOACHIMIAK, M. P., LUO, F., DENG, Y., BENDER, K. S., HE, Q., KEASLING, J. D., STAHL, D. A., FIELDS, M. W., HAZEN, T. C., ARKIN, A. P., WALL, J. D. & ZHOU, J. 2010. Hydrogen peroxide-induced oxidative stress responses in *Desulfovibrio vulgaris* Hildenborough. *Environmental Microbiology,* 12**,** 2645-2657.